Functional Impacts of Neurogenesis and Axonal Sprouting in Epilepsy

By

William D. Hendricks

A DISSERTATION

Presented to the Vollum Institute, Neuroscience Graduate Program;

and Oregon Health & Science University

School of Medicine

In partial fulfillment of

the requirements for the degree of:

Doctor of Philosophy

April 2019

School of Medicine

Oregon Health & Science University

CERTIFICATE OF APPROVAL

This is to certify that the PhD Dissertation of

William D. Hendricks

has been approved:

_____

Advisor, Eric Schnell, MD/PhD

_____

Member and Chair, John T. Williams, PhD

_____

Member, Gary L. Westbrook, MD

_____

Member, Laurence O. Trussell, PhD

_____

Member, Skyler L. Jackman, PhD

Table of Contents

Acknowledgements

This work would not have been possible without the persistence, patience, and dedication of my mentor, Eric Schnell. His mentorship has been truly instrumental in my success and growth as both a scientist and a person. During the course of countless discussions and impromptu meetings, Eric taught me to be thoughtful with my research, in order to design and conduct elegant and creative experiments. His support during tough scientific and personal times, and his enthusiasm during scientific and personal high-points is unmatched. I am lucky to have him as a mentor.

Additionally, I would like to thank Gary Westbrook for his senior mentorship and support all along the way. I would like to thank my other committee members, Larry Trussell, John Williams, and Skyler Jackman for their support and enthusiasm. I also want to thank all of the people who came through the labs during this time who provided technical, scientific, and collegial support; specifically: Kathleen Beeson, Cory Butler, Christina Chatzi, Chris Vaaga, Brian Jones, Kunal Gupta, Austin Peters, Yang Chen, Arielle Isakharov, Alex Wilson, and many others. I would like to thank my first mentor, Elizabeth Meyer-Bernstein for taking me into her lab and giving me an opportunity that would change my life.

Separately, I would like to thank my incredible classmates that quickly become my closest friends for the climbing, skiing, concerts, vacations, and other fun times we shared together. Most importantly, I would like to thank my

family and dedicate this dissertation to them. Their guidance led me to graduate school, and none of this would have been possible without their support.

Abstract

Seizures are patterns of abnormal electrical activity in the brain that can result in altered sensory perception, loss of consciousness, and involuntary motor spasms. Epilepsy is the diagnosis of spontaneous and recurrent seizures. Of the many varieties of epilepsy, temporal lobe epilepsy is a common acquired epilepsy in adults and is in many cases medically intractable. Acquired temporal lobe epilepsy can result following brain trauma; however, the mechanism for the development of epilepsy from a precipitating neurological insult has remained elusive. Temporal lobe epilepsy is correlated with altered structure and function of neural circuits, changes that are hypothesized as a primary factor in epilepsy etiology, though it is unclear how individual circuit changes affect excitability in epileptic brains. One such example of circuit rearrangement in epilepsy is the pathologic retrograde sprouting of granule cell mossy fiber axons within the hippocampal dentate gyrus. Despite their proximal location, large presynaptic terminals, and excitation of target neurons, the ultimate impact of sprouted mossy fiber activity is unclear. Additionally, the dentate gyrus is a locus for adult neurogenesis and adult-born granule cells have been hypothesized to directly give rise to sprouted mossy fibers. If sprouted mossy fibers do primarily arise from adult-born dentate granule cells, then seizure-enhanced neurogenesis might play a role in establishing these aberrant connections. Using the pilocarpine model of epilepsy and transgenic labeling of age-defined cohorts of granule cells in mice, I demonstrate that adult-born neurons contribute to

sprouting and are more likely to develop sprouted mossy fibers than their neonatally-born counterparts. Using super resolution confocal microscopy and whole-cell recordings from acute brain slices, I reveal sprouted mossy fiber axons form large synapses in the inner molecular layer that release glutamate and excite other dentate granule cells. Despite a prominent short-term depression of sprouted mossy fiber terminals, these cells had an increased probability of release during single stimulation episodes. Additionally, optogenetic activation of sprouted mossy fibers reliably triggered action potential firing in postsynaptic dentate granule cells and triggered polysynaptic bursts of EPSCs. A high probability of release and lack of tonic adenosine signaling at sprouted synapses contributed the generation of these bursts and activation of presynaptic adenosine 1 receptors decreased bursting of EPSCs. Taken together, my data suggest that sprouted mossy fibers from adult-born granule cells can quickly propagate recurrent excitation through the dentate gyrus and initiate bursts of recurrent excitation.

Introduction and Background

A delicate balance of wiring in the central nervous system is responsible for our sensation, reflexes, and behaviors within the environment. These functions arise from a complex system of neurons and neural circuits that balances neural excitation, inhibition, and modulation to a high degree of precision. However, neural circuits are not fixed and have an extraordinary flexibility to respond to natural and traumatic stimuli (Münte et al., 2002; Levin, 2003; Draganski et al., 2004; Dimyan and Cohen, 2011). This plasticity is critical for proper brain function and likely responsible for dynamic processes such as learning and memory (Draganski et al., 2004; Dayan and Cohen, 2011). Neural plasticity occurs on many levels, from short-term changes in neurotransmitter release probability at synapses (Zucker and Regehr, 2002; Malenka and Bear, 2004), to large-scale neural circuit reorganization (Hensch, 2005; Lledo et al., 2006).

Circuit plasticity can also arise following brain trauma and trauma to neural circuits can result in psychiatric and neurological disease (Sutula et al., 1989; Sloviter, 1991; Levin, 2003; Anderson et al., 2005; Dimyan and Cohen, 2011). Although diseases of the brain were originally thought to be spiritual in nature, Hippocrates in his famous work *On the Sacred Disease* first proposed diseases such as epilepsy were of natural and neurological origins and these diseases are now known to result from altered neural circuit function (McNamara, 1994; Chang and Lowenstein 2003).

Seizures and epilepsy constitute a large collection of neural circuit dysfunction

Seizures are patterns of abnormal electrical activity that can cause loss of consciousness, altered perception, and most notoriously, violent motor spams. Seizures can be comorbid with many psychiatric and neurological diseases and syndromes including epilepsy, autism, Angleman syndrome, Down syndrome, and anti-NMDA-receptor encephalitis, as examples (Hauser and Hesdorffer, 1990; McNamara, 1994; Chang and Lowenstein 2003; Sansing et al., 2007). Seizures can occur throughout the brain, either locally within a seizure focus or globally, generalizing throughout the brain. Generalized seizures are characterized by abrupt changes in global brain function from the onset, whereas focal seizures can "generalize" bilaterally but initiate locally within a seizure focus (Engel, 2013). Surgical removal of seizure foci is a treatment for focal epilepsies (Wiebe et al., 2001); therefore, it is hypothesized structural and functional changes occurring within a seizure focus is a critical component of epilepsy etiology.

Epilepsy specifically is the diagnosis of idiopathic, spontaneous recurrent seizures. Seizures and epilepsy has been described since at least 2000 BC (Magiorkinis et al., 2010) and epilepsy currently affects roughly 3% of the world population (Hauser and Hesdorffer, 1990). Epilepsies can be both generalized and focal, originate from genetic mutations, or be acquired from neurological insults such as fevers, traumatic brain injury, stroke and infections (McNamara, 1994; Chang and Lowenstein 2003).

The number and variety of possible causes of epilepsies and seizures underscores the delicate balance of the nervous system and the dramatic consequences of perturbations to brain circuitry. Yet, epilepsy etiology is still poorly understood. Both circuit alterations and neural hyperactivity are hypothesized as likely mechanisms and are consistent between human patients with epilepsy and rodent models of epilepsy (Mello et al., 1993; McNamara, 1994; Chang and Lowenstein 2003). However, despite well-characterized models of epilepsy in rodents and high clinical research importance, the mechanisms that drive disease progression of epilepsy, a process named "epileptogenesis", is still largely unknown.

Temporal lobe epilepsy is a common focal, acquired epilepsy

A temporal lobe focus is identified in the majority of patients with focal epilepsy making temporal lobe epilepsy (TLE) the most common focal epilepsy (Semah et al., 1998). TLE can develop following severe brain trauma and up to 40% of patients have ongoing seizures despite anticonvulsant treatment (Hauser and Hesdorffer, 1990). TLE involves altered neural circuitry of the temporal lobe (Williamson et al., 1993) and resection of the hippocampus from the temporal lobe is a highly effective treatment for TLE in patients who are not fully seizure free with medication (Wiebe et al., 2001). Thus, it is likely circuit changes in the hippocampus are be responsible for seizures and epilepsy (Turski et al., 1983; Mello et al., 1993; Löscher, 2017). Indeed, there are a variety of circuit changes including the loss (death) of inhibitory interneurons (Sloviter,

1987; Doherty and Dingledine, 2001), loss of pyramidal cells (Nadler et al., 1980; Babb et al., 1984a; DeGiorgio et al., 1992; Mello et al., 1993), and neurite outgrowth (Nadler et al., 1980; Ribak et al., 2000). Understanding how these processes impact circuit function would provide insight into how the brain regulates itself during both health and disease and could ultimately lead to greater understanding of epilepsy etiology, leading to more effective treatment options.

TLE can be induced in rodents genetically, by repeated electrical or chemical stimulation (eg. kindling), or chemical convulsants (ie. kainic acid or pilocarpine) (Shibley and Smith, 2002; Löscher, 2011). In both the kainic acid and pilocarpine models, currently the most widely used rodent models of TLE, animals are injected with a bolus dose of convulsant, have acute seizures, survive, enter a latent period that is followed by the development of spontaneous seizures. Rodent models of TLE share many of the same structural and functional changes within the hippocampus with human TLE such as cell loss, sprouting of axons and dendrites, and enhanced neurogenesis (Babb et al., 1984b; Babb et al., 1984a; Sutula et al., 1989; Sloviter, 1991; DeGiorgio et al., 1992; Represa et al., 1995; Shibley and Smith, 2002). Thus, it is likely these structural and functional circuit changes within the hippocampus represent a common, underlying mechanism of epileptogenesis in TLE.

Dentate gyrus circuitry and function

Circuit changes within the dentate gyrus of the hippocampus are intimately linked to TLE. Information flow through the hippocampus in healthy brains generally follows a tri-synaptic circuit (Figure 1) and the dentate gyrus receives the primary inputs to the hippocampus. Perforant path inputs from entorhinal cortex synapse onto dentate granule cell dendrites in the outer and middle molecular layers (OML and MML), with mixed feedback excitation and inhibition comprising the most proximal synaptic inputs in the inner molecular layer (IML) (Amaral et al., 2007). High synaptic divergence onto the over 1 million dentate granule cells is responsible for the "sparse-coding" nature of the dentate gyrus. Combined with low intrinsic activity the dentate gyrus effectively performs pattern separation (Jung and McNaughton, 1993; Leutgeb et al., 2007; Severa et al., 2017).

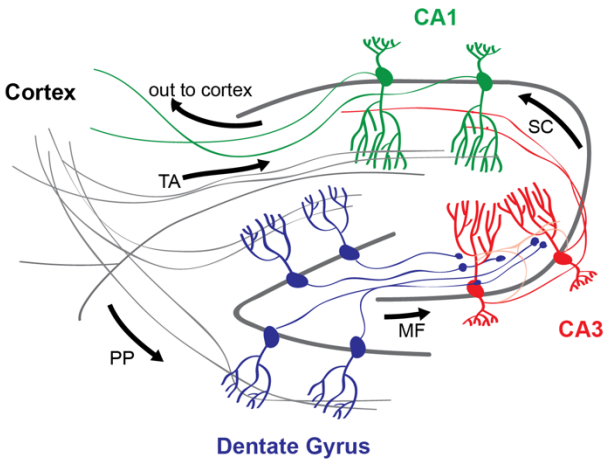

Figure 1: Hippocampal circuitry. The basic circuit architecture of the hippocampus follows a unidirectional, tri-synaptic circuit with a few minor modifications. Cortical inputs (grey) synapse onto dendrites of dentate granule cells (purple) via the perforant pathway (PP), the principal cell of the dentate gyrus. Granule cells send mossy fiber axons (MF) to CA3 pyramidal cells (red) and interneurons (not pictured). CA3 pyramidal cells are highly interconnected but send output to CA1 pyramidal cells (green) via Schaffer collaterals (SC). Pyramidal cells in CA1 also receive entorhinal input onto distal dendrites via the temporammonic pathway (TA). CA1 send information back out to cortex and other brain regions.

Facilitating unidirectional information flow out of the dentate, granule cells project mossy fiber axons to region CA3 where they make potent synaptic connections onto CA3 pyramidal cells (Amaral et al., 2007). Strong facilitation of

mossy fiber - CA3 synapses (mf-CA3) (Salin et al., 1996) and single bouton "detonation" of post-synaptic cells (Vyleta et al., 2016) engage the highly interconnected CA3 network to perform pattern completion (Guzman et al., 2016). From here, Schaffer collaterals, CA3 axonal projections to CA1, synapse onto CA1 pyramidal cells, cells that in turn send axons out of the hippocampus proper to the subiculum (Amaral et al., 2007).

Mossy fiber synapses in CA3, the output of the dentate gyrus

Mossy fiber axons from dentate granule cells terminate in region CA3 forming unusually complex and potent synapses onto pyramidal cells and interneurons (Henze et al., 2000; Nicoll and Schmitz, 2005). The mossy fiber axon terminal is large, over 3 μm in diameter, and engulfs complex dendritic spines on CA3 pyramidal cells known as "thorny excrescences" (Henze et al., 2000). Mossy fiber synapses are also highly specialized. Contacts onto CA3 inhibitory interneurons (mf-IN) are weaker (Toth et al., 2000) and lack the complex thorny excrescence morphology of mf-CA3 synapses (Henze et al., 2000). These weaker mf-IN synapses form as filopodia extending from the main bouton (Acsady et al., 1998), highlighting the highly complex, yet tightly compartmentalized and regulated nature of the mossy fiber synapse.

The properties of short-term plasticity at mf-CA3 synapses differentiate them from most other synapses within the hippocampus. Despite the multiple release sites at these synapses all having individually low probability of release (P_r) (von Kitzing et al., 1994), a single granule cell (Henze et al., 2002) or even a

single bouton (Vyleta et al., 2016) is capable of “detonating” or firing a post-synaptic CA3 pyramidal cell. Mossy fiber synapses undergo dramatic facilitation at almost any increase in stimulation frequency and 1 Hz electrical stimulation can facilitate mossy fiber EPSCs by upwards of 400% (Salin et al., 1996). Though granule cells typically fire infrequently *in vivo*, ranging from 0.04 - 3 Hz (Mistry et al., 2011), a modest increase in activity could drive CA3 cell firing (Vyleta et al., 2016) and potently influence hippocampal circuit activity.

Such dramatic facilitation is largely due to the very low probability of release at mf-CA3 synapses (von Kitzing et al., 1994). The presence of tonic adenosine in stratum lucidum (SL) lowers probability of release via presynaptic adenosine 1 receptor (A1R) inhibition (Moore et al., 2003) of Ca^{2+} channels in the terminal (Wu and Saggau, 1994; Manita et al., 2004). Indeed, blocking presynaptic A1Rs with DPCPX, a potent and selective A1R antagonist, largely occludes frequency facilitation (Moore et al., 2003; Fedele et al., 2005). Other components identified as critical in preserving frequency-dependent facilitation are the expression of trans-synaptic signaling molecules (Ben-Simon et al., 2015), specialized calcium-sensors (Jackman et al., 2016), and pre-synaptic kainate receptors (Sachidhanandam et al., 2009).

It also is worth recognizing other unique features of plasticity at mf-CA3 synapses. Although the debate over the locus of expression of long term potentiation (LTP) eventually settled on the now canonical post-synaptic mechanism (Kerchner and Nicoll, 2008), mf-CA3 synapses violate this rule. Expression of LTP at mf-CA3 synapses is not dependent on NMDAR receptors

(Harris and Cotman, 1986) or post-synaptic Ca^{2+} (Mellor and Nicoll, 2001), but rather entirely regulated and expressed pre-synaptically (Nicoll and Malenka, 1995) through increases in pre-synaptic Ca^{2+} and cAMP during high rates of activity that trigger PKA (Weisskopf et al., 1994) and increase release probability. Additionally, despite the low expression of NMDARs post-synaptically (Jonas et al., 1993), mf-CA3 synapses can undergo NMDAR-LTP (Kwon and Castillo, 2008), whereby the relative contribution of NMDARs is increased and drives increased excitability and spike bursting (Hunt et al., 2013). These unique features of mf-CA3 synapses make them interesting in the context of epilepsy given presynaptic activity alone could drive known long-term changes in release probability (Goussakov et al., 2000) and epilepsy-associated changes in NMDAR expression can alter granule cell spiking properties (Sutula et al., 1996; Lynch et al., 2000).

Dentate gyrus dysfunction in epilepsy

Resection of the hippocampus is an effective treatment for TLE (Wiebe et al., 2001) and circuit changes within the dentate gyrus are hypothesized to contribute to epileptogenesis (McNamara, 1994), making dentate gyrus dysfunction a leading candidate for epileptogenesis. Indeed, decades of research have documented physical and functional circuits changes that could conceivably lead to hippocampal hyperexcitability. I will briefly review two major dentate gyrus circuit changes in epilepsy: cell death and aberrant growth of dendrites and axons (Figure 2).

Excitatory and inhibitory cell death

Perhaps the most striking example of seizure-related brain damage in the hippocampus is the death of CA1 and CA3 pyramidal cells (Babb et al., 1984b; Babb et al., 1984a; DeGiorgio et al., 1992; Represa et al., 1995). Epileptic tissue from human patients with TLE show profound CA3 cell loss and rodent models of epilepsy phenocopy this phenomena (Mello et al., 1993; Cavalheiro et al., 1996). CA3 cell loss occurs within days after status epilepticus in animal models (Mello et al., 1993), though this process may be more gradual in humans (Babb et al., 1984b) given the more chronic onset of epilepsy in humans as opposed to the highly acute seizure induction in animal models.

Excitatory mossy cells in the hilus are highly vulnerable to seizures, and few remain in epileptic dentate gyrus (Mello et al., 1993). Mossy cells receive a major output from dentate granule cells and facilitate both feedback inhibition and excitation onto granule cells (Scharfman, 1995). Thus the death of mossy cells could counterintuitively drive either increased (Santhakumar et al., 2000) or decreased (Sloviter, 1991) excitation in epileptic brains. A decrease in the number of mossy cells would decrease the degree of feedback excitation, but would similarly decrease excitatory drive onto surviving interneurons, thereby decreasing feedback inhibition. How mossy cells loss affects dentate function is still unclear and could be further dependent on the properties of remaining mossy cells (Sloviter, 1991; Santhakumar et al., 2000; Bui et al., 2018).

In addition to cell death of excitatory neurons in epileptic brains, there is a profound decrease in inhibitory interneurons throughout the hippocampus, including hilar interneurons that provide feedback inhibition onto dentate granule cells (Sloviter, 1987; de Lanerolle et al., 1989; Doherty and Dingledine, 2001). A common feature to both human patients and animal models, the loss of inhibitory interneurons could lead to an increased excitation to inhibition ratio (ie. more excitation) and a hyperexcitable environment where seizures could originate.

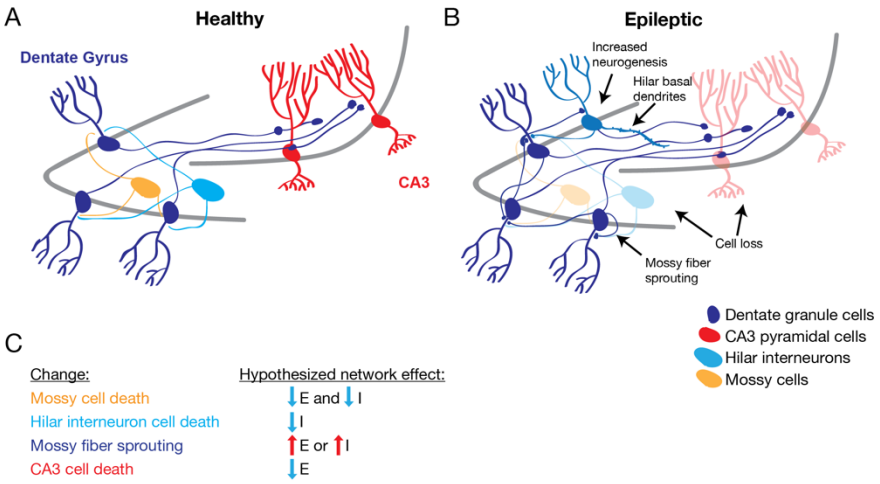

Figure 2: Alterations to dentate gyrus circuitry in epilepsy. A Dentate gyrus circuity in healthy (non-epileptic) rodent brains. Granule cells (blue) project mossy fiber axons to CA3 pyramidal cells (red). Mossy cells (yellow) and hilar interneurons (blue) provide feedback excitation and inhibition, respectively. **B** Dentate gyrus circuitry is dramatically altered in epileptic tissue. Cell loss (faded cells) involves CA3 pyramidal cells, hilar interneurons, and hilar mossy cells. Recurrent circuits from hilar basal dendrites and mossy fiber sprouting are formed. Dentate granule cell neurogenesis is increased, increasing the number of adult-born granule cells. Other changes (not pictured) include granule cell dispersion and ectopic cellular migration. **C** Hypothesized network effects of circuit changes. See text for further discussion.

The loss of these cell types may not be directly responsible for seizures or epilepsy *per se*, because cellular death is presumed to be permanent, and humans and rodents do not continuously seize. Yet, the death of both inhibitory cells and excitatory cells that drive feedforward inhibition creates a condition where the generation of epileptiform activity is more likely. In agreement, functional analysis of the dentate gyrus after seizures shows heightened

excitability (Tauck and Nadler, 1985); however, this is in concert with other network alterations, including changes to granule cells.

Aberrant growth of dendrites and axons

Dentate granule cells receive multi-contextual input along their apical dendrites with a high degree of segregation (Amaral et al., 2007). At the most distal points, in the outer molecular layer (OML), dentate granule cells synapse with excitatory lateral perforant path axons arising from lateral entorhinal cortex. More proximally, there is another laminated input to granule cells from medial entorhinal cortex along the medial perforant path. Because mossy fiber axons are restricted to the hilus in healthy brains (Amaral et al., 2007), granule cell apical dendrites do not receive any monosynaptic granule cell afferents. However, in TLE, granule cells form large hilar basal dendrites that receive mossy fiber input and create an excitatory recurrent network, and contribute to hyperexcitability (Spigelman et al., 1998; Ribak et al., 2000; Kelly and Beck, 2017).

Another seizure-induced morphological change to the granule cells is the sprouting of aberrantly targeted, mossy fiber axons onto other dentate granule cells (Nadler et al., 1980). Mossy fiber synaptic transmission produces large excitatory post-synaptic currents at their normal targets in CA3, and sprouted mossy fibers could create strong recurrent excitatory feedback loops if sprouted synapses had these functional properties (Nicoll and Schmitz, 2005). As sprouted mossy fibers and monosynaptic granule cell – granule cell connections

are absent under non-pathological conditions, such connections could induce run-away excitation resulting in hippocampal hyperexcitability (Tauck and Nadler, 1985; Sutula et al., 1988; Sutula et al., 1989; Okazaki et al., 1995; Buckmaster et al., 2002).

However, electron microscopy studies have also suggested sprouted mossy fibers could also target inhibitory interneurons located in the inner molecular layer (Sloviter et al., 2006b), thus compensating for the loss of interneurons by increasing inhibitory drive within the dentate, in which case sprouted mossy fibers would actually tend to reduce excitability. Although increased dentate excitation is seen in temporal lobe epilepsy, the challenge of isolating and selectively stimulating sprouted mossy fibers has severely limited the examination of the sprouted granule cell – granule cell synapse. Thus, the target(s) and effects of mossy fiber sprouting remain undefined and await functional confirmation.

Functional evidence of mossy fiber sprouting

Early functional evidence of sprouted mossy fibers

Functional analysis of sprouted mossy fibers has been an area of intense interest since 1985, with the discovery that antidromic stimulation of granule cells caused repeated population spiking in the dentate granule cell layer in epileptic rats (Tauck and Nadler, 1985). Importantly, this effect was absent in

low extracellular Ca^{2+} suggesting it was synaptically-mediated. However, this population spiking was only apparent in less than half the slices, despite robust mossy fiber sprouting (Tauck and Nadler, 1985). Additionally, hilar stimulation does not selectively activate sprouted mossy fibers (Figure 3), leaving open the possibility of contamination from other cell types such as interneurons and mossy cells as well as activation of alternate sources of recurrent excitation (Spigelman et al., 1998; Ribak et al., 2000).

Nevertheless, subsequent studies generally supported a role for sprouted mossy fibers in dentate gyrus hyperexcitability. Recurrent circuits in the dentate gyrus formed after seizures, presumed to be sprouted mossy fibers, have been studied using antidromic stimulation (Tauck and Nadler, 1985; Wuarin and Dudek, 1996; Okazaki et al., 1999), perforant path stimulation (Cronin et al., 1992; Golarai and Sutula, 1996; Masukawa et al., 1996; Okazaki et al., 1999), focal glutamate applications using glutamate microdrops (Wuarin and Dudek, 1996; Lynch and Sutula, 2000) and uncaging (Molnar and Nadler, 1999; Wuarin and Dudek, 2001) in the granule cell layer, and paired sharp-electrode recordings (Scharfman et al., 2003b). Together, these experiments offer supportive

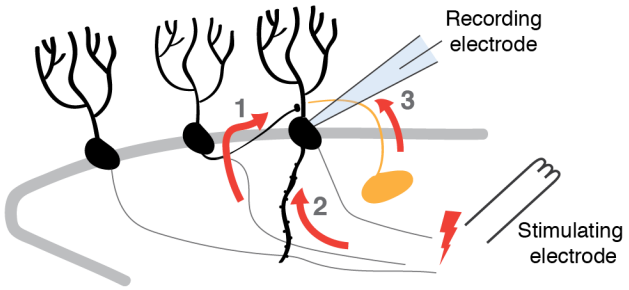

Figure 3: Difficulties with electrical stimulation of sprouted mossy fibers. Physiologic analysis of sprouted mossy fibers has traditionally relied upon electrical stimulation of mossy fiber axons to drive antidromic action potentials in granule cells that in turn activates sprouted mossy fibers (1). However, activation of mossy fibers could also drive recurrent activity through hilar basal dendrites (2) or activate remaining mossy cell feedback excitation (3), leading to contamination of evoked responses. Electrical stimulation of the inner molecular layer (not pictured) causes similar problems.

evidence that sprouted mossy fibers constitute a possible source of recurrent excitation within the epileptic dentate gyrus and highlight the potential for sprouted mossy fibers to drive hyperexcitability and epileptogenesis.

However, use of the above techniques, with the exception of paired recordings, required “unmasking” of sprouted mossy fibers (Patrylo and Dudek, 1998) as sprouted mossy fiber responses were unreliable and infrequent. Increased concentrations of extracellular potassium (Patrylo and Dudek, 1998; Hardison et al., 2000), blocking $GABA_A$-mediated inhibition (Cronin et al., 1992; Patrylo and Dudek, 1998), or both (Wuarin and Dudek, 1996; Wuarin and Dudek, 2001), more reliably evoked putative sprouted mossy fiber responses and led to the conclusion that sprouted synapses were “conditionally expressed” (Sutula and Dudek, 2007) and required a breakdown of inhibition or modest increases in extracellular potassium for sprouted fibers to drive hyperexcitability. It is unclear whether this “conditional expression” is an intrinsic property of sprouted mossy fibers or rather an epiphenomenon due to either the imprecise methods of stimulation or occurring as a consequence of acute slice preparation. Regardless, as neuromodulatory factors strongly affect basal properties of mf-CA3 neurotransmission (Castillo et al., 1996; Moore et al., 2003), it is conceivable that neuromodulators or other factors may strongly influence the expression and impacts of mossy fiber sprouting on hippocampal hyperexcitability, such that it is conditional (Simmons et al., 1997; Gouder et al., 2003; Amorim et al., 2016; Sandau et al., 2016).

Relevance of mossy fiber sprouting in epilepsy

Despite the initial assumption that sprouted mossy fibers could drive increased hyperexcitability, the artificial conditions in which sprouted mossy fibers were detected (Cronin et al., 1992; Wuarin and Dudek, 1996; Patrylo and Dudek, 1998; Hardison et al., 2000) left unresolved how sprouted mossy fibers drive epileptogenesis *in vivo* (Buckmaster, 2014). In other words, can sprouted mossy fibers drive epileptiform activity in physiological conditions? Complicating the matter, mossy fiber axons can also sprout onto remaining inhibitory cells (Sloviter et al., 2006b) and increase feedforward excitation of interneurons (Sloviter, 1992; Buckmaster and Dudek, 1997; Wu and Leung, 2001), thereby offsetting the effects of inhibitory cell loss (Sloviter, 1987; Doherty and Dingledine, 2001). However, reconstruction of long stretches of sprouted axons reveals that the majority of sprouted synapses are on excitatory cells (Buckmaster et al., 2002), yet relatively limited functional data exists.

Although an experimentally-obtained individual connection probability of 0.67% (Scharfman et al., 2003b) may also lead some to question the functional significance of sprouting, this low connection probability is a function of the large numbers of granule cells. It is worth noting that by the same calculation, if 60% of cells sprout (Sutula et al., 1998) 510 boutons (Buckmaster et al., 2002), over 300 million new recurrent, sprouted synapses would result in up to a 300:1 convergence of sprouted synapses onto granule cells, if all granule cells could receive 300 new synapses per cell. In agreement, computer simulations show

the extent of sprouting positively correlates with dentate excitability (Santhakumar et al., 2005).

Thus, sprouted fibers could drive dentate hyperexcitability and therefore seizures. However, the degree of staining for mossy fiber sprouting in the IML does not necessarily correlate with seizure frequency (Shibley and Smith, 2002) as might be expected if mossy fiber sprouting was directly linked to seizure generation. Furthermore, seizures can occur in the absence of mossy fiber sprouting (Longo and Mello, 1997, 1998) and inhibition of sprouting with rapamycin (Buckmaster and Lew, 2011; Heng et al., 2013) or cycloheximide (Longo and Mello, 1997) does not robustly reduce seizure frequency. Although this observation is controversial, as the effect may be timing- and/or dose-dependent (Williams et al., 2002; Zeng et al., 2009; Huang et al., 2010).

Functional properties of sprouted mossy fiber synapses

The relevance and impact of sprouted mossy fibers is also likely to depend on their functional characteristics. Given that mf-CA3 synapses are potent "detonator" synapses (reviewed above), sprouted mossy fibers with features of frequency facilitation and post-synaptic cell detonation could have a large impact and increase excitability, particularly given the high level of convergence and proximal dendritic location on individual granule cells. However, properties of mf-CA3 synapses can be altered after seizures (Goussakov et al., 2000) and also differ depending on post-synaptic targets (Toth et al., 2000).

Mossy fiber sprouting is associated with (and often held responsible for) repeated population spiking of granule cells (Tauck and Nadler, 1985; Patrylo and Dudek, 1998; Patrylo et al., 1999), bursts of EPSCs/EPSPs (Wuarin and Dudek, 1996; Patrylo and Dudek, 1998; Molnár and Nadler, 1999; Okazaki et al., 1999), overall increases in excitatory drive (Wuarin and Dudek, 2001), and epileptiform discharges (Patrylo and Dudek, 1998; Wuarin and Dudek, 2001). However, repetitive antidromic stimulation of sprouted mossy fibers reduced epileptiform activity of granule cells (Hardison et al., 2000), an unexpected result if sprouted mossy fibers functioned similarly to mf-CA3 synapses. Indeed, 1 Hz antidromic stimulation in also produced minimal facilitation of excitatory responses in granule cells (Feng et al., 2003). Though the experimental design assumed these were sprouted mossy fiber responses, there was minimal inhibition by DCG-IV (Feng et al., 2003), suggesting that the stimulation paradigm used was not selective. Paired recordings of dentate granule cells showed a similar effect; high failure rates and strong EPSP depression was observed when multiple evoked APs were triggered in the presynaptic neuron (Scharfman et al., 2003b). Despite robust mossy fiber sprouting and a lack of hilar basal dendrites, the connection probability was extremely low (6 in 903 simultaneous pairs), and the recording technique used (sharp electrode) prevented further analysis. Functional properties of sprouted mossy fibers have remained elusive, in part due to the imprecise methods of stimulation (Figure 3).

Adult neurogenesis and epilepsy

A distinguishing feature of the dentate gyrus is the continued generation of dentate granule cells postnatally (Parent, 2007). These adult-born granule cells survive and integrate into local circuitry (van Praag et al., 2002; Toni et al., 2008; Gu et al., 2012), becoming become virtually indistinguishable from their neonatally-born counterparts. However, during initial stages of maturation and integration, adult-born granule cells develop greater levels of excitability and plasticity (Gu et al., 2012).

Adult granule cell neurogenesis is dynamically regulated by several factors, both positively (Parent et al., 1997; Kempermann et al., 1998; Van Praag et al., 1999; Van Praag et al., 2005) and negatively (Kuhn et al., 1996; Gould et al., 1998). However, disease-associated enhancement of neurogenesis and heightened plasticity of immature, adult-born cells could also leave them vulnerable to disease (Figure 4). Indeed, seizures increase the rate of neurogenesis and accelerates integration of new cells into local circuitry (Parent et al., 1997; Parent et al., 1999; Overstreet-Wadiche et al., 2006; Parent et al., 2006; Jessberger et al., 2007) and adult-born cells born after seizures have morphological and functional changes that could implicate them in epileptogenesis (Parent et al., 1997; Parent et al., 2006; Jessberger et al., 2007; Walter et al., 2007; Kron et al., 2010; Kelly and Beck, 2017). Increased neurogenesis following epilepsy has been linked to cognitive dysfunction (Cho

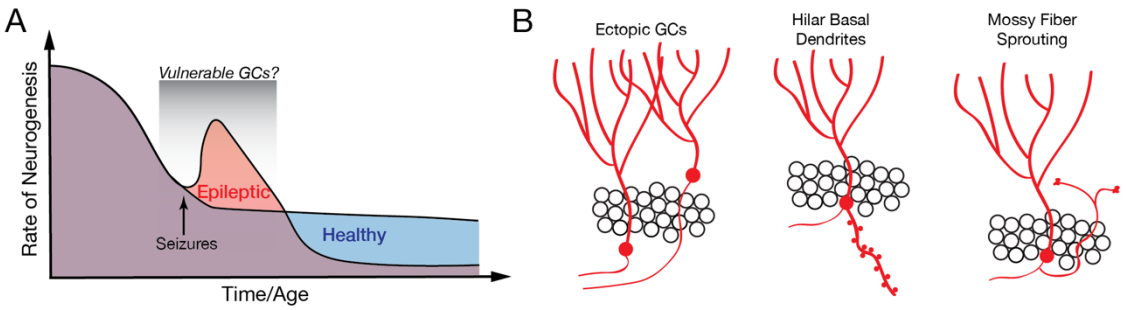

Figure 4: Interactions between neurogenesis and epilepsy. A Representation of rate of hippocampal dentate granule cell neurogenesis over time. Granule cell neurogenesis is highest in the neonatal brain and decreases with age in healthy animals (blue). Following a seizure insult (red), neurogenesis transiently increases and is sustained for weeks, prior to decreasing to very low rates, chronically. Adult-born granule cells born around the time of seizures are hypothesized to be the most vulnerable to circuit changes (gray highlighting). **B** Examples of circuit changes in adult-born granule cells (red cells). Adult-born granule cells can migrate ectopically in the hilus and molecular layer (left), develop hilar basal dendrites (middle), or sprout recurrent mossy fiber axons (right).

et al., 2015) and inhibition of seizure-enhanced neurogenesis can possibly halt disease progression (Hosford et al., 2017). Thus, it is of keen interest as to how newborn granule cells modulate epileptogenesis.

Neurogenesis contributes to altered dentate circuitry

Early research suggested that adult-born dentate granule cells, primarily, if not exclusively, contributed to mossy fiber sprouting (Kron et al., 2010). Though the evidence that neurogenesis is increased in epilepsy is strong (Parent et al., 1997; Jessberger et al., 2005; Parent et al., 2006; Jessberger et al., 2007), experimental ablation of neurogenesis has produced conflicting results with regard to mossy fiber sprouting (Parent et al., 1999; Cho et al., 2015; Hosford et al., 2016; Hosford et al., 2017).

The first study proposing that sprouting was related to enhanced neurogenesis used a combination of BrdU injections into epileptic rats and cytoskeletal staining with neurofilament (NF-M) to reveal sprouted mossy fiber axons originating from BrdU+ cell nuclei (Parent et al., 1997). These results

indicated that adult-born dentate granule cells were at least capable of sprouting mossy fibers into the IML after seizures. In subsequent studies using irradiation to reduce seizure-enhanced neurogenesis to near control levels (Parent et al., 1999), mossy fiber sprouting was unaffected, calling into question the hypothesized interactions between sprouting and neurogenesis.

The advent of virally-mediated gene transfer as a tool capable of labeling adult-born dentate granule cells (van Praag et al., 2002; Van Praag et al., 2005; Tashiro et al., 2006) enabled researchers to more directly assay the contribution of adult-born cells to mossy fiber sprouting (Jessberger et al., 2007; Kron et al., 2010; Althaus et al., 2016). Using a GFP-expressing retrovirus that only infects dividing cells (such as stem cells in the sub-granular zone) (Lewis and Emerman, 1994), researchers have elegantly characterized that granule cells migrate ectopically to the hilus or IML, form hilar basal dendrites, and sprout mossy fibers (Jessberger et al., 2007; Kron et al., 2010; Althaus et al., 2016). Initially, these alterations were thought to be most prominent in cells that were either immature or born soon after seizure-induction rather than granule cells born neonatally. Specifically, GFP+ sprouted axons were only found from adult-born granule cells (Jessberger et al., 2007; Kron et al., 2010), although enhanced retroviral plasmids have since revealed substantial sprouting from neonatally-born cells as well (Althaus et al., 2016) and ablation of neurogenesis with gamma radiation does not entirely block mossy fiber sprouting (Parent et al., 1999; Kron et al., 2010). Thus, while the exclusivity has been challenged, adult-

born granule cells significantly contribute to mossy fiber sprouting and potentially epileptogenesis as well.

Open Questions and Approach

Do sprouted mossy fibers from adult-born granule cells contribute to dentate gyrus hyperexcitability?

Given the above, it is possible that excessive excitability in the dentate gyrus might arise from sprouted mossy fibers, and in particular those fibers from adult-born dentate granule cells. Therefore, it is of particular interest to examine functional properties smf-GC synapses in order to understand how they impact circuit function. However, sprouted mossy fibers cannot be reliably stimulated using conventional electrical stimulation as it is not possible to selectively stimulate only those fibers from adult-born dentate granule cells.

It seems critical to determine which populations of dentate granule cells sprout (Figure 5). While the bulk of attention has been directed at granule cells born *after* seizures, granule cells *immature at the time of seizures* also sprout recurrent collaterals (Kron et al., 2010), and may contribute to disease progression (Jung et al., 2004; Jung et al., 2006; Cho et al., 2015; Hosford et al., 2016). Because the interplay of neurogenesis and sprouting remains in question (Parent et al., 1997; Parent et al., 1999; Bender et al., 2003; Kron et al., 2010), a

carefully designed experiment capable of robustly labeling adult-born neurons could settle this question.

A basic question regarding adult-born granule cells is whether they possess the ability to drive hippocampal hyperexcitability. There are fundamental questions about whether sprouted fibers from adult-born cells are functional and whether they release glutamate or other neurotransmitters. Currently, there is no direct evidence that sprouted fibers from adult-born neurons functionally contribute to hippocampal hyperexcitability.

Furthermore, do sprouted mossy fibers possess functional properties, such as 1 Hz facilitation, that could exacerbate hyperexcitability further during increased firing? Because sprouted mossy fibers could not be stimulated selectively using prior methods, it is unknown whether these recurrent fibers possess functional properties that could drive seizure activity. Immature adult-born granule cells do have heightened plasticity (Gu et al., 2012), but it is unknown whether sprouted mossy fibers from adult-born cells acquire divergent functional properties that contribute to or mitigate hyperexcitability or epileptogenesis. Additionally, synaptic function can be controlled by neuromodulatory factors and influence expression of short (Moore et al., 2003) and long (Wagner et al., 1993; Weisskopf et al., 1993) term plasticity. Factors that control mf-CA3 function are altered in epilepsy (McGinty et al., 1983; Kanamatsu et al., 1986; Ekonomou et al., 2000; Boison, 2008, 2012; Sandau et al., 2016). How any of these factors modulate sprouted mossy fiber function is unknown, and sprouted mossy fiber function may be differentially expressed as

a consequence of altered neuromodulator presence or function. If any of these factors could be identified and manipulated experimentally, it could be used to test the role of sprouted mossy fibers in epileptogenesis and eventually lead to potential avenues to treatment.

Recent technological advances make addressing the specific function of sprouted fibers from adult-born cells possible

Recent developments in Cre-dependent transgenic labeling have opened an approach to isolate cohorts of dentate granule cells with optogenetic stimulation. For example, the popular *Nestin-CreER^{T2}* mouse lines pulse-labels stem cells in the subgranular layer of the dentate gyrus (Dubois et al., 2006), but lacks temporal specificity as labeled stem cells will go through multiple rounds of division. Thus, pulse labeling of a population of immature granule cells would be ideal and could create a more tightly controlled labeling window. Indeed, *DcxCreER^{T2}* mice label an immature population of dentate granule cells upon tamoxifen administration (Cheng et al., 2011). This has the advantage of both labeling terminally differentiated granule cells and having a window large enough to label the high number of cells needed for physiologic analysis.

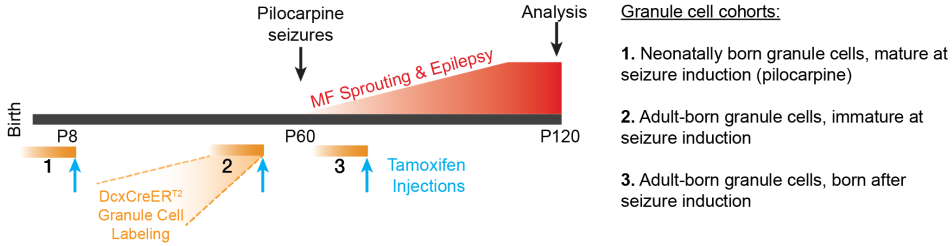

Figure 5: Experimental timeline and approach. Mice will be given pilocarpine to induce seizures at ~2 months old (P60). Following a brief latent period of no seizures, mice develop spontaneous recurrent seizures (epilepsy) and mossy fiber sprouting (mf sprouting). All analysis will be performed 2 months after pilocarpine (P120). Granule cells will be labeled using DcxCreER^{T2} mice, in which upon tamoxifen administration (blue arrows) labels immature granule cells born in the previous 2-3 weeks (yellow bars). Granule cell cohorts will consist of cells born neonatally (1), just prior to seizures (2), and immediately after seizures (3).

How would this approach vary from previous studies characterizing either the relationship between adult-neurogenesis and mossy fiber sprouting or the function of sprouted mossy fibers? There is substantial evidence to support sprouted mossy fibers arise from adult-born granule cells developing during or born into the epileptic brain (Parent et al., 1997; Jessberger et al., 2007; Kron et al., 2010; Althaus et al., 2016) and the function and presumed impact of recurrent circuitry in the epileptic dentate gyrus has been elegantly demonstrated (Tauck and Nadler, 1985; Wuarin and Dudek, 1996; Okazaki et al., 1999). Yet, an obvious and appealing question still remains: given the unique features and plasticity of adult-born granule cells, what are the functional properties of sprouted mossy fiber synapses, specifically from adult-born granule cells, and do they function in a way contributes to epileptogenesis or hippocampal hyperexcitability?

Unfortunately, technical limitations have been challenging to overcome. Even though newborn granule cells can be labeled with ChR2-YFP using retroviral injections (van Praag et al., 2002), the number of cells infected is extremely low and the temporal window of labeling is very tight (van Praag et al., 2002; Tashiro et al., 2006), both limiting the possibility of identifying post-synaptic cells to record from and require precisely timed injections into epileptic brains. By sacrificing the extreme temporal specificity of retrovirus, transgenic labeling approaches such as the *DcxCreER*^{T2} mouse (discussed above) that integrate labeling over longer periods (Cheng et al., 2011; Yang et al., 2015)

provide an opportunity to increase the number of adult-born cells labeled, critical for electrophysiologic analysis.

Summary of Work

In Chapter 1, I examine the relative contribution that various age-defined cohorts of granule cells make to mossy fiber sprouting. I demonstrate that adult-born granule cells, born either before or after seizures, sprout mossy fibers, consistent with some reports (Jessberger et al., 2007; Kron et al., 2010; Althaus et al., 2016), but not others (Parent et al., 1999). I also use the same transgenic labeling method to demonstrate that sprouted mossy fibers from adult-born granule cells born *before*, but not *after*, epilepsy induction form recurrent excitatory synapses with other dentate granule cells. Additionally, I characterize the basic functional properties of these synapses. Whereas mf-CA3 synapses are known to be “detonator synapses” with strong frequency facilitation, sprouted mossy fibers have strong frequency depression, a feature even more prominent in sprouted fibers from adult-born cells.

In Chapter 2, I examine further the functional changes in sprouted mossy fibers and identify one potential mechanism for the observed changes in the functional properties of sprouted mossy fibers. I show that sprouted mossy fibers have a high probability of release that contributes to bursts of EPSCs and post-synaptic cell firing. I find that unlike mf-CA3 synapses (Moore et al., 2003), there is a lack of tonic adenosine at sprouted mossy fiber synapses in the IML,

and the lack of this adenosine inhibition contributes to increased release probability and the recurrent network's ability to propagate excitability and bursts of EPSCs.

Chapter 1: Short-term Depression of Sprouted Mossy Fiber Synapses from Adult-born Granule Cells

William D. Hendricks[1,3], Yang Chen[2], AeSoon L. Bensen[2], Gary L. Westbrook[2], Eric Schnell[* 3,4]

[1]Graduate Program in Neuroscience; [2]Vollum Institute; Oregon Health and Science University, Portland, OR, 97239; USA; [3]Department of Anesthesiology and Perioperative Medicine; Oregon Health and Science University, Portland, OR, 97239; USA; [4]VA Portland Health Care System; Portland, OR, 97239; USA

Published in The Journal of Neuroscience, June 2017

(https://doi.org/10.1523/JNEUROSCI.0761-17.2017)

Abstract

Epileptic seizures potently modulate hippocampal adult neurogenesis, and adult-born dentate granule cells contribute to the pathologic retrograde sprouting of mossy fiber axons, both hallmarks of temporal lobe epilepsy. The characteristics of these sprouted synapses, however, have been largely unexplored, and the specific contribution of adult-born granule cells to functional mossy fiber sprouting is unknown, primarily due to technical barriers in isolating sprouted mossy fiber synapses for analysis. Here, we used DcxCreER^{T2} transgenic mice to permanently pulse-label age-defined cohorts of granule cells born either before or after pilocarpine-induced status epilepticus (SE). Using optogenetics, we demonstrate that adult-born granule cells born prior to SE form functional recurrent monosynaptic excitatory connections with other granule cells. Surprisingly, however, although healthy mossy fiber synapses in CA3 are well characterized "detonator" synapses that potently drive post-synaptic cell firing through their profound frequency-dependent facilitation, sprouted mossy fiber synapses from adult-born cells exhibited profound frequency-dependent depression, despite possessing some of the morphological hallmarks of mossy fiber terminals. Mature granule cells also contributed to functional mossy fiber sprouting, but exhibited less synaptic depression. Interestingly, granule cells born shortly after SE did not form functional excitatory synapses, despite robust sprouting. Our results suggest that although sprouted mossy fibers form recurrent excitatory circuits with some of the morphological characteristics of typical mossy fiber terminals, the

functional characteristics of sprouted synapses would limit the contribution of adult-born granule cells to hippocampal hyperexcitability in the epileptic hippocampus.

Significance Statement

In the hippocampal dentate gyrus, seizures drive retrograde sprouting of granule cell mossy fiber axons. We directly activated sprouted mossy fiber synapses from adult-born granule cells to study their synaptic properties. We reveal that sprouted synapses from adult-born granule cells have a diminished ability to sustain recurrent excitation in the epileptic hippocampus, questioning the role of sprouting and adult neurogenesis in sustaining seizure-like activity.

Introduction

Repeated seizures lead to epilepsy through the process of epileptogenesis, which likely results from alterations in neural circuits (Chang and Lowenstein 2003). However, it is unclear how network alterations in the brain contribute to circuit hyperexcitability. Temporal lobe epilepsy is associated with dramatic morphological changes to the hippocampus, including death of CA1 and CA3 pyramidal neurons (Babb et al., 1984a; DeGiorgio et al., 1992), loss of interneurons (Sloviter, 1987; Doherty and Dingledine, 2001), and the aberrant growth of dentate granule cell dendrites and axons (Nadler et al., 1980; Ribak et al., 2000).

The sprouting of mossy fiber axons away from their normal targets in the hilus and CA3 and into the inner molecular layer of the dentate gyrus has long been particularly intriguing. After sprouting, these axons contact the dendrites of other granule cells, forming a connection that is largely, if not entirely, absent in healthy animals (Tauck and Nadler, 1985; Sutula et al., 1988; Okazaki et al., 1995; Buckmaster et al., 2002). Mossy fibers in region CA3 produce large unitary excitatory post-synaptic currents (EPSCs) that profoundly facilitate glutamate release during repetitive activation and have been designated as "detonator synapses" due to their ability to potently drive postsynaptic cell spiking (Salin et al., 1996; Sachidhanandam et al., 2009; Vyleta et al., 2016). Thus, sprouted fibers with the same characteristics could conceivably form strong recurrent excitatory feedback loops and drive seizure generation.

Mossy fibers originate from mature dentate granule cells, but the hippocampal circuit is constantly refined by ongoing postnatal neurogenesis (van Praag et al., 2002). Interestingly, seizures increase the generation of new granule cells (Parent et al., 1997; Jessberger et al., 2005; Parent et al., 2006; Jessberger et al., 2007), which integrate into local circuitry (Bengzon et al., 1997; Parent et al., 1997; Overstreet-Wadiche et al., 2006; Parent et al., 2006; Jessberger et al., 2007; Kron et al., 2010), and contribute to mossy fiber sprouting (Jessberger et al., 2007; Kron et al., 2010; Althaus et al., 2016). The low connection probability between any one adult-born granule cell and its potential post-synaptic targets, as well as the challenges of definitively isolating fibers derived from adult-born granule cells, has limited direct assessment of

adult-born cells in epileptic brains. Thus, despite the evidence that adult-born granule cells contribute to mossy fiber sprouting, the functional properties of these sprouted synapses are still not known.

Here we isolated cohorts of age-defined granule cells using genetically modified mice to examine the contribution of adult-born granule cells to mossy fiber sprouting, and to determine the functional properties of sprouted mossy fiber synapses. Despite similar structural characteristics, sprouted mossy fiber synapses had distinct functional properties from mossy fiber-CA3 synapses, most notably a profound frequency-dependent synaptic depression, which was most prominent in synapses emanating from adult-born dentate granule cells. Additionally, granule cells born after seizures did not appear to make functional excitatory synapses with other granule cells, despite the morphological identification of boutons in the IML.

Materials and Methods

Animals

Homozygous Doublecortin-CreER^{T2} transgenic mice (line F18, generously supplied by Drs. Xuewen Cheng and Zhi-Qi Xiong; Cheng et al., 2010; RRID:MGI:5438982) were maintained on a C56Bl6/J background and crossed with either homozygous Gt(ROSA)26Sor$^{tm9(CAG-tdTomato)Hze}$ (Ai9; RRID:IMSR_JAX:007905) or Gt(ROSA)26Sor$^{tm32(CAG-COP4*H134R/EYFP)Hze}$ (Ai32; RRID:IMSR_JAX:012569) Cre-reporter lines for imaging and physiology experiments, respectively. Cre-mediated recombination was induced by

administration of tamoxifen. To label newborn granule cells in adult mice, tamoxifen (40 mg/kg in corn oil, i.p.) was administered twice daily for 5 days. Neonatally-born granule cells were labeled with 2 injections of tamoxifen (20 mg/kg in corn oil, i.p.) 12 hours apart on post-natal day 6. Veterinary care was provided by Oregon Health and Science University's Department of Comparative Medicine in an AAALAC-accredited vivarium, and all experiments and animal care were performed in accordance with state and federal guidelines and IACUC-approved protocols.

Seizure Induction

Two-month old male mice were pretreated with an intraperitoneal (i.p.) injection of 1 mg/kg scopolamine methyl bromide (Sigma) to block the peripheral cholinergic effects of pilocarpine. 20 minutes later, mice were treated with 325 mg/kg i.p. pilocarpine (Cayman Chemicals) to induce seizures. Animals were continuously monitored and seizures were graded on a modified Racine Scale (Shibley and Smith, 2002). Status epilepticus (SE) was defined by a state of continuous Grade 2 seizures following 3 or more Grade 3-5 seizures. Following 2 hours of continuous SE, animals were given 10 mg/kg diazepam (Sigma) to terminate seizures. Mice were given soft food and i.p. injections of 1 mL of 5% glucose in 0.45% normal saline every 12 hours until normal activity resumed. Mice that did not develop SE were humanely euthanized; non-injected littermates were used as controls. Although not quantified, mice treated with

pilocarpine were noted to have spontaneous seizures in the months following acute SE.

Immunofluorescence

4 month old mice were deeply anesthetized by inhalation of 4% isoflurane followed by injection of 1 mL of 1.2% avertin (Sigma), and transcardially perfused with 5 mL phosphate buffered saline (PBS) followed by 20 mL of 4% paraformaldehyde-PBS (PFA-PBS). Mice were then decapitated, and brains were removed and post-fixed overnight in 4% PFA-PBS. 50 µm coronal sections were cut using a Leica VT1000S microtome and stored in PBS. Sections were permeabilized and blocked with 0.4% triton-PBS (PBST) containing 10% normal goat serum (NGS) for 90 minutes at room temperature. For BrdU birth-dating experiments, slices were permeabilized by incubation in K^+-containing PBST (K-PBST) for 45 minutes, followed by 2N HCl K-PBST for 30 minutes at 37° C. Following 3 x 15 minute washes in PBST, slices were incubated in PBST with 1.5% NGS and varying combinations of: 1:500 guinea-pig anti-ZnT3 (Synaptic Systems Cat# 197 004, RRID:AB_2189667), 1:500 rabbit anti-DsRed (Clontech Laboratories, Inc. Cat# 632496, RRID:AB_10013483), 1:500 mouse anti-GAD67 (Millipore Cat# MAB5406, RRID:AB_2278725), rat anti-BrdU (Abcam Cat# AB6326, RRID:AB_305426), 1:400 guinea-pig anti-doublecortin (Millipore Cat# AB2253, RRID:AB_1586992), or 1:400 rabbit anti-GFP AlexaFluor 488 conjugate (Molecular Probes Cat# A-21311, RRID:AB_221477). Following overnight (18-24 hour) incubations at 4° C, slices were washed in PBST, and incubated with

secondary antibodies: goat anti-guinea-pig AlexaFluor 488, goat anti-rabbit AlexaFluor 568, goat anti-mouse AlexaFluor 647 (Life Sciences) at 1:500, overnight at 4° C. Slices were then briefly washed in standard PBS, post-fixed in 4% PFA for 20 minutes, counter-stained with 1:30,000 DAPI, and mounted onto slides with CMFR2 high-refractive index mounting media (Citifluor).

Standard confocal images were acquired from sections of the dorsal hippocampus of perfusion-fixed DcxCre::tdT mice using a Zeiss LSM 780 with a 40x/1.4NA oil objective; super-resolution images were performed on a Zeiss LSM 710 equipped with an AiryScan detector and 63x/1.NA oil objective. For bouton counting experiments, 20 μm vertical z-stacks were captured at a 1024 x 1024 pixel density with 0.38 μm step width. Linear adjustments (brightness, contrast, and intensity) were applied to the whole image in ImageJ/FIJI (NIH) to aid in counting, and kept constant across samples. For each animal, the central portion of the suprapyramidal blade of the dentate gyrus in 4 separate hippocampal sections was imaged to include both the full GCL and IML cross-section as well as portions of the MML and hilus. Only boutons that distinctly colocalized with ZnT3 on all three imaging planes were counted as mossy fiber boutons in the IML. tdTomato-positive cell bodies were counted if they were fully located within the GCL of these images, as delineated with DAPI. IML volume was calculated from three-dimensional renders and bouton volume measurements were conducted using the surface render and analysis suite in Imaris (Bitplane). Filopodia were manually identified from 3D renders as >1 μm protrusion from the main bouton not connected to longer axonal fibers. Bouton

measurements and tdT+ bouton density quantification was performed by an experimenter blind to experimental group assignment.

Slice Preparation and Physiological Recordings

4 month old DcxCre::ChR2 mice used for *ex vivo* electrophysiology experiments were deeply anesthetized with isoflurane and avertin as described above, and transcardially perfused with ice-cold choline- or N-methyl-D-glucamine (NMDG)-based solution, as during the course of this work we found better cell preservation in slices prepared from NMDG-perfused animals (Ting et al., 2014). We otherwise did not find any electrophysiologic differences that resulted from a change in perfusion solution. Choline-based solution contained (in mM):110 Choline Cl, 25 $NaHCO_3$, 10 Glucose, 7 $MgCl_2$, 3 Na-Pyruvate, 2.4 KCl, 1.3 Na-Ascorbate, 1.25 NaH_2PO_4*$2H_20$, and 0.5 $CaCl_2$. NMDG-based solution contained (in mM): 93 NMDG, 30 $NaHCO_3$, 24 Glucose, 20 HEPES, 5 Na-Ascorbate, 5 N-Acetyl Cysteine, 3 Na-Pyruvate, 2.5 KCl, 2 Thiourea, 1.2 NaH_2PO_4, 10 $MgSO_4$, and 0.5 $CaCl_2$. Mice were then rapidly decapitated the hippocampus was dissected, and 300 μm transverse hippocampal sections were prepared in ice-cold perfusion solution using a Leica VT1200S vibratome. For CA3 recordings, hippocampal dissection was omitted and brains were cut into 300 μm sagittal sections to preserve CA3 pyramidal cells and mossy fiber axons. After choline-based preparation, slices were allowed to recover in warm ACSF for 30 minutes followed by an additional 30 minutes at room temperature prior to recordings. After NMDG-based preparation, sections were allowed to

recover in warm NMDG-based cut solution for 15 minutes, followed by an additional 45-minute recovery in standard ACSF at room-temperature.

Electrophysiological recordings were made with 3-5 MΩ borosilicate glass pipettes filled with Cs^+-based internal solution: (in mM) 113 Cs-gluconate, 17.5 CsCl, 10 HEPES, 10 EGTA, 8 NaCl, 2 Mg-ATP, 0.3 Na-GTP, 0.05 AlexaFluor 568 (pH 7.3 adjusted with CsOH, osmolarity adjusted to 295 mOsm). For voltage clamp experiments, QX-314-Cl (5 mM; Tocris) was included in the internal solution to block unclamped action potentials. Pipettes were wrapped with parafilm to minimize pipette capacitance. Granule cells were identified and patched using live IR-DIC microscopy, after a lack of ChR2-YFP expression in a particular cell was confirmed using fluorescence microscopy. High resistance seals (>5 GΩ) were made and whole-cell recordings were obtained by applying brief suction. A hyperpolarizing (-10 mV) voltage step was applied prior to each sweep and used to monitor series resistance, input resistance, and cell capacitance. Series resistance was not compensated; cells with a >30% change in series resistance during experiments were excluded from analysis. All cells were filled with 50 μM AlexaFluor 568 to confirm granule cell identity and to verify the absence of hilar basal dendrites. For optogenetic stimulation, blue (1 ms, 470 nm, 8 mW/mm^2) light was delivered through a 40x WI objective at 20 sec intervals, powered by LED (ThorLabs), targeted at the inner molecular layer (for granule cell recordings) or stratum lucidum (for CA3 recordings). All experiments were performed in the presence of the $GABA_A$-receptor blocker SR95531 (10 μM; Ascent) to isolate excitatory currents and to avoid possible

contamination of responses by feed-forward inhibition or any off-target labeling of interneurons. Stimulation frequency was adjusted for frequency facilitation and paired pulse facilitation experiments as stated in the text. For some CA3 recordings, electrical stimulation of mossy fiber axons in CA3 was accomplished using a constant voltage stimulator (Digitimer, Inc.) and a bipolar electrode (FHC Inc.) placed in stratum lucidum. Signals were amplified with an AxoClamp 200B (Axon Instruments) amplifier, low-pass bessel filtered at 5 kHz, sampled at 10 kHz, and digitized with a National Instruments A/D board. Data were captured with a custom script in Igor Pro 6 (Wavemetrics) for online and offline analysis and further statistical analysis. For presentation, offline filtering was accomplished with a 2 kHz Gaussian filter. Cells were voltage clamped to -70mV for AMPAR-mediated response analysis, and to +40mV to unmask NMDAR-mediated responses. AMPAR:NMDAR ratios were determined by measuring the peak current in voltage clamp at -70 mV for the AMPAR-component and the remaining current at 60 ms post-stimulus at +40 mV for the NMDAR-component. Evoked responses were included if maximal current amplitude was >5 pA within 20 ms of stimulus. Drugs were included in the ACSF when indicated: NBQX (Ascent), 10 μM; SR95531 (Ascent), 10 μM; DCG-IV (Tocris), 1 μM. The liquid junction potential was 8 mV and was uncorrected.

Experimental Design and Statistical Analysis

Statistical analysis was performed in Igor Pro 6 (Wavemetrics) and data are presented as mean ± SEM unless otherwise noted. T-tests were performed

on continuous data containing 2 independent data sets. Experiments with 3 or more data sets were compared with 1-way ANOVA with *post-hoc* Dunnett's test when compared to a control (Figure 2), or Tukey's Test between groups (Figure 8). Fischer's Exact test was used to compare categorical data. Unless otherwise noted, data followed a binomial distribution and parametric tests were performed. For all experiments, significance was determined at $p < 0.05$.

Results

Faithful pulse labeling of temporally distinct dentate granule cell cohorts

To analyze the structure and synaptic function of sprouted mossy fibers from neonatally-derived and adult-born dentate granule cells, we used transgenic Dcx-CreER^{T2} mice (Cheng et al., 2011) to pulse label discrete, temporally defined cohorts of immature granule cells. Crossed DcxCreER^{T2}::Gt(ROSA)26Sor$^{tm9(CAG\text{-}tdTomato)Hze}$ (Ai9) mice (henceforth referred to as DcxCre::tdT mice) were given intraperitoneal (i.p.) injections of tamoxifen (TAM) to initiate Cre-dependent tdTomato expression in immature granule cells. These cells continue to express tdTomato after their maturation (Figure 1A-E). BrdU co-labeling (Figure 1B), demonstrated that labeled cells were born during a two-week window prior to TAM administration, consistent with the normal expression pattern of *doublecortin*, which is high for the first 2-3 weeks after granule cell mitosis (Brown et al., 2003). Labeling efficiency of granule cells born during this two-week window was approximately 40%, with negligible labeling of cells born even one week earlier or later (data not shown). Similar results

were obtained with DcxCreER^{T2}::Gt(ROSA) 26Sor$^{tm32(CAG-COP4*H134R/EYFP)Hze}$ (Ai32) mice (Figure 1F; henceforth referred to as DcxCre::ChR2).

Importantly, cell labeling in DcxCreER^{T2} mice occurs after neuronal differentiation, such that following removal of TAM, pulse-labeled cells continue to express reporter proteins while subsequently born dentate granule cells are not labeled. Adult-born cells were never labeled in animals that had received neonatal TAM, as assessed by Dcx co-staining (data not shown) or with BrdU injections in adults (0.0% of adult-born BrdU+ cells labeled with ChR2-YFP in DcxCre::ChR2 mice, n = 0/137 cells, 3 mice; see also (Villasana et al., 2015)). Although all granule cell labeling was restricted to temporally-isolated cohorts, in some animals we observed labeling of a few GAD+ interneurons in the hilus, CA1, and CA3, as determined by GAD co-staining, cell location, and morphology, in both epileptic and control mice, as previously observed (Cheng et al., 2011; also see Stratum radiatum of region CA3 in Figure 1C and D).

To examine mossy fiber synaptic function, we used optogenetics to activate pulse-labeled granule cell cohorts in DcxCre::ChR2 mice (Figure 1G-J). Short (1 ms) pulses of 470 nm blue light (8 mW/cm^2) reliably produced photocurrents (Figure 1G) and action potential firing (Figure 1I) in ChR2-expressing granule cells. ChR2+ granule cells demonstrated robust spike fidelity during 1 Hz LED illumination (fidelity during a 50-pulse train: 96.1 ± 1.2%, n = 8 cells), but spike failures became evident during longer duration trains at higher frequencies (>15 pulses at 20 Hz, data not shown). Photostimulation of CA3 stratum lucidum in hippocampal slices from labeled DcxCre::ChR2 animals

evoked mossy fiber EPSCs in CA3 pyramidal cells, which were blocked by the Group II mGluR agonist DCG-IV, as is typical for electrically evoked mossy fiber EPSCs (Figure 1I-J).

Adult-born granule cells sprout mossy fiber boutons after pilocarpine-induced seizures

Retroviral labeling techniques have demonstrated that adult-born granule cells contribute to mossy fiber sprouting after seizures (Jessberger et al., 2007; Kron et al., 2010; Althaus et al., 2016); however, their functionality remains unclear (Walter et al., 2007; Althaus et al., 2016). To determine how immature adult-born granule cells respond to pilocarpine-induced status epilepticus (SE) evoked at P60, we administered TAM to DcxCre::tdT mice one week prior to SE so that the labeled cohort of adult-born granule cells was 1-3 weeks post-mitosis during SE. Mice were examined 2 months later, when mossy fiber sprouting becomes well established with this model (Figure 2A; (Cavalheiro et al., 1996). To identify sprouted mossy fiber boutons in the inner molecular layer (IML) of the dentate, we stained tissue with antibodies against Zinc Transporter 3 (ZnT3), a vesicular transporter protein highly enriched in mossy fiber terminals.

Despite sparse tdT+ granule cells in adult-labeled mice, there were abundant tdT+/ZnT3+ boutons in the IML of DcxCre::tdT mice after SE (Figure 2B), indicating that granule cells born just before SE robustly contributed to mossy fiber sprouting, consistent with prior reports (Jessberger et al., 2007; Kron et al., 2010; Althaus et al., 2016). As expected, healthy control animals had

abundant tdT+/ZnT3+ boutons in the hilus and CA3, but had no mossy fiber sprouting, evidenced by the lack of ZnT3 staining or tdT+ boutons in the IML (Figure 2A, top, and Figure 1B, bottom). Super-resolution confocal images of adult-born mossy fiber boutons (Figure 2C) were rendered and measured in 3 dimensions (Figure 2D), revealing that seizures altered mossy fiber bouton morphology. Mossy fiber boutons in region CA3 had larger volumes in epileptic mice (Figure 2E) than CA3 mossy fiber boutons in control (healthy) mice after SE, whereas their sprouted counterparts in the IML were decreased in size (Figure 2E). The surface area of sprouted boutons was also reduced (Figure 2F). Mossy fiber terminals in healthy CA3 form filopodial extensions that directly contact interneurons (Acsady et al., 1998). Interestingly, sprouted mossy fiber boutons from adult-born granule cells had fewer filopodial extensions than their CA3 counterparts (Figure 2G), suggesting that sprouted mossy fiber boutons may predominantly contact excitatory cells, as has previously been described using electron microscopy (Buckmaster et al., 2002).

Adult-born granule cells drive recurrent excitation via sprouted mossy fibers after SE

Sprouted mossy fibers are interspersed amongst other inputs to granule cells and cannot be electrically stimulated as a distinct population, which has limited their functional assessment. By selectively labeling granule cells in DcxCre::ChR2 mice, we were able to optogenetically isolate sprouted mossy

fiber inputs and thus directly analyze the function of sprouted synapses originating from adult-born granule cells.

In whole-cell voltage clamp recordings from post-SE mouse brain slices (Figure 3A), optogenetic stimulation of adult born granule cells often evoked EPSCs in ChR2-YFP negative dentate granule cells (n = 15 of 28 cells), whereas these responses were rarely observed in slices from healthy control animals (n = 2 of 15 cells; Figure 3B,C). These data are consistent with the formation of functional recurrent synapses in epileptic mice (Tauck and Nadler, 1985) and minimal granule cell-granule cell connectivity in the dentate gyrus of healthy animals (Ribak and Shapiro, 2007). To determine whether these EPSCs truly reflected the formation of monosynaptic granule cell-granule cell contacts, we blocked polysynaptic activity with NBQX and optogenetically evoked NMDA receptor (NMDAR)-mediated EPSCs at a holding potential of +40 mV. In epileptic mice, monosynaptic NMDAR-mediated EPSCs were present in one-third of granule cells tested (n = 5 of 15; Figure 3D), whereas these responses were not observed in control animals (n = 0 of 15 cells). Sprouted mossy fiber responses were strongly inhibited by DCG-IV, similar to LED-evoked mossy fiber-CA3 (mf-CA3) responses in control animals (Figure 3E).

Monosynaptic, granule cell-granule cell EPSCs could either originate from aberrantly sprouted mossy fiber synapses in the IML or alternatively from mossy fiber synapses acquired by newly-formed hilar basal dendrites (Ribak et al., 2000). To differentiate between these possibilities, granule cells were routinely filled with Alexa Fluor 568 dye during recording, fixed, and imaged. In all cells

imaged, all dendrites projected into the molecular layer, with no branches detected in the hilus (0%, n = 15), unequivocally demonstrating that these *de novo* monosynaptic EPSCs arose from retrogradely sprouted mossy fibers forming synapses onto granule cell apical dendrites.

Functional properties of the sprouted mossy fiber synapse

Understanding the functional properties of sprouted mossy fiber synapses is critical to determining their contribution to hyperexcitable circuit formation in epilepsy. Although sprouted mossy fiber boutons are smaller than their counterparts in CA3 (Figure 2), they are still much larger than typical CNS synapses and thus might be expected to retain many of the properties of healthy mossy fiber synapses in CA3. For example, mossy fiber synapses in CA3 have a low complement of post-synaptic NMDARs (Weisskopf and Nicoll, 1995). Surprisingly, however, sprouted mossy fiber responses had substantially greater complement of NMDARs than mf-CA3 synapses in age-matched healthy animals (AMPA:NMDA ratio: healthy mf-CA3, 2.87 ± 0.43, n = 6; sprouted mf, 1.06 ± 0.21 n = 7; Unpaired t-test, p = 0.006; Figure 3F). The finding that these new synapses contain many NMDARs is consistent with the well-characterized increase in hippocampal hyperexcitabtility due to NMDAR activation in epileptic tissue (Sutula et al., 1996; Lynch et al., 2000).

One of the most striking functional characteristics of mf-CA3 synapses is a profound frequency-dependent presynaptic facilitation of glutamate release (Salin et al., 1996). This phenomenon occurs with increased mossy fiber firing

frequency, and therefore if sprouted mossy fibers possessed a similar form of short-term plasticity, they could strongly contribute to recurrent excitatory network activation. Surprisingly, however, sprouted mossy fiber synapses did not exhibit frequency-dependent facilitation during higher frequency (1 Hz) stimulation, but instead displayed frequency-dependent synaptic depression (Figure 4A and 4B).

This frequency-dependent synaptic depression could be due to altered release probability (P_r) at the sprouted mossy fiber synapse. Consistent with this possibility, sprouted mossy fiber synapses had a decreased paired-pulse ratio (PPR) compared to mf-CA3 connections (Figure 4C and 4D), suggesting an increased initial P_r, in stark contrast with the well-characterized low P_r of mf-CA3 synapses (Bischofberger et al., 2006). Together, these data indicate that sprouted mossy fiber synapses have distinctly different release properties from healthy mf-CA3 synapses.

Sprouted mossy fibers from mature cells form functional monosynaptic connections with granule cells

Despite post-natal neurogenesis in the dentate gyrus, the majority of granule cells are born neonatally (Kuhn et al., 1996). Studies examining whether these mature cells contributed to mossy fiber sprouting have yielded conflicting results (Kron et al., 2010; Althaus et al., 2016), raising the question of whether this population of cells contributes to recurrent excitatory circuit formation.

Thus, we sought to determine whether cells born during neonatal development, contributed to functional mossy fiber sprouting.

To identify sprouted mossy fiber boutons from neonatally-born granule cells, we labeled these cells by administering TAM to DcxCre::tdT mice at P6, so the labeled cells would be fully mature at the onset of SE (P60). TAM injections at P6 labeled on average 346,200 ± 70,300 granule cells/mm^3, (n = 4 mice; Figure 1C), comparatively greater than the labeling in adult mice (19,600 ± 3,400 granule cells/mm^3, n = 4 mice; Figure 1D), consistent with the known age-related decline in neurogenesis (Kuhn et al., 1996). First, we stained tissue from DcxCre::tdT mice with anti-ZnT3 antibodies two months after pilocarpine-induced SE, to assess whether any of the neonatally-born cells contributed to mossy fiber sprouting. As shown in Figure 5A, we found a substantial number of tdT+/ZnT3+ sprouted mossy fiber boutons in the IML, indicating that neonatally born granule cells contributed to mossy fiber sprouting.

In whole cell voltage clamp recordings from unlabeled granule cells in slices from neonatally-labeled DcxCre::ChR2 mice, 76% of dentate granule cells had optogenetically-evoked AMPAR-mediated EPSCs (average EPSC, cells with response: -81.6 ± 13.3 pA, n = 13 of 17 cells; Figure 5B-D). In the presence of NBQX to block polysynaptic activity, we again confirmed that sprouted mossy fiber EPSCs arose from monosynaptic granule cell – granule cell synapses (Figure 5E and 5F). These EPSCs were blocked by DCG-IV (Figure 5B and 5E), and no hilar basal dendrites were observed in granule cells filled with Alexa Fluor 568 dye (n = 0 of 13 cells), together confirming that the optogenetically-evoked

EPSCs derived from sprouted mossy fiber synapses. Sprouted mossy fiber synapses from these cells also had significantly increased NMDAR-mediated transmission (Figure 5G), paired pulse depression (Figure 5H), and frequency-dependent synaptic depression at 1 Hz (Fig 5I) when compared with mossy fiber responses in recorded in region CA3 from healthy (control) mouse slices. Together, our data definitively demonstrate that neonatally-born granule cells sprout mossy fiber axons into the IML after seizures, and that these fibers form functional recurrent excitatory synapses.

Adult-born sprouted mossy fibers have diminished ability to sustain recurrent excitation

Sprouted mossy fiber synapses from both mature and adult-born granule cells shared many of the same functional properties, including similar AMPAR:NMDAR ratios (Mature, 1.38 ± 0.35, n = 7; Adult-born, 1.05 ± 0.20, n = 8; Unpaired t-test, p = 0.443), block by the Group II mGluR agonist DCG-IV (Figure 6A), and paired-pulse depression (Figure 6B). Notably, although both adult-born and neonatally-born granule cells exhibited frequency-dependent depression of sprouted mossy fiber synaptic responses (Figure 6C), this was much more pronounced at synapses formed by adult-born granule cells (Figure 6D), despite similar presynaptic release probabilities (Figure 6B) and EPSC kinetics (single exponential decay: Mature, τ = 10.4 ± 0.9 ms, n = 8; Adult-born, 12.3 ± 1.6 ms, n = 7, p = 0.32). The enhanced synaptic depression of adult-born cells occurred at the onset of higher frequency stimulation (1 Hz) and was

sustained throughout the 50 pulse train (Figure 6D). Thus, recurrent excitatory synapses from adult-born granule cells were less able to sustain repetitive activation than their neonatally-derived counterparts.

No functional sprouted synapses from granule cells born after SE

Hippocampal neurogenesis is increased by seizures, and granule cells born after SE contribute to mossy fiber sprouting, albeit with some delay (Kron et al., 2010; Althaus et al., 2016). We examined whether synapses from cells born after SE shared similar functional properties with other sprouted mossy fiber synapses. We pulse-labeled granule cells born after pilocarpine-induced SE in DcxCre mice, by administering TAM 2 weeks after SE. Despite the presence of tdT-labeled sprouted mossy fiber synapses from this cohort of cells in DcxCre::tdT mice (Figure 7A), we were not able to optogenetically evoke any sprouted mossy fiber EPSCs when we examined acute slices from this same cell cohort in DcxCre::ChR2 mice (response frequency: post-SE, 0%, n = 0 of 18 cells; pre-SE, 54%, 15 of 28 cells; pre-SE vs. post-SE $p < 0.0001$, Fisher's Exact Test; Figure 7B and 7C).

Because the circuit impact of sprouted mossy fibers depends on when the respective granule cells from which they derived were born (Figures 6 and 7), we attempted to roughly determine the relative contribution of the different granule cell cohorts (neonatally born, adult-born prior to SE, adult-born after SE) to mossy fiber sprouting. Using confocal microscopy to examine thin optical sections (0.38 μm) of tissue from DcxCre::tdT mice, we found comparable

densities of tdT+ sprouted mossy fiber boutons in slices labeled at the corresponding timepoints for each cohort of granule cells (Figure 8A-D) despite marked differences in the number of labeled cells across cohorts (Figure 1C-D). We calculated a "sprouting ratio" for each animal, defined as the ratio of tdT+/ZnT3+ mossy fiber bouton density in the IML to the density of tdT+ labeled granule cells in the granule cell layer, to represent the relative likelihood that a cell from a given cohort formed sprouted boutons. The sprouting ratio of either cohort of adult-born granule cells was significantly higher than that of neonatally-born granule cells (Figure 8E), suggesting these cells may be the most likely to sprout.

Discussion

Here, we demonstrate that both neonatally-born and adult-born granule cells generate sprouted mossy fibers and form functional monosynaptic excitatory granule cell-granule cell connections. Sprouted synapses had strikingly different functional properties than mf-CA3 synapses in healthy brains, despite retaining similar morphological characteristics. Adult-born granule cells generated just before SE were most susceptible to developing sprouted fibers, and had more pronounced functional changes than sprouted synapses formed by granule cells generated neonatally.

Divergence of function in sprouted mossy fiber boutons

Mossy fiber-CA3 synapses in healthy tissue form potent synapses onto proximal CA3 dendrites, and tend to dramatically facilitate in response to repetitive stimulation (Salin et al., 1996), leading to their designation as "detonator" synapses that can drive CA3 cell spiking in response to activity at a single synapse (Henze et al., 2002; Sachidhanandam et al., 2009; Vyleta et al., 2016). Thus, recurrent mossy fiber synapses with these properties could easily drive synchronized granule cell discharges through recurrent circuits, and upon repetitive activation, lead to ever-increasing positive feedback. Our data, however, suggest that sprouted mossy fiber synapses rapidly fatigue during repetitive activation, as evidenced by their paired-pulse depression and 1 Hz frequency-dependent depression, which would be expected to dampen the ability of these synapses to drive multiple rounds of recurrent excitation. However, sprouted mossy fiber synapses might still be able to potently drive granule cell spiking due to the epilepsy-induced increase in post-synaptic kainate receptor expression in granule cells (Epsztein et al., 2005; Artinian et al., 2011). Slower kinetics of kainate receptor-mediated EPSPs could enhance temporal summation and contribute to granule cell firing (Sachidhanandam et al., 2009), which might explain the demonstrated involvement of kainate receptors and sprouted mossy fibers in driving epileptiform activity and spontaneous seizures (Peret et al., 2014; Kourdougli et al., 2017).

The epileptic environment of the hippocampus may also play a role in determining presynaptic mossy fiber function. In our model, we could not directly compare mossy fiber physiology at sprouted synapses with that at

mossy fiber-CA3 synapses in epileptic animals, due to a paucity of surviving CA3 cells in our model (Nadler et al., 1980; Mello et al., 1993). Sprouted mossy fiber boutons are somewhat smaller than CA3-targeted boutons in both epileptic and healthy animals (Figure 2; also seeFrotscher and Zimmer, 1983; Represa et al., 1993; Danzer et al., 2009), consistent with the concept that post-synaptic specification may play some role in determining pre-synaptic functional parameters (Toth et al., 2000), which may partially account for our observed functional divergence. However, using a different model of temporal lobe epilepsy (intraperitoneal kainic acid injections) and field EPSP recordings, Goussakov et al. (2000) observed a loss of both paired pulse facilitation and high-frequency dependent facilitation at mossy fiber-CA3 synapses in epileptic rats compared to mossy fiber-CA3 synapses in healthy animals. Given the similarities between our results and those found by Goussakov et al. (2000), the increased P_r that we observed at sprouted mossy fiber synapses might be a general property of all mossy fiber synapses in an epileptic environment. The mechanisms underlying altered P_r likely involve complex interactions between expression and phosphorylation of pre-synaptic proteins, neuromodulatory factors, and the potentiation state of synapses, all of which could broadly alter synaptic function in the epileptic brain.

Consequences of sprouted mossy fiber activity on hippocampal hyperexcitability

The intermingling of sprouted mossy fibers with other granule cell inputs has impeded our understanding of their impact on neural network dynamics in epileptic brains, and functional evidence that sprouted mossy fibers form recurrent excitatory synapses has long relied upon indirect, albeit elegantly designed, experiments. The presence/absence of mossy fiber sprouting has been correlated with abnormal responses of granule cells to antidromic hilar/CA3 stimulation (Tauck and Nadler, 1985; Wuarin and Dudek, 1996; Okazaki et al., 1999), suprathreshold perforant pulse stimulation (Cronin et al., 1992; Golarai and Sutula, 1996; Masukawa et al., 1996; Patrylo et al., 1999), focal glutamate application (Wuarin and Dudek, 1996; Lynch et al., 2000), or glutamate uncaging in the granule cell layer (Molnar and Nadler, 1999; Wuarin and Dudek, 2001). Using paired recordings of granule cells, Scharfman et al. (2003b) observed putative monosynaptic granule cell – granule cell connectivity in epileptic rats with seizure-induced mossy fiber sprouting. However, disynaptic pathways remained intact, and although response latencies were appropriately short (4 ms), there remained the possibility that some evoked EPSPs were polysynaptic. Regardless, the low connection probability between any two granule cells (6 connected in 902 pairs) and inability to perform voltage clamp recordings in these experiments precluded functional characterization of these synapses.

By pulse-labeling and optogenetically stimulating granule cell cohorts, we bulk-activated sprouted synapses, dramatically improving our ability to directly study the connections formed by these fibers. This selective stimulation of

sprouted mossy fiber synapses eliminates the need to use paired recordings selectively stimulate pre-synaptic granule cells, and as such, allowed us to characterize sprouted mossy fiber function in a direct manner to more precisely determine its impacts on the hippocampal circuit.

Despite the potential for recurrent mossy fiber synapses to drive seizure activity, questions have been raised regarding the involvement of sprouted mossy fibers in the occurrence of spontaneous seizures in epilepsy (Buckmaster, 2014). In some studies, suppression of mossy fiber sprouting with rapamycin reduced seizure frequency (Zeng et al., 2009; Huang et al., 2010). However, rapamycin has multiple other effects (Wong, 2013) and does not reduce seizure frequency when sprouting is diminished but remains present at a lower level (Buckmaster and Lew, 2011; Heng et al., 2013). Additionally, both the nature of the synaptic connection (excitatory vs. inhibitory; (Gutiérrez, 2000), as well as the targets of the sprouted mossy fibers (Sloviter et al., 2006a) have been questioned. Although our results demonstrate that mossy fibers form recurrent excitatory connections with other granule cells, the propagation of this activity out of the dentate gyrus might only occur in association with additional pathology such as the loss of various interneuron populations (Sloviter, 1987; Doherty and Dingledine, 2001), and sprouting into CA2 (Althaus et al., 2016; Haussler et al., 2016), any of which could be critical for the occurrence of spontaneous generalized seizures.

Significance of adult-born granule cells in the epileptic hippocampus

Consistent with prior work (Jessberger et al., 2007; Kron et al., 2010; Althaus et al., 2016), our results demonstrate that adult-born granule cells robustly contribute to mossy fiber sprouting, and form functional recurrent synapses (Figure 2 and 8). However, neonatally-born neurons also contributed substantially to sprouting, consistent with some reports (Parent et al., 1999; Althaus et al., 2016) but not others (Kron et al., 2010). These discrepancies could have resulted from the possibility that only a small proportion of neonatally-born cells sprout, or from differences in the detection of sprouted mossy fibers between various labeling techniques (Althaus et al., 2016). The ability of all cohorts of granule cells to form sprouted mossy fibers may explain why potent suppression of neurogenesis (Parent et al., 1999; Cho et al., 2015; Hosford et al., 2016) failed to block mossy fiber sprouting, and why inhibition of neurogenesis at earlier time points was only partially successful (Kron et al., 2010).

Considering the increase in neurogenesis after seizures (Parent et al., 1997; Jessberger et al., 2005; Parent et al., 2006; Jessberger et al., 2007), it seems likely that ongoing generation of adult-born granule cells leads to a continual accumulation of sprouted mossy fibers, which is further worsened by the recurrence of seizures in epileptic animals. However, although adult neurogenesis may continue to drive the accumulation of sprouted mossy fiber synapses over time, the enhanced frequency-dependent depression of these adult-born synapses may mitigate their contribution to hyperexcitability. Interestingly, disruption of adult neurogenesis reduced seizure frequency while

simultaneously increasing seizure duration (Hosford et al., 2016), further indicating that the role of adult-born granule cells in epileptogenesis is likely dualistic.

A surprising result was our inability to observe functional sprouted mossy fiber responses from granule cells born after SE (Figure 7), despite the presence of robust morphologic mossy fiber sprouting by these cells. This observation could be related to the previously described delay in the formation of anatomically detectable sprouted mossy fiber synapses by this population of cells (Kron et al., 2010), which could then lead to a delay in their functional activation. Although adult-born cells form functional output synapses as early as two weeks post-mitosis in healthy brains (Gu et al., 2012), fibers from cells born after SE likely arrive in the IML later than those from previously existing granule cells, further delaying their maturation. However, if these synapses remain unable to drive recurrent excitation, and sprouted boutons from adult-born neurons continue to accumulate over time, the majority of the recurrent synapses in the IML would be the least capable of sustaining repeated activation or could even remain functionally silent.

Acknowledgments:

This work was funded by the Department of Veterans Affairs, Veterans Health Administration, Office of Research and Development, Biomedical Laboratory Research and Development CDA-2 award 005-10S (ES), Department of Veterans Affairs Merit Review Award I01-BX002949 (ES), NIH F31-NS098597

(WDH), NIH RO1-NS080979 (GLW), Ellison Medical Foundation (GLW), NIH P30-NS061800 (OHSU Imaging Center; PI Aicher) awards. We would like to thank Drs. Zhi-Qi Xiong and Xuewen Cheng (Shanghai Institute for Neuroscience) for graciously providing the DcxCreER^{T2} mouse line, and members of the Schnell and Westbrook Labs for critical feedback and discussion on the manuscript.

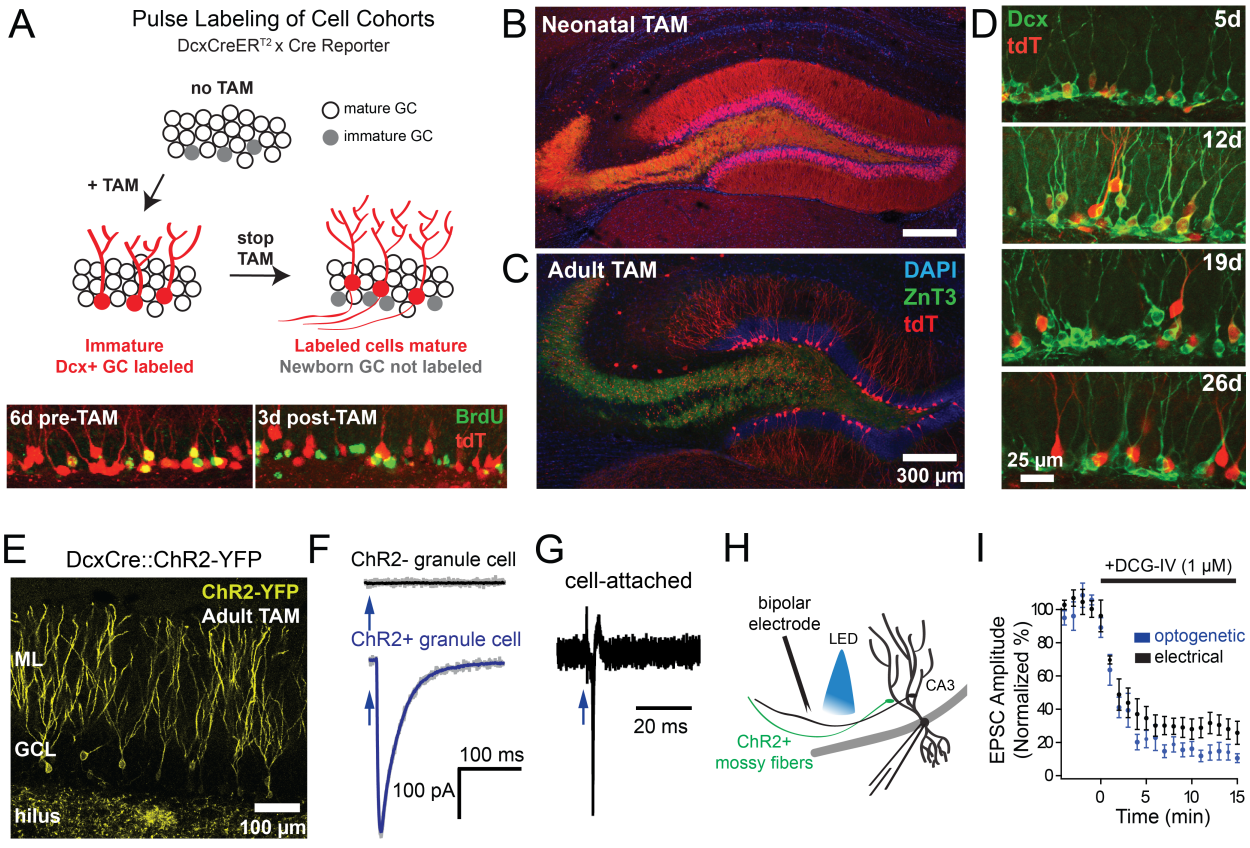

Figure 1. Transgenic pulse labeling of granule cell cohorts.

(A) Approach used to pulse-label temporally-defined cohorts of dentate granule cells in DcxCreER^{T2} transgenic mice. In the absence of tamoxifen (TAM), reporter genes are not expressed. Tamoxifen administration causes genetic recombination and marker gene expression (red) in immature neurons (gray), which persists after these cells mature. Cells born after TAM are not labeled. (B) BrdU/tdTomato (tdT) co-labeling in DcxCre::tdT mice. Mice were given BrdU injections to label mitotic cells at different time points relative to tamoxifen injections. Cells born prior to TAM (BrdU 6 days pre-TAM) co-label with tdT. Cells born after TAM (BrdU 3 days post-TAM) are not co-labeled.

(C) Neonatal (P6) TAM administration broadly labels mature dentate granule cells and mossy fiber axons in the adult (P120) DcxCre::tdTomato mouse (tdT; red). Mossy fiber terminals are labeled with ZnT3 (green) and nuclei with DAPI (blue).
(D) Adult-born granule cells are permanently labeled when TAM is administered to adult DcxCre::tdT mice. Image is from a mouse that received TAM at 2 months of age, and was imaged at 4 months of age.
(E) TAM was administered to adult DcxCre::tdT mice, and brains were fixed and stained at varying time intervals thereafter. At early time points (5-12 days post-TAM), tdTomato-marked cells (tdT; red) are immature, and co-label with the immature neuronal marker Doublecortin (Dcx; green). By 26 days post-TAM, co-staining of tdT+ cells with the immature marker Dcx completely disappears, and tdT+ cells assume a mature morphology, indicating that pulse-labeled cells have matured and that no younger cells were labeled.
(F) DcxCre::ChR2 mice express ChR2-YFP in dentate granule cell dendrites, somata, and mossy fiber axons following TAM administration. 20x confocal stack image of endogenous ChR2-YFP signal in the dentate granule cell layer from a 4 month-old animal given TAM at 2 months. ML: molecular layers, GCL: granule cell layer.
(G) LED stimulation (blue arrows; 1 ms, 8 mW/cm^2) reliably evokes photocurrents in ChR+ granule cells (bottom; blue), but not adjacent ChR- granule cells (top; black) in healthy mice during whole-cell voltage clamp recordings. Average traces are overlaid onto 10 individual sweeps (gray).

(H) Reliable spiking of granule cells after LED stimulation (blue arrows) is observed in cell-attached mode. 10 consecutive sweeps are overlaid.
(I) Experimental design for alternating optogenetic and electrical stimulation of mf-CA3 pyramidal cell synapses in DcxCre::ChR2 mice. Whole cell recordings were obtained from CA3 pyramidal cells in 4-month-old mice, while stimulating mossy fibers electrically or optogenetically in statum lucidum. TAM was given neonatally to label mossy fiber axons.
(J) Time course of EPSC inhibition by bath application of DCG-IV. Mossy fiber EPSCs elicited by LED or bipolar electrode stimulation in stratum lucidum follow similar timecourse of blockade upon wash-in of 1 μM DCG-IV (%EPSC amplitude of baseline following 15-minute drug wash-in, electrical stimulation: 26.0 ± 5.2%, n = 6; optogenetic stimulation: 14.1 ± 4.6%, n = 7, p = 0.3, unpaired t-test). Data represented as average ± SEM.

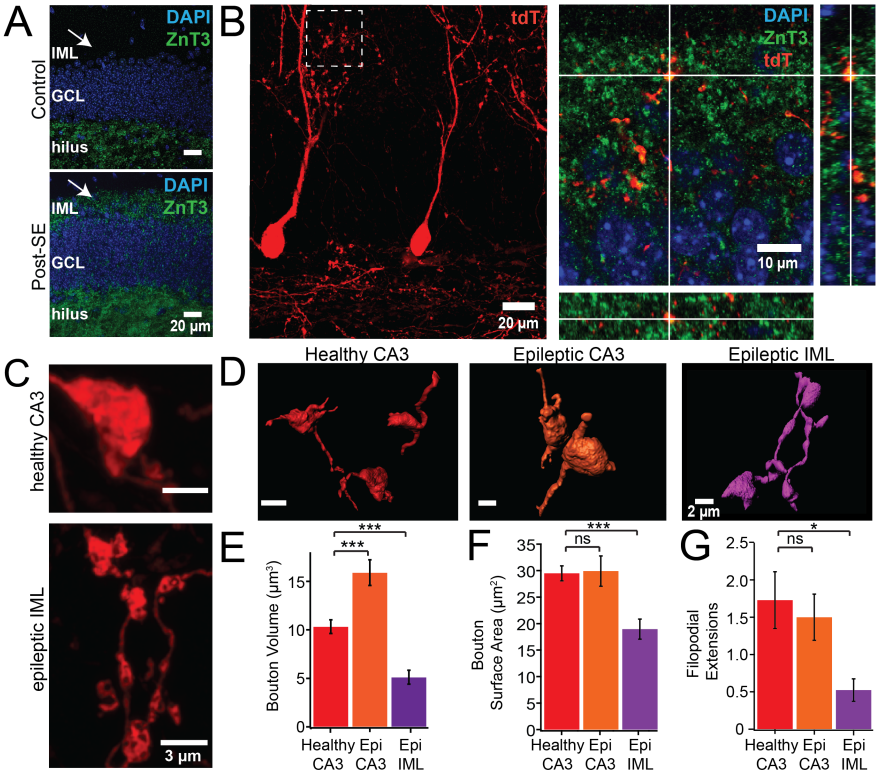

Figure 2. Adult-born granule cells sprout mossy fiber boutons following pilocarpine-induced SE.

(A) Mice treated with pilocarpine to induce status epilepticus (SE; bottom), but not control mice (top), have dense mossy fiber sprouting in the inner molecular layer (IML; arrow) of the dentate gyrus, as measured by ZnT3 immunoreactivity (green). Granule cell nuclei are marked with DAPI (blue).

(B) Representative confocal images from tdT-labeled adult-born granule cells (red) in DcxCre::tdT mice given tamoxifen (TAM) 1 week prior to SE demonstrate robust mossy fiber sprouting from these cells. Dashed box indicates corresponding locations from compressed stack image (left) represented in orthogonal single plane projection (right). Mossy fiber terminals are labeled with ZnT3 (green) and nuclei with DAPI (blue).

(C) Super-resolution images of tdT+ boutons from adult-born cells in healthy CA3 (top) and in epileptic mouse IML (bottom).

(D) Three-dimensional rendering of mossy fiber boutons.

(E) Measurements of mossy fiber bouton volume determined from 3-dimensional rendering. Mossy fiber bouton volume is greater in boutons from CA3 in epileptic animals, but sprouted mossy fiber boutons in the IML have decreased volume (control CA3 vs. epileptic CA3, $p = 0.0006$; control CA3 vs. epileptic IML, $p < 0.0001$; $n = 21, 27, 36$ for healthy CA3, epileptic CA3, and epileptic IML respectively; ANOVA with Dunnett's test).

(F) Mossy fiber boutons in epileptic IML have decreased surface area (control CA3 vs. epileptic CA3, $p = 0.99$; control CA3 vs. epileptic IML, $p = 0.0007$; ANOVA with Dunnett's test).

(G) The average number of filopodia emanating from sprouted mossy fiber boutons is significantly lower than the number of filopodia from boutons in healthy mice (healthy CA3 vs. epileptic IML, $p = 0.015$, ANOVA with Dunnett's test). All data represented as average ± SEM. * $p < 0.05$, *** $p < 0.001$

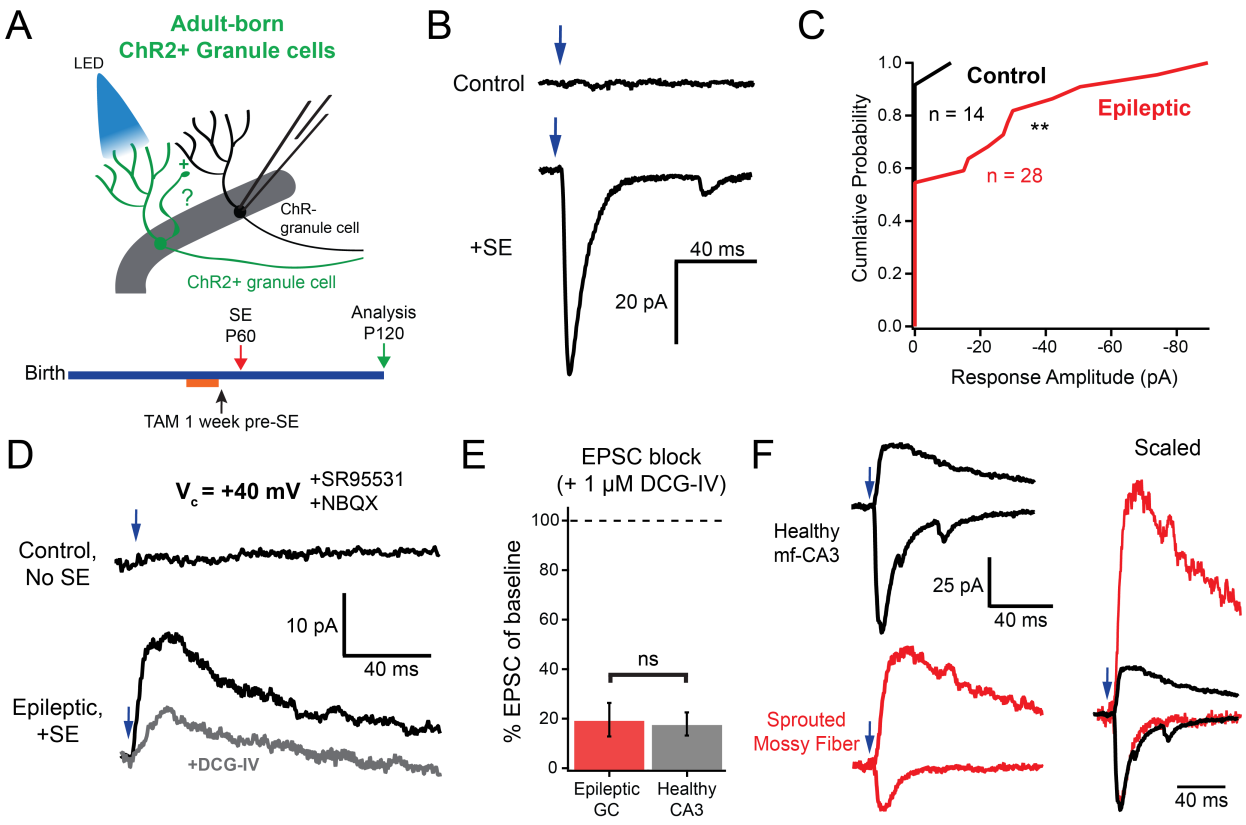

Figure 3. Sprouted mossy fibers from adult-born granule cells make monosynaptic excitatory connections with granule cells in pilocarpine treated mice.

(A) Experimental design for the recording of sprouted mossy fiber responses from adult-born granule cells. DcxCre::ChR2 mice received TAM to label granule cells that were immature at the time of SE; 2 months later, recordings were made from unlabeled granule cells. Timeline depicts the two week birth-dating window (orange) for labeled granule cells relative to TAM, SE and electrophysiologic analysis.

(B) Representative whole-cell voltage clamp traces from ChR2-negative dentate granule cells in adult-labeled control (top) and epileptic (bottom) mice during

optogenetic stimulation (1 ms, blue arrow) of labeled adult-born cells. Optogenetically-evoked EPSCs (oEPSCs) were rarely observed in healthy control animals (n = 2 of 15 cells).

(C) Cumulative probability plot for functional sprouted mossy fiber innervation by adult-born neurons, demonstrating infrequent responses in control cells (n = 2 of 15 cells), but higher likelihood of responses in animals that had SE (n = 15 of 28 cells; p = 0.02, Fisher's Exact Test).

(D) Sprouted mossy fibers from cells born shortly before SE formed functional monosynaptic excitatory connections with other granule cells. Monosynaptic currents were isolated in the presence of NBQX (10 μM) to block polysynaptic activity, while holding the target cell at +40 mV to unblock NMDARs. Monosynaptic responses were observed in n = 5 of 15 cells from epileptic mice, and in 0 of 15 cells from control mice.

(E) Sprouted mossy fiber currents were strongly inhibited by DCG-IV, similar to optogenetically evoked currents in healthy DcxCre::ChR2 mice in CA3 (% block by DCG-IV: control mf-CA3: n = 6 cells; sprouted mf, n = 6 cells).

(F) Representative EPSCs from healthy-CA3 (black traces) and sprouted mossy fiber synapses (red traces) at holding potentials of -70 mV and +40 mV. Overlaid, peak-scaled traces (right) show relative increased NMDAR activation at sprouted mossy fiber synapses (red trace) compared with that of healthy mf-CA3 synapses (black trace). Sprouted mossy fiber synapses had a significantly decreased AMPA:NMDA ratio compared with healthy mossy fiber synapses

(AMPA:NMDA ratio: healthy mf-CA3, 2.87 ± 0.43, n = 7; sprouted mf, 1.06 ± 0.21, n = 7, t-test, $p = 0.006$).

* $p < 0.05$

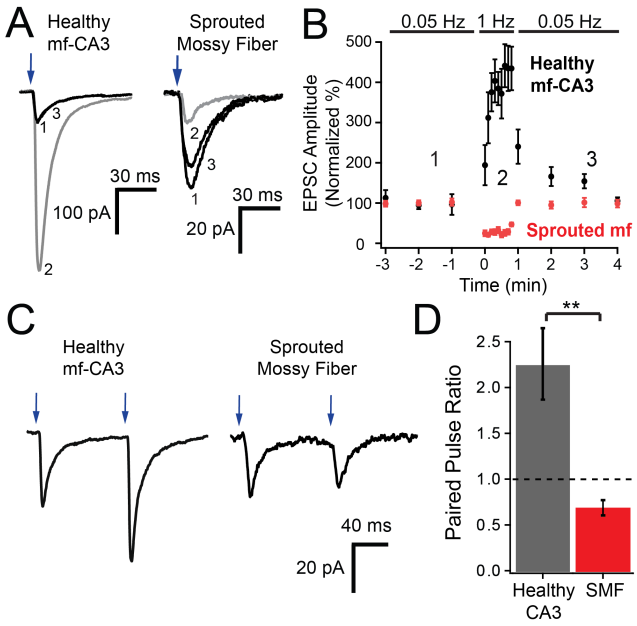

Figure 4. Short-term plasticity of sprouted mossy fiber synapses.

(A) Example traces comparing oEPSCs recorded from healthy mf-CA3 (left) and sprouted mossy fiber-granule cell (right) synapses during 0.05 Hz (black traces) and 1 Hz optogenetic stimulation (gray traces), taken from timepoints represented by the corresponding numbers in (B).

(B) Binned oEPSC amplitudes (normalized to baseline) from sprouted mossy fiber synapses onto granule cells (red) and healthy mf-CA3 synapses (black) recorded at 0.05 Hz and 1 Hz stimulation frequencies. Sprouted mossy fibers exhibit frequency-dependent depression whereas mf-CA3 connections exhibit frequency-dependent facilitation (control mf-CA3, n = 6; sprouted mossy fibers, n = 10; p = 0.0004, unpaired t-test).

(C) Example traces from paired-pulse experiments demonstrate short-term depression at sprouted mossy fiber synapses (right), in contrast to the paired-pulse facilitation typical of healthy mf-CA3 synapses (left).

(D) The paired-pulse ratio (100 ms interval) was significantly less at sprouted mossy fiber synapses after SE when compared with mf-CA3 responses ($EPSC_2$ /$EPSC_1$: healthy CA3, n = 6; sprouted synapses, n = 6; unpaired t-test, p = 0.0011). All data represented as average ± SEM. ** $p < 0.01$

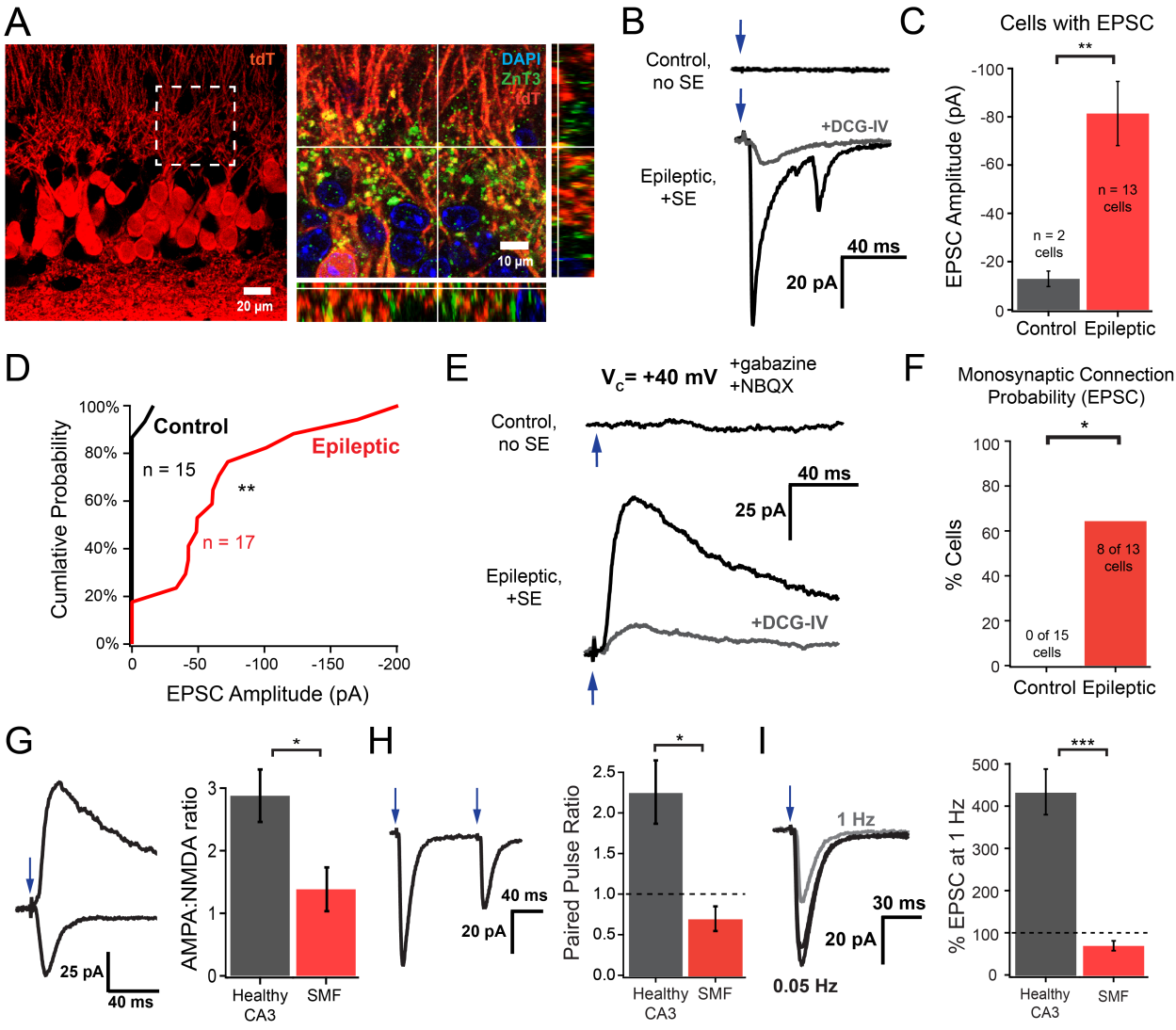

Figure 5. Neonatally-born granule cells contribute to functional mossy fiber sprouting.

(A) Representative confocal images of tdT-labeled neonatally-born granule cells (red) in DcxCre::tdT animals given TAM at P6 demonstrate mossy fiber sprouting from these cells. Dashed box indicates corresponding locations from compressed stack image (left) represented in an orthogonal single plane projection (right). Mossy fiber terminals are labeled with ZnT3 (green) and nuclei with DAPI (blue).

(B) Representative averaged evoked responses recorded from ChR2-negative granule cells in control (top) and epileptic (bottom) neonatally-labeled DcxCre::ChR2 animals during optogenetic stimulation of ChR2-expressing granule cells. Gray trace is the average evoked oEPSC following wash-in of 1 μM DCG-IV.

(C) In the subset of cells with an observable optogenetically-evoked response, average oEPSC amplitude was substantially greater in recordings from epileptic mice (Control, n = 2 cells; epileptic, n = 13 cells; p = 0.004, unpaired t-test).

(D) Cumulative probability plot for the occurrence of oEPSCs in control (black) and epileptic (red) mice recorded while voltage-clamping the recorded cell to -70mV. EPSCs from granule cells in epileptic mice were substantially larger and more frequent than those found in controls (response likelihood: Control, 2 of 15 cells with oEPSC; Epileptic, 13 of 18 cells with oEPSC, Fisher's Exact Test, p = 0.0013).

(E) Monosynaptic sprouted granule cell-granule cell synapses were only observed in pilocarpine-treated mice (bottom trace), and not in controls (top trace). Monosynaptic NMDAR-mediated currents were recorded from cells voltage clamped to +40 mV, while blocking polysynaptic responses with NBQX (10 μM).

(F) Probability of monosynaptic granule cell – granule cell connections. Neither of the two control cells that had oEPSCs depicted in (C) had an NMDAR-mediated response in the presence of NBQX, suggesting that these responses were polysynaptic. 8 cells assayed at +40mV in epileptic mice had a

monosynaptic recurrent connection. (Control: 0 of 15 cells; Epileptic: 8 of 13 cells; $p = 0.011$, Fisher's Exact Test).

(G) Representative EPSCs from sprouted mossy fiber synapses (left) at holding potentials of -70 mV and +40 mV. Mean AMPAR:NMDAR ratios (right) demonstrate a significantly increased relative NMDAR-mediated contribution at sprouted mossy fiber synapses (AMPAR:NMDAR ratio: healthy mf-CA3, $n = 6$; sprouted mf, $n = 7$; $p = 0.022$, unpaired t-test).

(H) Paired-pulse depression at sprouted mossy fiber synapses from neonatally-born granule cells (left). The mean paired-pulse ratio (right; 100 ms interval) was significantly less at sprouted mossy fiber synapses after SE when compared with mf-CA3 responses ($EPSC_2$ / $EPSC_1$: healthy mf-CA3, $n = 6$; sprouted mf, $n = 9$; unpaired t-test, $p = 0.02$).

(I) Example traces (left) of sprouted mossy fiber-granule cell synapses during 0.05 Hz (black traces) and 1 Hz stimulation (gray traces) of neonatally-born granule cells from post-SE mice. Sprouted mossy fibers exhibit frequency-dependent depression whereas mf-CA3 connections exhibit frequency-dependent facilitation (right) (control mf-CA3, $n = 6$; sprouted mf, $n = 8$; $p < 0.001$, unpaired t-test). All data presented as average ± SEM. * $p < 0.05$, ** $p < 0.01$, *** $p < 0.001$

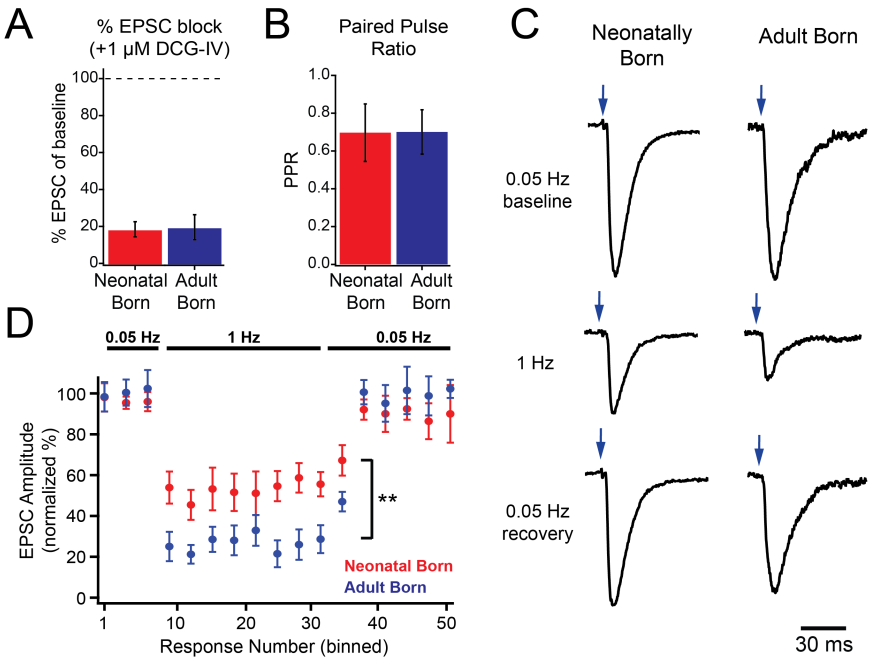

Figure 6. Sprouted mossy fiber synapses made by adult-born granule cells have enhanced short-term depression compared to those from neonatally-born cells.

(A) Sprouted mossy fiber synapses from neonatally-born and adult-born granule cells have comparable block by 1 μM DCG-IV (%EPSC: Neonatal, n =5; Adult-born, n = 7; Unpaired t-test, p = 0.4).

(B) Comparable paired-pulse depression in sprouted mossy fiber synapses from both neonatally-born and adult-born granule cells (PPR: Neonatal, n = 7; Adult-born, n = 7; Unpaired t-test, p = 0.2).

(C) Example frequency-dependent depression of sprouted mossy fiber oEPSCs from neonatally-born (left) and adult-born (right) granule cells upon 1 Hz stimulation. Baseline stimulation was 0.05 Hz. Vertical scale between cells are

normalized to the amplitude of the first EPSC; all responses for each cell are on the same vertical scale.

(D) Sprouted synapses from adult-born granule cells displayed enhanced short-term depression compared to cells born neonatally. Average steady-state (last 10 traces) EPSC depression from baseline was significantly greater in synapses from adult-born granule cells (Neonatal: n = 8, Adult-born: n = 6; p = 0.007, Unpaired t-test). All data represented as average ± SEM. ** $p < 0.01$

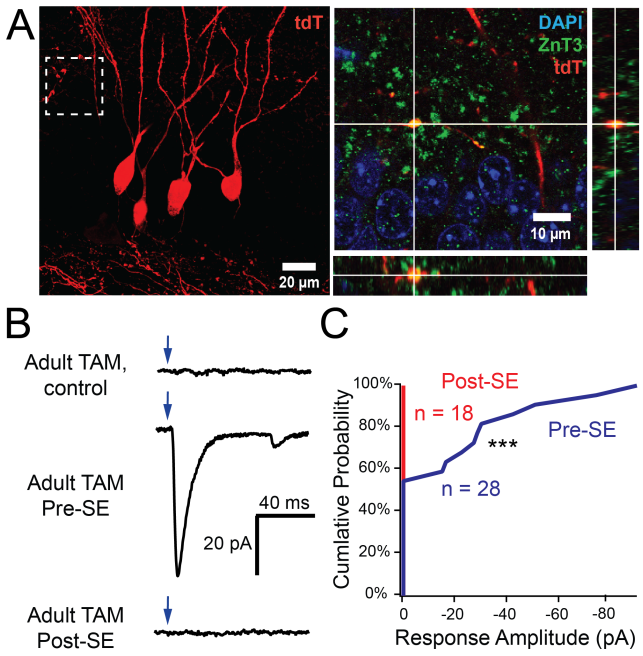

Figure 7. Sprouted mossy fiber synapses from granule cells born after seizures do not form functional excitatory synapses by 2 months after SE.

(A) Representative confocal images from tdT-labeled adult-born granule cells (red) in animals given TAM after SE demonstrate robust mossy fiber sprouting from cells born after SE. Dashed box indicates corresponding location from compressed stack image (left) represented in orthogonal single plane projection (right). Mossy fiber terminals are labeled with ZnT3 (green) and nuclei with DAPI (blue).

(B) Representative whole-cell voltage clamp traces from unlabeled dentate granule cells during stimulation of ChR2-expressing granule cells in adult-labeled healthy control mice (top), from adult-born cells generated prior to SE (mice given TAM pre-SE; middle), and granule cells born after SE (mice given

TAM 2 weeks post-SE; bottom). oEPSCs were not observed during stimulation of granule cells born after SE. Scale is identical for all traces.

(C) Cumulative probability plot for functional sprouted mossy fiber innervation by adult-born neurons, demonstrating no responses from ChR2-positive granule cells born post-SE (n = 0 of 18 cells), with frequent sprouted mossy fiber-mediated responses from ChR2-positive adult-born cells born pre-SE (n = 15 of 28 cells; $p < 0.0001$, Fisher's Exact Test). *** $p < 0.001$

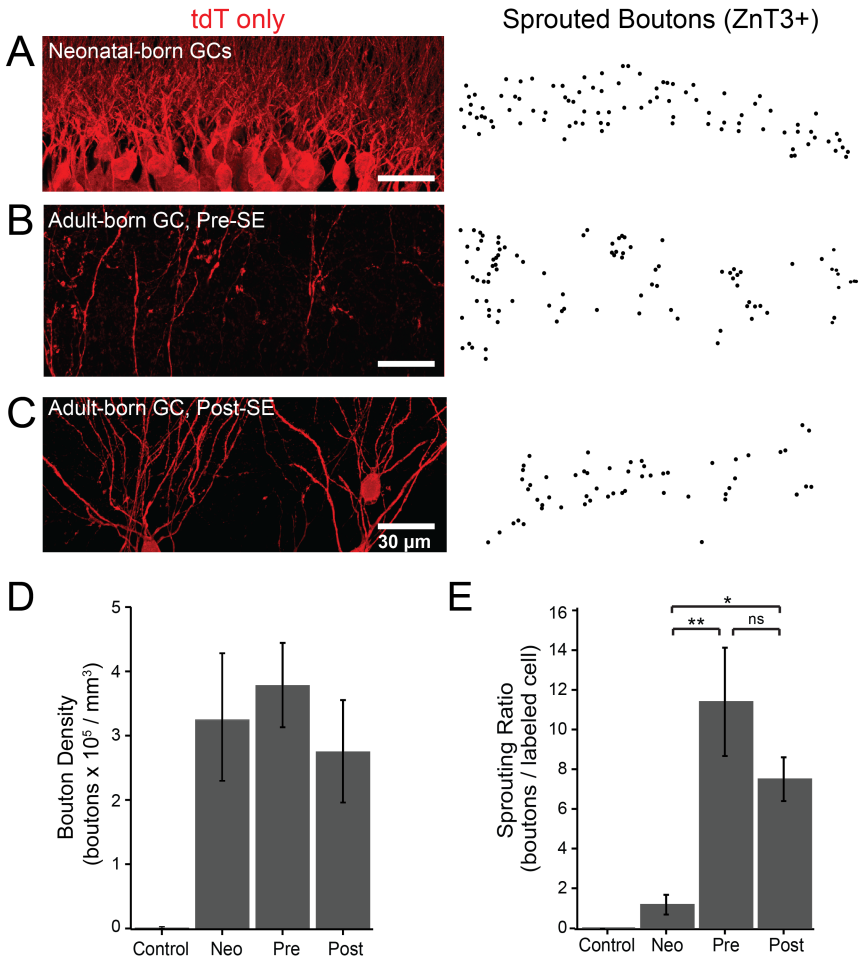

Figure 8. Adult-born granule cells are more likely to form sprouted mossy fiber boutons than neonatally-born granule cells.

(A) Example compressed 20 µm confocal stack of tdT-labeled, neonatally-born granule cells (red) from pilocarpine-treated DcxCre::tdT mice (left). Sprouted tdT+ boutons were identified using thin confocal sections and co-labeling with ZnT3 (as in Figure 5A) and the localization of sprouted mossy fiber boutons (tdT+/ZnT3+) in this stack is represented by black dots (shown on right). ZnT3 staining omitted for clarity.

(B) Example compressed confocal stack of tdT-labeled, adult-born granule cells born pre-SE (red) from pilocarpine-treated DcxCre::tdT mice (left) and corresponding localization of sprouted (tdT+ZnT3+) mossy fiber boutons (black dots, right).

(C) Example compressed confocal stack of tdT-labeled, adult-born granule cells born post-SE (red) from pilocarpine-treated DcxCre::tdT mice (left) and corresponding localization of sprouted (tdT+ZnT3+) mossy fiber boutons (black dots, right).

(D) Sprouted tdT+ bouton density in the IML after SE is similar across all labeling cohorts despite dramatic differences in the density of labeled neurons (bouton density: Control, n = 5 mice; Neonatal, n = 6; Pre-SE, n = 4; Post-SE, n = 4; $p = 0.6$, two-tailed ANOVA between Neonatal, Pre-SE, Post-SE). Controls did not have any sprouting (Control, n = 5 mice).

(E) Granule cells from adult-born cells had significantly more sprouted boutons per labeled neuron, represented as an increase in their sprouting ratio (sprouted bouton density/labeled cell density; Control, n = 5 mice, Neonatal, n = 6; Pre-SE, n = 4; Post-SE, n = 4; Neonatal vs. Pre-SE, $p < 0.002$; Neonatal vs. Post-SE, $p < 0.05$, ANOVA with Tukey's test; no difference between Pre-SE and Post-SE, $p = 0.08$).

Chapter 2: Early detonation by sprouted mossy fibers enables aberrant dentate network activity

William D. Hendricks[a,b], Gary L. Westbrook[c] & Eric Schnell[b,d]

[a]Neuroscience Graduate Program; [b]Department of Anesthesiology and Perioperative Medicine; Oregon Health and Science University, Portland, OR, 97239; USA; [c]Vollum Institute, Oregon Health and Science University, Portland, OR, 97239; USA; [d]VA Portland Health Care System; Portland, OR, 97239; USA

Published in Proceedings of the National Academy of Sciences USA (PNAS), May 2019

(https://doi.org/10.1073/pnas.1821227116)

Abstract

In temporal lobe epilepsy, sprouting of hippocampal mossy fiber axons onto dentate granule cell dendrites creates a recurrent excitatory network. However, unlike mossy fibers projecting to CA3, sprouted mossy fiber synapses depress upon repetitive activation. Thus, despite their proximal location, relatively large presynaptic terminals, and ability to excite target neurons, the impact of sprouted mossy fiber synapses on hippocampal hyperexcitability is unclear. We find that despite their short-term depression, single episodes of sprouted mossy fiber activation in hippocampal slices initiated bursts of recurrent polysynaptic excitation. Consistent with a contribution to network hyperexcitability, optogenetic activation of sprouted mossy fibers reliably triggered action potential firing in postsynaptic dentate granule cells after single light pulses. This pattern resulted in a shift in network recruitment dynamics to an “early detonation” mode and an increased probability of release compared to mossy fiber synapses in CA3. A lack of tonic adenosine-mediated inhibition contributed to the higher probability of glutamate release thus facilitating reverberant circuit activity.

Significance Statement

Sprouted mossy fibers are one of the hallmark histopathological findings in experimental and human temporal lobe epilepsy. These fibers form recurrent excitatory synapses onto other dentate granule cells that display profound short-term depression. Here, however, we show that although these sprouted

mossy fibers weaken substantially during repetitive activation, their initial high probability of glutamate release can activate reverberant network activity. Furthermore, we find that a lack of tonic adenosine inhibition enables this high probability of release and, consequently, recurrent network activity.

Introduction

Mossy fibers contacting CA3 pyramidal cells have a low probability of release (P_r), but show profound short-term facilitation (Nicoll and Schmitz, 2005). These “conditional detonator” synapses strongly drive post-synaptic cell firing during repetitive activation (Vyleta et al., 2016). In experimental and human epilepsy, mossy fiber axons sprout collaterals onto the proximal dendrites of other dentate granule cells (Sutula et al., 1988; Sutula et al., 1989; Houser et al., 1990; Okazaki et al., 1995), where conditional detonation could be highly epileptogenic. However, sprouted mossy fibers are smaller than mossy fiber synapses in CA3 (Sutula et al., 1998; Cavazos et al., 2003; Hendricks et al., 2017) and rapidly depress during repetitive activation (Hendricks et al., 2017), suggesting the extent with which they drive seizure activity could be limited (Smith, 2017).

Despite multiple lines of evidence demonstrating *de novo* recurrent connections in rodent models of epilepsy, the impact of mossy fiber sprouting on circuit dynamics remains uncertain (Mello et al., 1993; Longo and Mello, 1997, 1998; Buckmaster, 2014). Sprouted mossy fibers are absent under non-pathological conditions, and the formation of novel recurrent connections

capable of activating post-synaptic granule cells (Scharfman et al., 2003b) could induce run-away excitation, particularly if they robustly activate the typically quiescent dentate network. Although increased dentate excitation occurs in temporal lobe epilepsy (Cronin et al., 1992; Wuarin and Dudek, 2001), the challenge of isolating and selectively stimulating sprouted mossy fibers has severely hampered studies that directly examine sprouted mossy fiber synapses (Scharfman et al., 2003b) and an understanding of how the activation of these fibers might contribute to epileptiform activity.

Here, we selectively activated sprouted mossy fiber axons with optogenetics to determine their influence on post-synaptic granule cell firing and dentate gyrus activity. We find that sprouted mossy fibers reliably drive post-synaptic action potential firing in dentate granule cells and initiate recurrent circuit activity even in the absence of manipulations to increase excitability. This effect is mediated by increased release probability at these synapses, attributed to a lack of tonic adenosine signaling in the inner molecular layer of the dentate gyrus. The increased P_r allows sprouted mossy fiber activation to reliably recruit post-synaptic circuits, as primed network "spark plugs."

Results

As the functional contribution of mossy fiber sprouting to epileptogenesis remains controversial (Longo and Mello, 1997, 1998; Buckmaster, 2014; Smith, 2017), we combined the pilocarpine model of temporal lobe epilepsy with electrophysiology to directly examine the contribution of sprouted mossy fiber

activation to epileptiform activity, as this model reliably induces dense mossy fiber sprouting (see methods, also see ref. Hendricks et al., 2017). To isolate sprouted mossy fibers from other granule cell inputs, we used DcxCre::ChR2 mice (Cheng et al., 2011) to selectively label neonatally-born granule cells with channelrhodopsin2 (ChR2) (Fig. 1A). We then prepared acute mouse hippocampal slices, and optogenetically activated sprouted mossy fibers while recording from ChR2-negative (unlabeled) granule cells (Fig. 1B,C; SI Appendix, Fig. S1; also see ref. Hendricks et al., 2017). Optogenetic activation of sprouted mossy fibers evoked EPSCs in dentate granule cells only in slices from pilocarpine-treated mice (Fig. 1D,E; also see ref. Hendricks et al., 2017). Postsynaptic cells, filled with AlexaFluor 568 dye during recordings, did not have hilar basal dendrites (0 of 32 cells; Fig. 1C), indicating that LED-evoked responses originated from recurrent (sprouted mossy fiber) synaptic inputs.

In addition to monosynaptic sprouted mossy fiber – granule cell (smf-GC) EPSCs, we frequently observed LED-evoked epileptiform activity following single light pulses (Fig. 1D, right). Responses identified as bursts had, on average, 2.3 ± 0.3 EPSCs during a burst (n = 13 cells). These bursts were not a result of altered intrinsic properties compared to cells with single or no evoked recurrent EPSCs (R_i, input resistance: cells without bursts, 610 ± 47 MΩ, n = 19 cells; cells with bursts, 527 ± 77 MΩ, n = 13 cells; unpaired t-test, t_{30} = 0.9711, p = 0.3392; C_m, cell capacitance: cells without bursts, 51.5 ± 3.8 pF, n = 19 cells; cells with bursts, 46.8 ± 3.8, n = 13 cells; unpaired t-test, t_{30} = 0.8302, p = 0.4130). Optogenetic stimulation only elicited single spikes in ChR2-expressing

granule cells (number of AP per 1 ms light pulse: 0.98 ± 0.09, n = 5 cells), indicating that sprouted mossy fiber activation initiated recurrent activity. Consistent with polysynaptic activation, EPSC peaks during bursts (EPSC peaks 2 – 3) had high jitter (Fig. 1 F-G). One possible source of these bursts is through the activation of additional populations of granule cells with their own sprouted mossy fibers, if sprouted mossy fibers could effectively drive post-synaptic firing.

Unlike healthy mossy fiber – CA3 synapses (Nicoll and Schmitz, 2005) that are described as conditional detonators, sprouted mossy fiber synapses exhibit profound frequency-dependent short-term depression (SI Appendix, Fig. S2, see also ref. Hendricks et al., 2017), which may limit their ability to drive postsynaptic firing (Smith, 2017). Thus, we compared patterns of synaptically-evoked spike generation in post-synaptic target cells at these two different synapses using a short 10 Hz train of optogenetic stimulation. In striking contrast to synaptic facilitation and delayed CA3 pyramidal cell spike generation at mf-CA3 synapses, 10 Hz stimulation of sprouted mossy fiber synapses induced post-synaptic spikes only at the beginning of the train (Fig. 2). Importantly, this firing pattern did not result from a failure to activate sprouted mossy fibers in epileptic brains, as these fibers maintain action potential fidelity throughout optogenetic trains (SI Appendix, Fig. S1). Thus, the failure to maintain post-synaptic activation resulted instead from reduced glutamate release later in the train, consistent with short-term synaptic depression at these synapses (Hendricks et al., 2017). Despite this depression, however, single

pulses triggered circuit activation sufficient to recruit additional recurrent networks (Fig. 1D).

Both the frequency-dependent short-term depression and the robust initial recruitment of postsynaptic cell firing during recurrent activation (Fig. 2B) could result from a high initial P_r at sprouted mossy fiber synapses. To directly test for increased P_r, we measured use-dependent MK-801 block kinetics during activation of both types of mossy fiber synapses. Optogenetically-evoked NMDAR-mediated synaptic currents were isolated by voltage-clamping granule cells to -70 mV in Mg^{2+} free ACSF, in the presence of NBQX (10 μM) and SR95531 (10 μM) to block AMPA- and $GABA_A$-receptors, respectively. After baseline EPSC recording, LED stimulation was paused for 10 minutes while MK-801 (40 μM) was washed onto the slice and allowed to equilibrate. Upon resuming LED stimulation (0.05 Hz), MK-801 progressively blocked NMDAR-EPSCs from smf-GC and mf-CA3 synapses (Fig. 3A). The rate of block was faster for sprouted mossy fiber synapses (Fig. 3B), indicating a higher P_r. Interestingly, MK-801 block rate at smf-GC synapses was better fit by a double-exponential decay model (Fig. 3C), whereas at mf-CA3 synapses, a single exponential model was sufficient, suggesting increased synaptic heterogeneity at sprouted mossy fiber synapses (Rosenmund et al., 1993). Overall, the increased P_r at sprouted mossy fiber synapses likely contributes to target granule cell firing and therefore the spread of recurrent excitation in epileptic brains.

Extracellular adenosine inhibits neurotransmitter release at mossy fiber synapses in CA3 via A1-type adenosine receptors (A_1Rs) located on mossy fiber terminals. This tonic activation of pre-synaptic A_1Rs contributes to the profound short-term plasticity at these synapses (Moore et al., 2003; Fedele et al., 2005). As altered adenosine metabolism may be a contributing factor in epileptogenesis (Boison, 2008; Williams-Karnesky et al., 2013; Sandau et al., 2016), we posited that sprouted mossy fibers might manifest an increased P_r due to a reduction in A_1R-mediated inhibition. To measure tonic A_1R-mediated inhibition of sprouted mossy fibers in epileptic mice, we washed on the selective high-affinity A_1R antagonist, 8-Cyclopentyl-1,3-dipropylxanthine (DPCPX, 200 nM), while recording sprouted mossy fiber-mediated responses. In contrast to the enhancement of synaptic transmission at healthy mf-CA3 synapses (Fig. 4A,B, also see ref. Moore et al., 2003), DPCPX had no effect on sprouted mossy fiber EPSCs (Fig. 4A,B), indicating a lack of tonic A_1R signaling. The DPCPX-induced increase in EPSC amplitudes at mf-CA3 synapses coincided with decreased PPR (paired-pulse ratio, P_2/P_1: pre-DPCPX, 2.36 ± 0.37; post-DPCPX, 1.37 ± 0.12, n = 6 cells; paired t-test, $t_5 = 3.408$ $p = 0.0191$), as expected for a pre-synaptic effect on A_1Rs.

To determine whether the lack of tonic A_1R-mediated inhibition at sprouted mossy fiber synapses resulted from an absence of presynaptic adenosine receptors, we washed on the selective A_1R agonist, 2-Chloro-N^6-cyclopentyladenosine (CCPA, 1 μM). CCPA reduced sprouted mossy fiber EPSCs (Fig. 4C,D) and increased paired-pulse facilitation (SI Appendix, Fig. S3).

Thus, A_1Rs were present and functional on sprouted mossy fiber terminals, indicating that the lack of tonic A_1R modulation was due to a reduced extracellular adenosine concentration. CCPA decreased the probability of release at sprouted mossy fiber synapses, but it did not restore frequency facilitation (SI Appendix, Fig. S4), suggesting that the molecular mechanisms underlying synaptic facilitation at mossy fiber terminals cannot be restored solely by increasing A_1R activation.

Finally, to test whether reduced A_1R activation and increased P_r at sprouted mossy fiber synapses contributes to recurrent circuit activation, we examined the effect of A_1R activation using hippocampal slices from epileptic mice. When applied to slices demonstrating EPSC bursts after sprouted mossy fiber activation, the A_1R agonist CCPA reduced recurrent EPSCs (Fig. 3E,F) as well as the charge transfer carried by polysynaptic bursts (% of total charge transfer carried by burst: pre-CCPA, 36.5 ± 5.1%, post-CCPA 22.8 ± 4.4%, n = 5 cells, paired t-test, $t_4 = 3.497$, $p = 0.0250$). Together, these data indicate that reduced A_1R activation at granule cell outputs contributes to hyperexcitability in the dentate gyrus in epileptic brains.

Discussion

Here we show that sprouted mossy fibers can trigger reverberating network activity despite their profound short-term depression. This recurrent network activation is enabled by a high probability of release, resulting in “early detonation” of post-synaptic cells. Moreover, this is due, at least in part, to the

lack of tonic adenosine inhibition at sprouted mossy fiber synapses in the inner molecular layer.

The retrograde sprouting of mossy fibers is common to both animal models of epilepsy and human patients with temporal lobe epilepsy (Buckmaster), yet the functional impact of these recurrent synapses is not well understood (Buckmaster, 2014; Smith, 2017). We demonstrate that single optogenetic stimulation of these fibers can produce bursts of recurrent EPSCs, suggesting that sprouted mossy fibers effectively recruit the local network. This observation is consistent with paired granule cell recordings from epileptic mice (Scharfman et al., 2003b), which suggest that sprouted mossy fibers form recurrent excitatory connections capable of driving post-synaptic cell spiking. Critically, we find that sprouted mossy fibers can potently trigger granule cell action potential firing with single coordinated release events, which could lead to bursts as successive rounds of sprouted mossy fibers are activated through additional granule cell firing.

The functional effects of sprouted mossy fibers on dentate excitability in *ex vivo* slice preparations has been difficult to determine, as it sometimes requires modulation of the extracellular environment to reduce the masking effects of inhibition (Cronin et al., 1992; Wuarin and Dudek, 1996; Patrylo and Dudek, 1998; Hardison et al., 2000; Sutula and Dudek, 2007). This suggests that although the state of the epileptic dentate network may be relatively stable (Santhakumar et al., 2005), subtle changes in external K^+ concentration (Patrylo and Dudek, 1998; Hardison et al., 2000), inhibition (Cronin et al., 1992; Patrylo

and Dudek, 1998), or adenosine (Gouder et al., 2003; Amorim et al., 2016; Sandau et al., 2016) could shift the network to a more unstable, hyperexcitable state, during which sprouted mossy fibers can readily trigger epileptiform activity. The absence of tonic adenosine signaling appears to be intrinsic to epileptic slices, recorded using standard solutions. However, it remains likely that changes in adenosine-mediated signaling may serve as another conditional factor *in vivo*, which might vary over time and contribute to the occurrence (or avoidance) of seizure activity, given the presence of functional adenosine receptors at these synapses.

All EPSC bursts were self-limited, which may be a manifestation of the strong short-term depression of the smf-GC synapse (Scharfman et al., 2003b; Hendricks et al., 2017). This also helps explain prior indirect observations made using extracellular retrograde stimulation of mossy fibers, which caused self-limited episodes of granule cell population spiking in slices from epileptic rats (Tauck and Nadler, 1985). By using direct optogenetic stimulation of sprouted fibers, we demonstrate sprouted mossy fibers can indeed drive granule cell firing even with inhibition intact and low (3 mM) external K^+ concentrations. We recognize that the conclusions that can be made while using optogenetic stimulation in an acute slice preparation in regards to seizure activity *in vivo* are limited, primarily due to the isolation of slices from other brain networks and the cerebral extracellular environment and synchronized activation of sprouted terminals. However, our ability to robustly trigger recurrent network activation suggests that recurrent networks are widespread even within our 300 μm brain

slices, and that recurrent interconnectivity might be even more extreme within the intact brain.

The increased P_r at sprouted mossy fibers provides a reasonable mechanism that could enable sprouted mossy fibers to act as “spark plugs” to hyperactivate local dentate gyrus networks. Our direct comparisons of P_r between smf-GC and mf-CA3 synapses are consistent with previous data demonstrating a larger success rate at individual smf-GC connections (0.35) (Scharfman et al., 2003b) than the prior estimate of P_r at mf-CA3 synapses of 0.2-0.28 (von Kitzing et al., 1994). We propose that the increased P_r at these sprouted synapses is, at least in part, due to reduced tonic inhibition by adenosine at the smf-GC synapse.

Although we did observe an increase in PPR with CCPA (suggesting that it lowered P_r), our observation that 1 Hz facilitation was not restored by adenosine agonism was somewhat surprising, given the extent to which A1R antagonism occludes frequency facilitation at mf-CA3 synapses in healthy brains (Moore et al., 2003). This indicates that tonic adenosine alone is unlikely to be the only mechanism controlling short-term plasticity the smf-GC synapse. This is supported by the previous observation that healthy mossy fiber synapses still express small but significant frequency-dependent facilitation even in the presence of A1R blockade or A1R gene knockout (Moore et al., 2003). Thus, the short-term depression remaining at smf-GC synapses even in the presence of CCPA could be due to other changes in neuromodulatory tone in the epileptic dentate gyrus, or altered expression of specific components of the release

machinery required for facilitation (Ben-Simon et al., 2015; Jackman et al., 2016). Even in health brains, the expression of frequency-dependent facilitation by mossy fibers is target-specific (Toth et al., 2000) and thus the remaining differences may also partly derive from differences in the post-synaptic complement between granule cells and CA3 pyramidal cells.

Does the lack of tonic adenosine in the dentate gyrus contribute to seizure activity in epilepsy? Although systemic or local injections of A_1R agonists can reduce the severity of seizures (Gouder et al., 2003; Amorim et al., 2016), adenosine has broad inhibitory effects throughout the brain. Here, the absence of tonic adenosine signaling at these synapses heightens the excitability of dentate gyrus circuitry, which was reduced by pharmacological A_1R activation (Fig. 4). As the granule cell network is implicated in spontaneous seizures *in vivo* (Zhou et al., 2019), restoration or augmentation of extracellular adenosine could reduce recurrent circuit dynamics in the in the dentate gyrus and provide one mechanism for the observed *in vivo* effects of adenosine (Gouder et al., 2003; Amorim et al., 2016). Thus, although seizure activity in epileptic brains likely results from multiple hyperexcitable circuit elements, the lack of tonic adenosine signaling in the dentate gyrus shifts sprouted mossy fiber synapses from "conditional detonators" to "early detonators", which could contribute to the initiation of generalized seizures.

Methods

Animals

All experiments were carried out in accordance with local, state, and federal guidelines, and protocols were approved by OHSU and VA Institutional Animal Care and Use Committees (IACUC). Housing was provided by Oregon Health & Science University's Department of Comparative Medicine vivarium accredited by the Association for Assessment and Accreditation of Laboratory Animals. To generate DcxCre::ChR2 mice, homozygous *doublecortin-CreER*^{T2} (line F18; RRID:MGI:5438982) mice were bred with homozygous *Gt(ROSA)26Sor*$^{tm32(CAG-COP4*H134R/EYFP)Hze}$ (Ai32; RRID:IMSR_JAX:012569) and used as previously described (Cheng et al., 2011; Hendricks et al., 2017). Briefly, Cre-mediated combination was induced by tamoxifen (TAM) at P8 (2 injections, 12 hours apart, 20 mg/kg in corn oil, i.p.), to permanently label neonatally-generated granule cells with ChR2-eYFP in DcxCre::ChR2 heterozygous mice. Status epilepticus was induced in two-month-old male mice with pilocarpine (325 mg/kg i.p.; Cayman Chemicals) after pre-treating with an i.p. injection of scopolamine methyl bromide (Sigma-Aldrich). Seizures were graded on the modified Racine Scale (Shibley and Smith, 2002); status epilepticus (SE) was defined when a mouse had 3 or more Racine Grade 3 seizures, followed by continuous grade 2 seizing. Following 2 hours of SE, seizures were terminated with diazepam (10 mg/kg i.p.; Hospira, Inc.) and given soft food and i.p. injections of 5% glucose in 0.45% normal saline to aid in recovery. Mice that did not develop SE were humanely killed by carbon dioxide inhalation and cervical dislocation and excluded from further analysis. These criteria reliably produce dense mossy fiber sprouting as measured by ZnT3 staining in the IML, and a

high density of sprouted mossy fibers originating from granule cells specifically labeled at this timepoint (Hendricks et al., 2017). A total of 23 healthy control mice and 19 pilocarpine-treated mice were used in this study.

Slice Physiology

Acute brain slices for *ex vivo* electrophysiology were prepared as previously described (Hendricks et al., 2017). In brief, four-month-old male DcxCre::ChR2 mice were anesthetized with 4% isoflurane, followed by injection of 1.2% avertin (Sigma-Aldrich). Mice were transcardially perfused with 10 mL of ice-cold N-methyl-D-glucamine (NMDG)-based cutting solution, containing the following (in mM): 93 NMDG, 30 NaHCO3, 24 glucose, 20 HEPES, 5 Na-ascorbate, 5 N-acetyl cysteine, 3 Na-pyruvate, 2.5 KCl, 2 thiourea, 1.2 NaH2PO4, 10 MgSO4, and 0.5 CaCl2. Mice were rapidly decapitated and 300 µm sagittal slices were prepared with a Leica VT1200S vibratome. This method was chosen to best preserve CA3 pyramidal cell health and mossy fiber axons from these 4 month old mice. For some dentate granule cell recordings, the hippocampus was dissected, and 300 µm transverse hippocampal sections were prepared in ice-cold NMDG solution, which allowed us to maximize the number of slices obtained from epileptic animals. We did not observe any physiological differences between the two preparations during granule cell recordings, including the frequency of smf-GC bursts, so these results were combined. Slices from both preparations recovered in warm NMDG cut solution for 15 mins followed by standard ACSF at room temperature for 1 hour prior to recording.

Dentate granule cell and CA3 pyramidal cell recordings were obtained with 3-5 MΩ borosilicate glass pipettes filled with internal solution. The Cs^+-based internal solution for voltage-clamp experiments contained the following (in mM): 113 Cs-gluconate, 17.5 CsCl, 10 HEPES, 10 EGTA, 8 NaCl, 2 Mg-ATP, 0.3 Na-GTP, 0.05 Alexa Fluor 568, pH adjusted to 7.3 with CsOH, with a final osmolarity of 295 mOsm; QX-314-Cl (5 mM; Tocris Bioscience) was included to block unclamped action potentials. The K^+-based internal solution for current-clamp experiments contained the following (in mM): 130 K-gluconate, 20 KCl, 10 HEPES, 4 Mg-ATP, 0.3 Na-GTP, 0.1 EGTA, 0.05 AlexaFluor 568, pH adjusted to 7.2 KOH, with a final osmolarity of 295 mOsm. Granule cells and CA3 pyramidal cells were identified with infrared differential interference contrast microscopy on an Olympus BX-51WI microscope. Whole-cell recordings were obtained by making high-resistance seals (>5 GΩ) and applying brief suction. Cells were filled with Alexa Fluor 568 dye to visually confirm cell type and assess for presence of hilar basal dendrites. Series resistance was uncompensated and cells with a >30% change in series resistance were excluded from analysis. Liquid junction potential was 8 mV and was uncorrected. For current-clamp recordings, minimal negative current was injected if necessary to maintain a resting potential of -70 mV in dentate granule cells and CA3 pyramidal cells.

Pulses of blue LED-powered (Thorlabs) light (1 ms, 470 nm, 8 mW/cm^2, 0.05 Hz) were delivered through a 40x water immersion objective, targeted at the stratum lucidum for CA3 recordings and inner molecular layer for granule cell recordings. Stimulation frequency was modified for various experiments as

noted in the text. Signals were amplified with an AxoPatch 200B amplifier (Molecular Devices), low-pass Bessel-filtered at 5 kHz, and digitized and sampled at 10 kHz using a NIDAQ (National Instruments) analog-to-digital board. Data were captured using a custom Igor Pro 8 (Wavemetrics) script and NIDAQmx (National Instruments) plugins. For presentation of EPSCs, a 2 kHz Gaussian filter was applied, *post-hoc.*

Statistical Analysis

Curve fitting and EPSC trace averaging was carried out in Igor Pro 8 (Wavemetrics) using built-in and custom functions, respectively. Epileptiform burst activity (multiple EPSCs to single stimulus) was determined by eye, aided by fitting a single exponential curve to the initial decay and identifying delayed EPSC peaks rising above the decay fit line. Peak detection was implemented in Igor Pro by identifying zero-point crossings of thresholded peaks on the first-order derivative of the EPSC. Charge transfer measurements were implemented with Igor Pro's area function. Additional statistical analysis was performed in Prism 8 (GraphPad). Normality was tested with the Shapiro-Wilk normality test prior to statistical test selection. Paired and unpaired t-tests were used for normally distributed datasets; Mann-Whitney and Wilcoxon matched-pairs signed rank test were used for non-parametric datasets. For all experiments, significance was determined by $p < 0.05$ (*$p < 0.05$, **$p < 0.01$, ***$p < 0.001$). All summary data is presented as mean ± SEM.

Acknowledgments

We wish to thank Drs. Zhi-Qi Xiong and Xuewen Cheng (Shanghai Institute for Neuroscience) for providing the DcxCreER^{T2} mouse line, and members of the Schnell and Westbrook laboratories for critical feedback and discussion on the manuscript. Research funding was provided by Department of Veterans Affairs, Veterans Health Administration, Office of Research and Development, Biomedical Laboratory and Development CDA-2 award 005-10S (ES); Department of Veterans Affairs Merit Review Award I01-BX002949 (ES); a Department of Defense CDMRP Award W81XWH-18-1-0598 (ES); a National Institutes of Health (NIH) Grant F31-NS098597 (WDH); NIH Grant R01-NS080979 (GLW); and NIH Grant P30-NS061800 (Oregon Health and Science University Advanced Light Microscopy Core). The contents of this manuscript do not represent the views of the U.S. Department of Veterans Affairs or the United States government.

Figures:

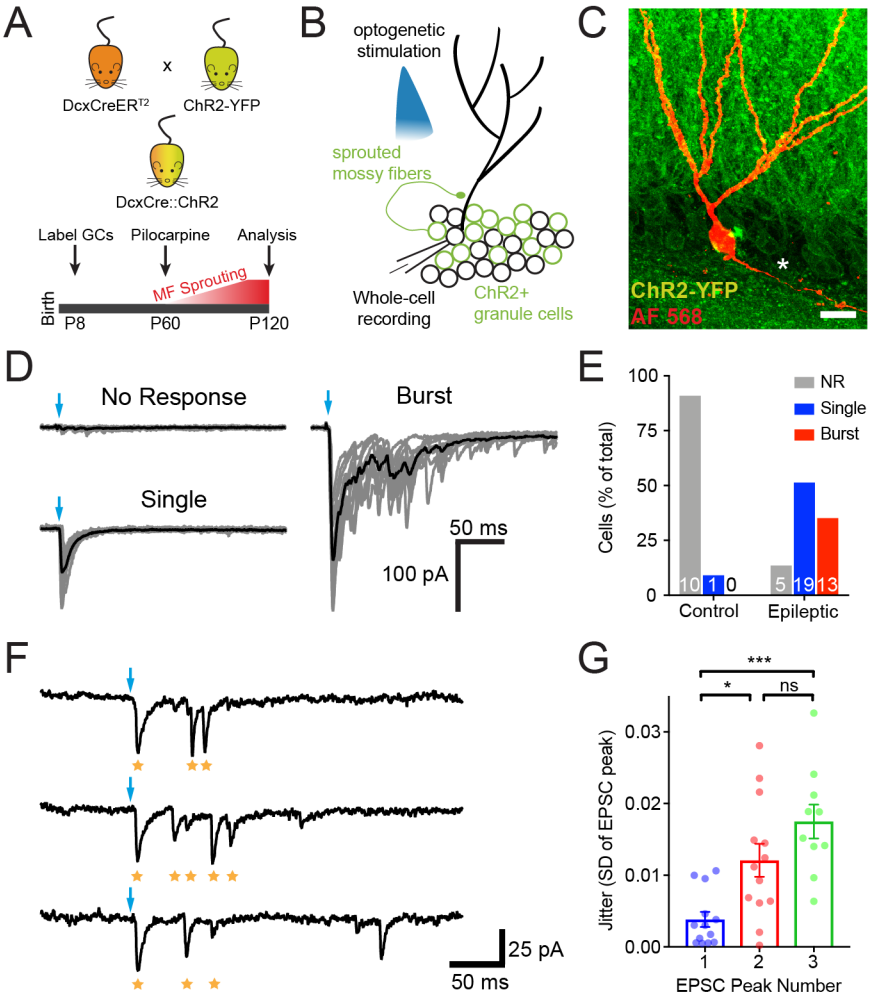

Figure 1: Stimulation of sprouted mossy fibers triggers spiking in post-synaptic dentate granule cells and recurrent network activity. (*A*) Experimental design for granule cell labeling and induction of epileptic mossy fiber sprouting. DcxCreER^{T2} mice were bred with conditional ChR2-YFP (Ai32) reporter mice (top) and given tamoxifen (TAM) at P8 to turn on reporter gene expression (bottom). At 2 months (P60), mice were given pilocarpine to induce seizures and

mossy fiber sprouting or kept as controls. All analysis was at P120. (*B*) Whole-cell recordings were performed on ChR2-negative dentate granule cells (black circles) and sprouted mossy fiber axons were stimulated with blue (470 nm) LED light delivered through the objective. (*C*) Representative confocal image of a recorded granule cell filled with AlexaFluor 568 (50 μM) during whole-cell recording (levels and gamma adjusted for clarity). Star designates mossy fiber axon; no basal dendrites were present (scale, 10 μm). (*D*) Example traces from cells with no response (top left), single EPSCs (bottom left), and epileptiform bursts (right) after single optogenetic stimulation of ChR2+ granule cells (blue arrows). Scale bar on right applies to all traces. (*E*) Frequency of cells with no response (NR), single EPSCs (Single), and EPSC bursts (Burst) in control and epileptic mice. Number of cells in each category are listed on the graph. (*F*) Three consecutive traces taken from a cell with EPSC bursts. Optogenetic stimulation (blue arrow) evoked an initial EPSC (likely monosynaptic) followed by variably timed burst EPSCs. Gold stars designate detected EPSCs. EPSCs occurring later in the sweep were not counted, as they did not occur within our 100 ms post-stimulus timeframe to be considered part of the burst. (*G*) Jitter (trial to trial variability of EPSC onsets, as standard deviation) taken from the first 3 peaks in an EPSC burst is increased after the first EPSC peak (EPSC jitter: Peak 1, n = 13; Peak 2, n = 13; Peak 3, n = 10; One-way ANOVA, $F_{2,33} = 12.0$, $p = 0.0001$; Tukey's test, Peak 1 vs. Peak 2, $p = 0.0105$; Peak 1 vs. Peak 3, $p < 0.0001$; Peak 2 vs. Peak 3, $p = 0.1544$). High variability in second and third EPSC peaks within a burst suggest that they result from polysynaptic activity.

Summary data presented as mean ± SEM. *$p < 0.05$, ***$p < 0.001$, ns = not significant

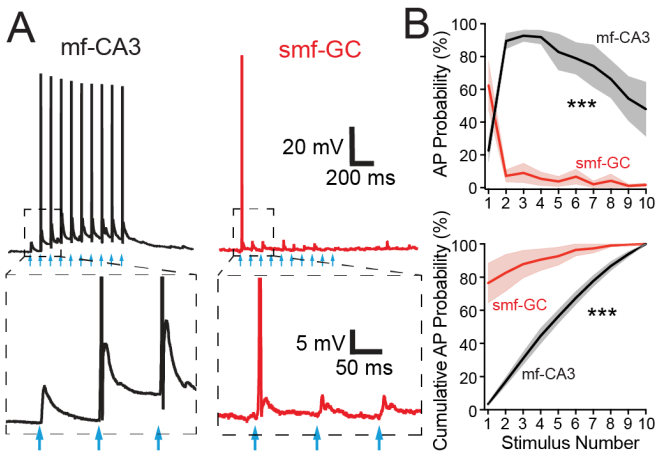

Figure 2: Sprouted mossy fiber activation drives post-synaptic granule cell firing early during brief trains. (*A*) Representative current clamp recordings during mossy fiber – CA3 (mf-CA3, black trace) and sprouted mossy fiber – granule cell (smf-GC, red trace) activation by 10 Hz, 10 pulse LED trains (blue arrows). Dashed boxes represent insets (below) highlighting facilitation of mf-CA3 EPSPs (left) and depression of smf-GC EPSPs (right). (*B*) Action potential (AP) probability (top) is shifted to the first stimulus after smf-GC activation relative to mf-CA3 activation (mf-CA3, n = 6 cells; smf-GC, n = 8 cells, 2-way RM ANOVA, $F_{1,12} = 85.68$, $p < 0.0001$; Sidak's multiple comparisons test, Stimulus 1, $p = 0.0048$, Stimuli 2 – 9, all $p < 0.0001$, Stimulus 10, $p = 0.0006$). Cumulative action potential distribution (bottom) was also significantly shifted (Kolmogorov-Smirnov test, $p = 0.0006$). Summary data presented as mean ± SEM. ***$p < 0.001$

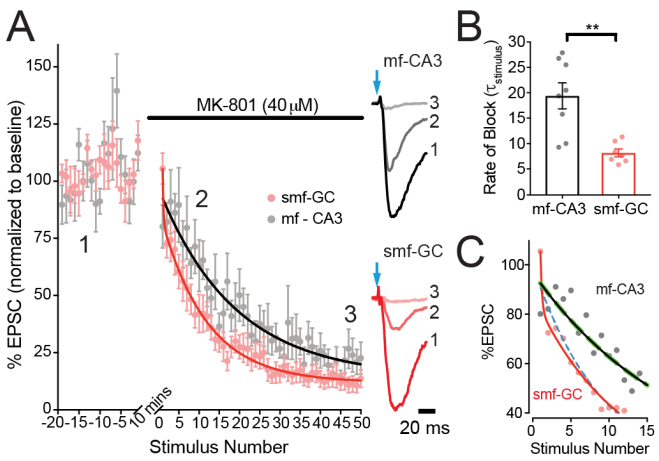

Figure 3: Elevated probability of release at sprouted mossy fiber synapses. (*A*) Probability of release (P_r) was measured from the kinetics of use-dependent MK-801 block of NMDAR-mediated EPSCs during 0.05 Hz LED stimulation. Averaged and normalized responses (left) are plotted before and after bath application of MK-801 (40 μM; mf-CA3, n = 8; smf-GC, n = 7). Representative, peak-scaled NMDAR EPSC averages (right) were taken during baseline, shortly after resuming LED stimulation, and at the end of the experiment, numbered 1, 2, 3, respectively. (*B*) Average rate of MK-801 block measured in individual cells. MK-801 rate of block was significantly faster at sprouted mossy fiber synapses (unpaired t-test, $t_{13} = 3.942$, $p = 0.0017$), indicating higher P_r. (*C*) Same as in (*A*), but only showing the first 15 sweeps in MK-801. Single (solid lines) and double (dashed lines) exponential fits are plotted for smf-GC (red and blue) and mf-CA3 (black and green). Sprouted mossy fibers are better fit by double exponential decays (extra sum of squares F-test, $F_{2,395} = 5.07$, $p = 0.0067$) whereas mf-CA3 synapses are fit identically by single and double models. All data are presented as mean ± s.e.m. **$p < 0.01$

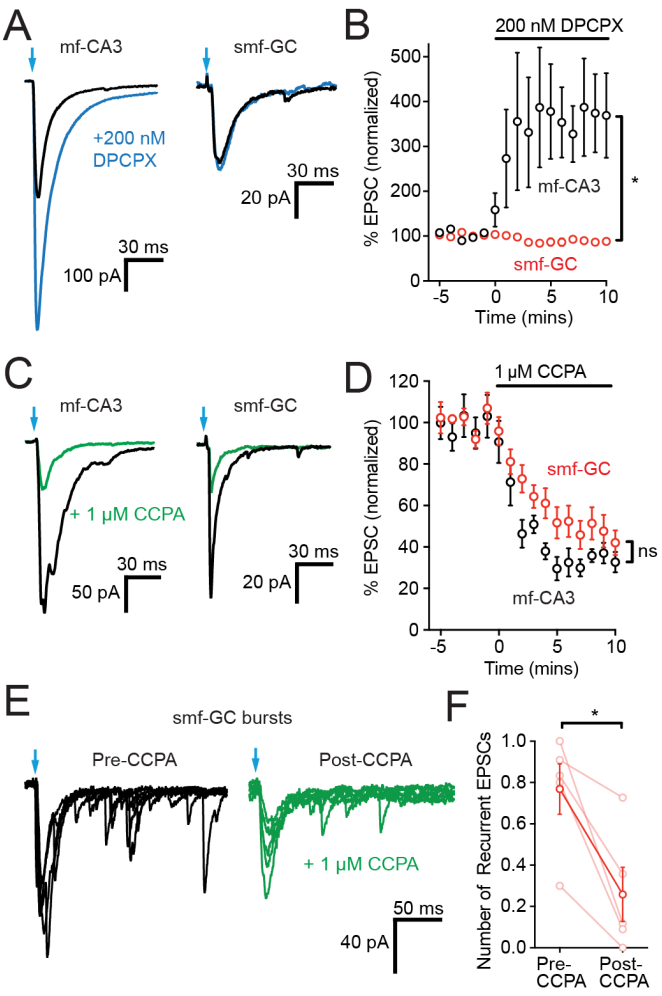

Figure 4: Lack of tonic adenosine contributes to increased release probability and polysynaptic activity. (*A*) Mossy fiber – CA3 (left) and sprouted mossy fiber-GC (right) EPSCs before (black traces) and after (blue traces) washing on the adenosine 1a receptor (A_1R) antagonist DPCPX (200 nM). Bath application of DPCPX facilitates mf-CA3 EPSCs (n = 8 cells, paired t-test, $t_7 = 5.77$, p = 0.0007), but has no effect on EPSC amplitudes at smf-GC synapses (n = 5 cells, paired t-test, $t_4 = 1.39$, p = 0.2364). (*B*) Normalized EPSC amplitudes of mf-CA3 (black, n = 8 cells) and smf-GC (red, n = 5 cells) responses before and during DPCPX administration (unpaired t-test, $t_{11} = 3.63$ p = 0.0040). (*C*) The A_1R

agonist CCPA (1 μM) inhibits both mf-CA3 (left) and smf-GC (right) EPSCs similarly (baseline, black example traces; CCPA, green traces). (*D*) Normalized mf-CA3 (black) and smf-GC (red) EPSC amplitudes during CCPA application, demonstrating intact A_1R responses at both synapses (mf-CA3, n = 7 cells, smf-GC, n = 12 cells; unpaired t-test, $t_{17} = 1.08$, $p = 0.2954$). (*E*) Adenosine A_1R agonism inhibits recurrent polysynaptic network activity evoked by single pulse optogenetic stimulation of sprouted mossy fibers. Examples are 5 consecutive EPSC traces overlaid from the same cell, pre- and post-CCPA (black and green, respectively). (*F*) Quantification of EPSC burst inhibition by CCPA at smf-GC synapses. CCPA (1 μM) reduces the mean number of recurrent EPSCs during a burst (number of recurrent EPSCs per epoch, n = 5 cells, $t_4 = 3.963$, $p = 0.0166$). Summary data presented as mean ± SEM. *$p < 0.05$, ns = not significant

SI Figures:

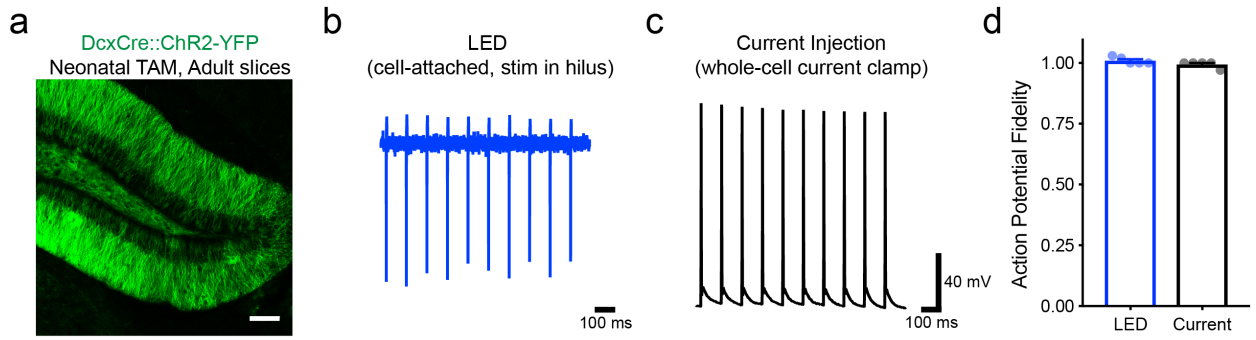

Fig. S1. Action potential fidelity at 10 Hz stimulation in epileptic mice. (A) Single confocal image from DcxCre::ChR2 mouse given tamoxifen neonatally (P8) and perfused at 4 months, demonstrating mature granule cell labeling. Scale bar, 100 μm. (B) Example trace from a cell-attached recording of a ChR2 expressing dentate granule cell from an epileptic mouse reliably firing action potentials in response to optogenetic stimulation at 10 Hz (1 ms LED pulse, 470 nm, 8 mW/cm^3). LED light was delivered via a 40x objective placed over the hilus to trigger antidromic action potential propagation and avoid direct stimulation of ChR2-expressing cell bodies. (C) Example trace from a whole-cell current clamp recording of a dentate granule cell from an epileptic mouse, demonstrating that these cells reliably fire actions potentials during repeated brief current injections (1 ms, 500 pA, 10 Hz). (D) Summary of action potential fidelity upon optogenetic (blue; n = 5) or current-injection (black; n = 5) stimulus trains. Actual potential fidelity potted as number action potentials evoked per LED stimulus. Data plotted as mean ± SEM.

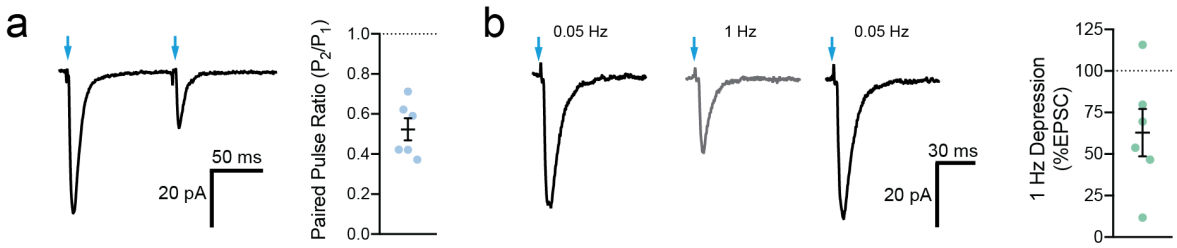

Fig. S2. Sprouted mossy fibers exhibit short-term depression during paired-pulse and 1 Hz stimulation.

(A) Example trace of paired pulse stimulation (100 ms ISI) of sprouted mossy fibers axons (left) and summary plot (right). Sprouted mossy fibers have a low paired-pulse ratio (PPR: 0.523 ± 0.06, n = 6). Blue arrows mark optogenetic stimulation. (B) Example average EPSC responses during baseline (0.05 Hz, left trace), 1 Hz stimulation (middle trace), and recovery (0.05 Hz, right trace). Summary data is plotted on the right. Sprouted mossy fibers display prominent depression during 1 Hz stimulation (%EPSC of baseline: 62.9 ± 14.3%, n = 6). Blue arrows mark optogenetic stimulation. All data presented as mean ± SEM.

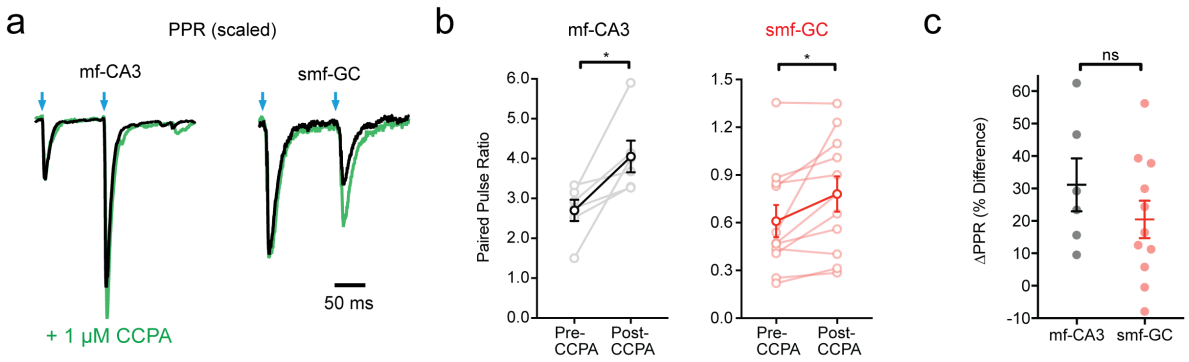

Fig. S3. The A_1R agonist CCPA increases the paired pulse ratio at both mossy fiber – CA3 and sprouted mossy fiber – GC synapses.

(A) Representative EPSCs from paired-pulse experiments (100 ms ISI) from both mf-CA3 (left) and smf-GC (right) recordings before (black traces) and after (green traces) bath application of CCPA (1 μM, A_1R agonist). Traces are scaled and normalized to the first EPSC peak. Larger relative EPSC peaks on the second pulse in CCPA indicates an increased paired-pulse ratio (PPR). (B) Quantification of paired-pulse experiments exemplified in (A). CCPA increases the PPR in both mf-CA3 (left) and smf-GC (right) experiments (PPR, mf-CA3: n = 6, paired t-test, $t_5 = 3.195$, $p = 0.0241$; PPR, smf-GC: n = 11, paired t-test, $t_{10} = 2.74$, $p = 0.0208$). Group averages are overlaid over individual experiments. (C) Change in PPR from bath application of CCPA (% Difference) is similar for mf-CA3 and smf-GC synapses (ΔPPR: mf-CA3, n = 6; smf-GC, n = 11, unpaired t-test, $t_{15} = 1.082$, $p = 0.2962$). All data presented as mean ± SEM. *$p < 0.05$, ns = not significant

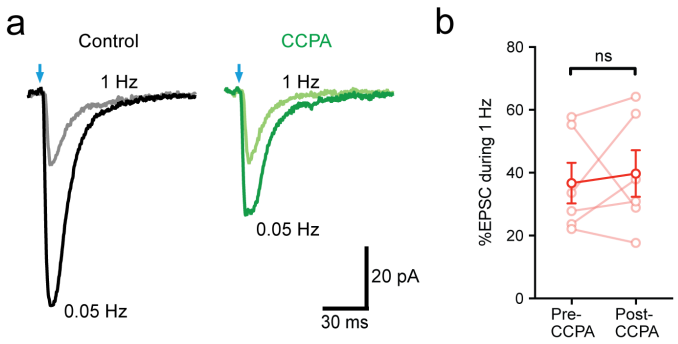

Fig. S4. Restoring A_1R tone with CCPA does not restore frequency-dependent facilitation at sprouted mossy fiber synapses.

(A) Example traces taken at baseline stimulation frequency (0.05 Hz, darker traces) and during 1 Hz frequency trains (lighter traces) before (black traces) and after (green traces) bath application of CCPA (1 μM), demonstrating decreased EPSC amplitudes when evoked at 1 Hz. Examples are taken from the same cell/experiment. Scale bar is the same for both examples. (B) Quantification of experiments shown in (A). Bath application of CCPA does not alter EPSC depression during 1 Hz LED trains (% EPSC during 1 Hz, 50 pulse trains: pre-CCPA, n = 6; t_5 = 0.422, paired t-test, p = 0.6905). All data presented as mean ± SEM, ns = not significant.

Summary and Conclusions

The work presented here focused on understanding the functional contribution of adult neurogenesis in recurrent axonal sprouting and whether these recurrent synapses have properties that could drive excessive or runaway excitation in epileptic brains. In Chapter 1, I used a combination of immunofluoresence and confocal imaging, transgenic mouse lines, and whole-cell electrophysiology from epileptic mice to establish the age-defined cohorts of granule cells that sprout mossy fibers, determine whether they formed functional excitatory synapses, and identified their basic physiologic properties. In Chapter 2, I used whole-cell recordings and optogenetic stimulation to determine if the consequence of “altered” synaptic properties (divergent of that from mf-CA3 synapses) contributed to dentate hyperexcitability and identified a mechanism underlying the high probability of release at these synapses. Overall, these results reveal that sprouted mossy fibers can function to drive hyperexcitability after seizures and sprouted mossy fiber synapses are most likely to form from adult-born dentate granule cells. Whether this directly leads to epileptogenesis will require future study.

Adult-born cells sprout functional recurrent axons in epilepsy

By using a transgenic labeling strategy to non-invasively and permanently label large numbers of adult-born dentate granule cells, I was able to identify the

populations of granule cells that sprout in response to seizures. In fact, all granule cell cohorts, including those born in the neonatal brain, contributed to mossy fiber sprouting, consistent with some reports (Parent et al., 1999; Althaus et al., 2016), but not all (Kron et al., 2010). Discrepancies between the literature and the results presented here might be explained by the robustness of labeling. By counting the total number of boutons in the IML and normalizing to the number of granule cells labeled, we determined a "sprouting ratio" that represents the relative likelihood of any granule cell cohort to contribute to sprouting (Chapter 1). In spite of all granule cells sprouting, the sprouting ratio reveals that sprouted axons are more likely to form from adult-born granule cells. Thus, prior studies using retroviral labeling techniques may have simply missed sprouted fibers from neonatally-born granule cells due to low labeling efficiency. Indeed, in experiments using improved retroviral constructs, a recent report (Althaus et al., 2016) identified sprouted mossy fibers from neonatally-born dentate granule cells, as well as those generated postnatally.

While settling a dispute about which specific populations of granule cells sprout may on the surface seem purely semantic, understanding if and how the developmental stage of granule cells determines their contribution to sprouting is important for interpreting the broader role of adult neurogenesis in the development of epilepsy, particularly if sprouted mossy fibers drive hyperexcitability.

Future Directions – Autaptic connections from adult-born granule cells?

The work presented here documents sprouted mossy fiber synapses from adult-born granule cells forming onto mature, likely neonatally-born granule cells. This assumption is based upon the relatively low number of adult-born granule cells, cellular morphology obtained from cells filled with dye, intrinsic properties (eg. low input resistance, high cell capacitance), and location within the GCL, all of which suggest recordings were made from neonatally-born or at least matured granule cells. However, the development of granule cell dendrites from granule cells born during post-seizure neurogenesis aligns with the approximate timing of mossy fiber sprouting (Wuarin and Dudek, 2001; Overstreet-Wadiche et al., 2006). Therefore, it is conceivable that sprouted mossy fibers might *preferentially* target the maturing dendrites of other adult-born dentate granule cells, or even their own dendritic trees. Autaptic connections or hyper-innervated populations of adult-born granule cells could form micronetworks and "hubs" for excitation to generate within the granule cell layer.

Indeed, preliminary observations suggest this is possible. Using DcxCre::tdT mice to label granule cells born after seizures, super-resolution imaging revealed tdT+ boutons forming putative synapses onto tdT+ granule cell dendrites (Figure 1). Additionally, sprouted mossy fiber boutons from adult-born cells were clustered around tdT+ granule cell dendrites. In my initial attempts at performing autatptic recordings from adult-born granule cells in epileptic mice, I found evidence of autaptically connected granule cells (Figure

1), though the frequency at which they were observed was moderately low for continued analysis (4 of 14 cells with putative autaptic responses). However, recording configurations and experimental approach might not have been optimal, as only autaptic connections were tested, leaving open the possibillity adult-born granule cells contacting *other* adult-born granule cells (ie. not autaptic) were more prevalent throughout the slice.

Enhanced dentate hyperexcitability is a product of high release probability at sprouted synapses

Heightened dentate excitability is a fundamental feature of TLE (Tauck and Nadler, 1985; Wuarin and Dudek, 1996; Okazaki et al., 1999) and how sprouted mossy fibers contribute to hyperexcitability is unclear. The presence of recurrent circuits does not result in hyperexcitability *per se* and even the relevance of mossy fiber sprouting has been questioned (Buckmaster, 2014) due to the requirement that sprouted mossy fibers must be “unmasked” experimentally by increased levels of K^+ (Patrylo and Dudek, 1998; Hardison et al., 2000) or blocking $GABA_A$Rs (Cronin et al., 1992; Patrylo and Dudek, 1998) to facilitate recurrent excitation in slices. Using an optogenetic approach that directly activates sprouted mossy fibers, analysis of their functional impacts could be isolated from other circuit changes and the altered excitatory to inhibitory balance occurring through cell death.

Probability of neurotransmitter release influences the expression of short-term plasticity and the functional impacts a synapse has on circuit dynamics (Abbott and Regehr, 2004; Rothman et al., 2009; Klug et al., 2012). In these experiments, I applied optogenetic activation at sprouted mossy fibers to determine synaptic properties that could reveal their function. Furthermore, I determined how one factor, adenosine —or rather the lack of adenosine— contributes to sprouted mossy fiber function.

Restoring tonic adenosine alters PPR but does not restore frequency facilitation, thus it is possible adenosine is only a single factor in a complex system regulating short-term properties of mossy fiber synapses. Indeed, components of release machinery, including calcium sensors (Jackman et al., 2016) and SNARE-complex interacting molecules (Ben-Simon et al., 2015) are critical for expression of frequency facilitation at mf-CA3 synapses and could be differentially expressed in epilepsy.

It is unclear why sprouted mossy fiber synapses do not express similar characteristics to their healthy mf-CA3 counterparts. Notably, high probability of release is thought to be characteristic of immature mossy fiber synapses (Marchal and Mulle, 2004) and mossy fiber synapses rely upon trans-synaptic signaling to fully mature at mf-CA3 and mf-IN synapses (Williams et al., 2011; Martin et al., 2015). Perhaps the appropriate signaling mechanisms are lacking at recurrent, granule cell - granule cell synapses and sprouted mossy fibers do not fully mature. However, as they can form functional synapses (Chapter 1), the

full maturation and expression of low P_r and short-term facilitation may be independent of bouton formation.

Future Directions – Are adenosine-related proteins absent or mislocalized?

How adenosine regulates sprouted mossy fiber excitability is interesting future line of research, particularly as adenosine injections into the hippocampus can reduce seizure activity (Amorim et al., 2016). Regulation of extracellular adenosine is tightly controlled within the hippocampus. Most hippocampal synapses have some adenosine tone (Moore et al., 2003; Sandau et al., 2016); however, the elevated level of extracellular adenosine at mossy fiber synapses appears to be due to high levels of 5'-ectonucleotidase (NT5E) in stratum lucidum (Zimmermann et al., 1993; Langer et al., 2008), which is notably absent from the IML. Additionally, dysregulation of adenosine metabolism is implicated as a contributing factor in epileptogenesis, where increased adenosine kinase (ADK) levels can cause circuit hyperexcitability (Fedele et al., 2005; Boison, 2008, 2012). Although NT5E is observed on sprouted mossy fiber terminals soon after seizures (Schoen et al., 1999), it is unknown whether these changes persist to longer timelines examined here. In initial experiments examining 5 adenosine-related genes, there was no difference in RNA expression 2 months after pilocarpine treatment (Figure 2). However, this does not exclude the possibility of chronic changes in expression or mislocalization of adenosine-related enzymes and receptors, as protein expression may stabilize at longer time-points after SE and subtle changes specific to the IML could be missed during

whole-dentate preparations, all of which are experiments worthy of further investigation.

Altered functional properties of sprouted mossy fiber are enhanced in adult-born cells

Because adult-born dentate granule cells provide a significant fraction of sprouted mossy fibers in the epileptic brain (Jessberger et al., 2007; Kron et al., 2010; Althaus et al., 2016) (also see Chapter 1), understanding their functional properties is critical for revealing their potential role in driving hyperexcitability. My results are the first to demonstrate functional sprouted synapses from adult-born granule cells from those born *prior* to seizures. This suggests adult-born cells can drive recurrent excitation onto dentate granule cells and potentially drive hyperexcitability.

Interestingly, even though there was strong morphological support for sprouted terminals in the IML from granule cells born *after* seizures (also see Jessberger et al., 2007; Kron et al., 2010; Althaus et al., 2016), there was no physiological evidence of these synapses during optogenetic stimulation and whole-cell recordings. Whether or not this indicates the synapses are non-functional, targeting different cell types or populations, or releasing different neurotransmitter is unclear. Although previous studies do indicate this newborn granule cells born after seizures contribute to seizure activity *in vivo* (Hosford et al., 2016; Hosford et al., 2017), this could arise through independently of mossy

fiber sprouting via other mechanisms such hilar basal dendrites (Ribak et al., 2000; Kelly and Beck, 2017) or ectopic locations of granule cells (Dashtipour et al., 2001; Scharfman et al., 2003a; Pierce et al., 2005; Zhan et al., 2010).

Though sprouted mossy fibers from all cohorts of granule cells lack the frequency-dependent facilitation characteristic of mf-CA3 synapses and acquire 1 Hz depression (at least from those cohorts where functional synapses were identified), sprouted mossy fibers from adult-born cells had higher levels of frequency depression. Notably, sprouted fibers from these cells retained similar functional properties to other sprouted mossy fibers such as paired-pulse depression, DCG-IV sensitivity, and high NMDAR activation. On the surface, this suggests adult-born granule cells born immediately prior to seizures are less capable of propagating recurrent excitation. However, because 1 Hz and paired-pulse depression is associated with the switch from "conditional detonation" to "early detonation" and the degree of 1 Hz depression is further increased in this population, this actually suggests sprouted mossy fibers from adult-born cells may have an even greater early detonation phenotype and thus more strongly drive recurrent activation and bursts of EPSCs.

Future Directions – Release of GABA from "silent" sprouted mossy fibers?

The functional properties of sprouted synapses are regulated, at least in part, by the absence of tonic adenosine within the IML (Chapter 2). However, this does not explain why sprouted mossy fibers from adult-born neurons show greater levels of depression during 1 Hz stimulation. Therefore, it would be

interesting to determine whether these sprouted fibers have an even higher probability of release than their neonatally-derived counterparts and whether adenosine signaling or other mechanisms conferring synaptic facilitation are more severely impaired in these cells. Targeted genetic comparisons of granule cells born neonatally and in the adult brain via TU-tagging or laser-capture (Chatzi et al., 2016; Chatzi et al., 2019) may reveal subtle expression differences of key pathways of synaptic maturation (Chatzi et al., 2016) and regulators of facilitation (Ben-Simon et al., 2015; Jackman et al., 2016).

Heightened activity of adult-born cells could also result in plasticity neurotransmitter phenotypes. High levels of activity, including seizures, can induce expression of glutamic acid decarboxylase (GAD) (Ramírez and Gutiérrez, 2001), the enzyme responsible for GABA synthesis from glutamate, in mossy fiber terminals. Indeed, following seizure induction with kainic acid or electrical kindling, stimulation mf-CA3 synapses can produce monosynaptic *inhibition*, suggesting release of GABA from mossy fiber terminals (Gutiérrez, 2000; Gutiérrez and Heinemann, 2001; Gutierrez et al., 2003). Do sprouted mossy fibers transiently or permanently release GABA onto granule cells? Preliminary immunofluorescence experiments indicate increased GAD expression in sprouted terminals from adult-born cells (Figure 3). Technical limitations of the *DcxCre* mouse line prevented obtaining any functional evidence of GABA release; therefore, whether sprouted mossy fibers release GABA following seizures and how this would impact circuit function remains unknown. Alternative mouse lines with less off-target interneuron labeling such

as the *AsclCreER*^{T2} (Yang et al., 2015) or *POMC-Cre* (Gao et al., 2007; Zucca et al., 2017) lines may sacrifice temporal specificity, but provide greater cellular specificity and allow an unambiguous functional result.

Implications for epileptogenesis

Sprouted mossy fibers have remained an attractive mechanism for epileptogenesis; however, this view is not held universally and is still being debated (Buckmaster, 2014). In reality, the contribution of *any* one circuit rearrangement is unlikely to be sufficient to drive the development of epilepsy on its own. It is most likely a combination of various circuit changes, some of which discussed here, contribute to the development of epilepsy. Of course, this should not imply mossy fiber sprouting is unimportant; sprouted mossy fibers drive hyperexcitability in the dentate gyrus, which is a prominent feature of TLE (Babb et al., 1984a; Tauck and Nadler, 1985; Santhakumar et al., 2005; Sloviter et al., 2006b).

Additionally, the influence sprouted mossy fibers have on seizure generation is also dependent on other systems influencing the properties of these synapses. For example, the levels of tonic adenosine surrounding sprouted mossy fibers influence their functional properties and their ultimate impact on the dentate (Chapter 2), and is a system that is likely independent of sprouting (Boison, 2012). Therefore, sprouted mossy fibers, in combination with, and modulated by other circuit changes, gene expression, and neural excitability

(McNamara, 1994; Chang and Lowenstein 2003) are expected to contribute to the development of epilepsy.

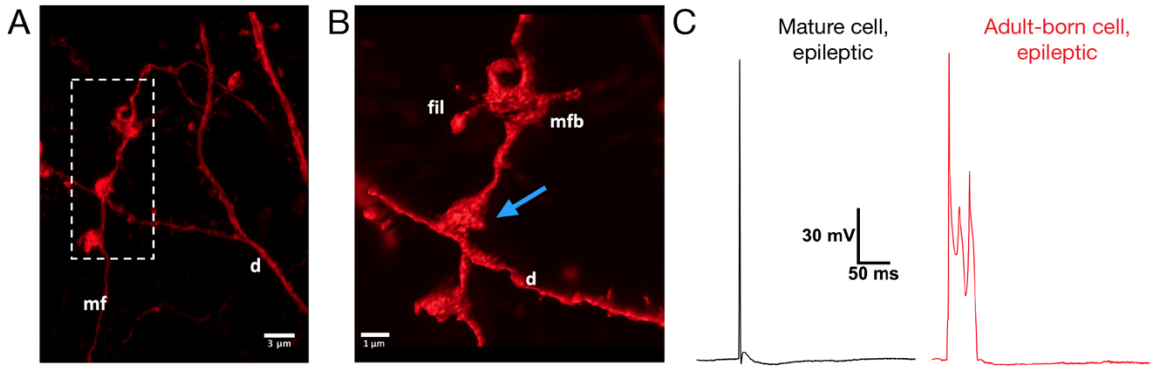

Figure 1: Autaptic connections from adult-born dentate granule cells

A) Super-resolution AiryScan image (10 µm z-stack) showing a cluster of adult-born (tdT+, red) sprouted mossy fiber boutons (mf) around adult-born granule cell dendrites (d) and site of putative crossing (dashed box).

B) 3D surface rendering of dashed box in (A). Blue arrow marks the site of a putative synapse. The main mossy fiber bouton (mfb) and filopodia (f) can be resolved.

C) Whole-cell current clamp recordings from tdT- (left, black trace) and tdT+ (right, red trace) granule cells from the same epileptic animal. The tdT+ cell was observed to have a recurrent axon projecting into its dendrites. Granule cells were given a 400 pA, 1 ms current injection to drive a single action potential. Note increased excitability in tdT+ cell in response to the same size and length current step.

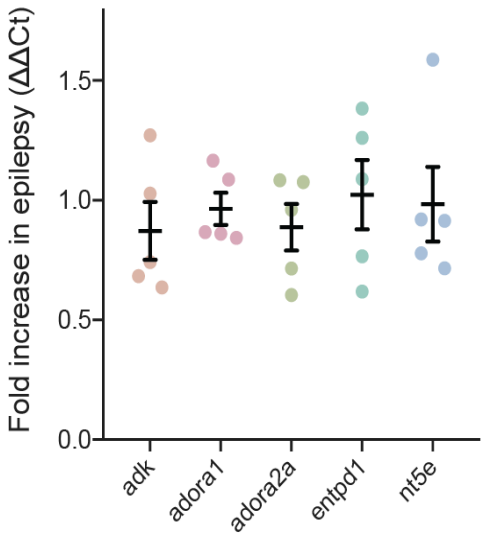

Figure 2: Expression of adenosine-related enzymes and receptors is stable by 2 months after pilocarpine

Fold change in gene expression in dentate gyri from epileptic mice (ΔΔCt) of adenosine kinase (adk), adenosine receptor 1 (adora1), adenosine receptor 2a (adora2a), ectonucleoside triphosphate diphosphohydrolase 1 (entpd1), 5'-ectonucleotidase (nt5e). No differences were observed between control and epileptic conditions for any genes. Dentate gyri were dissected from control and epileptic mice, homogenated in Trizol, and cDNA isolated from RNA. Gene expression was quantified with qPCR. Values of 1 indicate no change in following pilocarpine treatment.

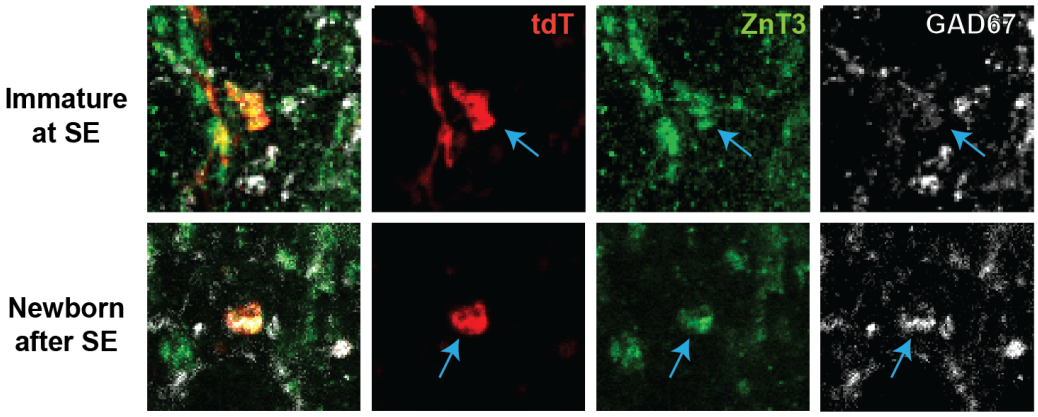

Figure 3: Increased GAD expression in sprouted mossy fibers from adult-born dentate granule cells

Single confocal section demonstrating the presence of GAD67 in sprouted mossy fiber boutons. Sprouted mossy fiber boutons born either before (top) or newborn after (bottom) SE were identified with tdT and ZnT3 co-labeling in the IML of epileptic mice. Sprouted mossy fibers from granule cells born after SE were observed to have higher levels of colocalization with GAD67.

References

Abbott LF, Regehr WG (2004) Synaptic computation. Nature 431:796-803.

Acsady L, Kamondi A, Sik A, Freund T, Buzsaki G (1998) GABAergic cells are the major postsynaptic targets of mossy fibers in the rat hippocampus. J Neurosci 18:3386-3403.

Althaus AL, Zhang H, Parent JM (2016) Axonal plasticity of age-defined dentate granule cells in a rat model of mesial temporal lobe epilepsy. Neurobiol Dis 86:187-196.

Amaral DG, Scharfman HE, Lavenex P (2007) The dentate gyrus: fundamental neuroanatomical organization (dentate gyrus for dummies). Prog Brain Res 163:3-790.

Amorim BO, Hamani C, Ferreira E, Miranda MF, Fernandes MJS, Rodrigues AM, de Almeida AG, Covolan L (2016) Effects of A1 receptor agonist/antagonist on spontaneous seizures in pilocarpine-induced epileptic rats. Epilepsy Behav 61:168-173.

Anderson V, Catroppa C, Morse S, Haritou F, Rosenfeld J (2005) Functional plasticity or vulnerability after early brain injury? Pediatrics 116:1374-1382.

Artinian J, Peret A, Marti G, Epsztein J, Crepel V (2011) Synaptic kainate receptors in interplay with INaP shift the sparse firing of dentate granule cells to a sustained rhythmic mode in temporal lobe epilepsy. J Neurosci 31:10811-10818.

Babb TL, Lieb JP, Brown WJ, Pretorius J, Crandall PH (1984a) Distribution of pyramidal cell density and hyperexcitability in the epileptic human hippocampal formation. Epilepsia 25:721-728.

Babb TL, Brown WJ, Pretorius J, Davenport C, Lieb JP, Crandall PH (1984b) Temporal lobe volumetric cell densities in temporal lobe epilepsy. Epilepsia 25:729-740.

Ben-Simon Y, Rodenas-Ruano A, Alvina K, Lam AD, Stuenkel EL, Castillo PE, Ashery U (2015) A Combined Optogenetic-Knockdown Strategy Reveals a Major Role of Tomosyn in Mossy Fiber Synaptic Plasticity. Cell Rep 12:396-404.

Bender RA, Dubé C, Gonzalez-Vega R, Mina EW, Baram TZ (2003) Mossy fiber plasticity and enhanced hippocampal excitability, without hippocampal cell loss or altered neurogenesis, in an animal model of prolonged febrile seizures. Hippocampus 13:399-412.

Bengzon J, Kokaia Z, Elmer E, Nanobashvili A, Kokaia M, Lindvall O (1997) Apoptosis and proliferation of dentate gyrus neurons after single and intermittent limbic seizures. Proc Natl Acad Sci U S A 94:10432-10437.

Bischofberger J, Engel D, Frotscher M, Jonas P (2006) Timing and efficacy of transmitter release at mossy fiber synapses in the hippocampal network. Pflugers Arch 453:361-372.

Boison D (2008) The adenosine kinase hypothesis of epileptogenesis. Prog Neurobiol 84:249-262.

Boison D (2012) Adenosine dysfunction in epilepsy. Glia 60:1234-1243.

Brown JP, Couillard-Despres S, Cooper-Kuhn CM, Winkler J, Aigner L, Kuhn HG (2003) Transient expression of doublecortin during adult neurogenesis. J Comp Neurol 467:1-10.

Buckmaster PS (2012) Mossy Fiber Sprouting in the Dentate Gyrus. Jasper's Basic Mechanisms of the Epilepsies.

Buckmaster PS (2014) Does Mossy Fiber Sprouting Give Rise to the Epileptic State? In: Issues in Clinical Epileptology: A View from the Bench (Scharfman HE, Buckmaster PS, eds), pp 161-168. Dordrecht: Springer Netherlands.

Buckmaster PS, Dudek FE (1997) Neuron loss, granule cell axon reorganization, and functional changes in the dentate gyrus of epileptic kainate-treated rats. J Comp Neurol 385:385-404.

Buckmaster PS, Lew FH (2011) Rapamycin Suppresses Mossy Fiber Sprouting But Not Seizure Frequency in a Mouse Model of Temporal Lobe Epilepsy. Journal of Neuroscience 31:2337-2347.

Buckmaster PS, Zhang GF, Yamawaki R (2002) Axon Sprouting in a Model of Temporal Lobe Epilepsy Creates a Predominantly Excitatory Feedback Circuit. The Journal of Neuroscience 22:6650-6658.

Bui AD, Nguyen TM, Limouse C, Kim HK, Szabo GG, Felong S, Maroso M, Soltesz I (2018) Dentate gyrus mossy cells control spontaneous convulsive seizures and spatial memory. Science 359:787-790.

Castillo PE, Salin PA, Weisskopf MG, Nicoll RA (1996) Characterizing the Site and Mode of Action of Dynorphin at Hippocampal Mossy Fiber Synapses in the Guinea Pig. The Journal of Neuroscience 16:5942-5950.

Cavalheiro EA, Santos NF, Priel MR (1996) The Pilocarpine Model of Epilepsy in Mice. Epilepsia 37:1015-1019.

Cavazos JE, Zhang P, Qazi R, Sutula TP (2003) Ultrastructural features of sprouted mossy fiber synapses in kindled and kainic acid-treated rats. J Comp Neurol 458:272-292.

Chang BS, Lowenstein DH (2003) Epilepsy. New England Journal of Medicine 349:1257-1266.

Chatzi C, Zhang Y, Shen R, Westbrook GL, Goodman RH (2016) Transcriptional profiling of newly generated dentate granule cells using TU tagging reveals pattern shifts in gene expression during circuit integration. eNeuro 3.

Chatzi C, Zhang Y, Hendricks WD, Chen Y, Schnell E, Goodman RH, Westbrook GL (2019) Exercise-induced enhancement of synaptic function triggered by the inverse BAR protein, Mtss1L. bioRxiv:545582.

Cheng X, Li Y, Huang Y, Feng X, Feng G, Xiong ZQ (2011) Pulse labeling and long-term tracing of newborn neurons in the adult subgranular zone. Cell Res 21:338-349.

Cho KO, Lybrand ZR, Ito N, Brulet R, Tafacory F, Zhang L, Good L, Ure K, Kernie SG, Birnbaum SG, Scharfman HE, Eisch AJ, Hsieh J (2015)

Aberrant hippocampal neurogenesis contributes to epilepsy and associated cognitive decline. Nat Commun 6:6606.

Cronin J, Obenaus A, Houser CR, Dudek FE (1992) Electrophysiology of dentate granule cells after kainate-induced synaptic reorganization of the mossy fibers. Brain Res 573:305-310.

Danzer SC, He X, Loepke AW, McNamara JO (2009) Structural plasticity of dentate granule cell mossy fibers during the development of limbic epilepsy. Hippocampus:NA-NA.

Dashtipour K, Tran PH, Okazaki MM, Nadler JV, Ribak CE (2001) Ultrastructural features and synaptic connections of hilar ectopic granule cells in the rat dentate gyrus are different from those of granule cells in the granule cell layer. Brain research 890:261-271.

Dayan E, Cohen LG (2011) Neuroplasticity subserving motor skill learning. Neuron 72:443-454.

de Lanerolle NC, Kim JH, Robbins RJ, Spencer DD (1989) Hippocampal interneuron loss and plasticity in human temporal lobe epilepsy. Brain Res 495:387-395.

DeGiorgio CM, Tomiyasu U, Gott PS, Treiman DM (1992) Hippocampal pyramidal cell loss in human status epilepticus. Epilepsia 33:23-27.

Dimyan MA, Cohen LG (2011) Neuroplasticity in the context of motor rehabilitation after stroke. Nature Reviews Neurology 7:76.

Doherty J, Dingledine R (2001) Reduced excitatory drive onto interneurons in the dentate gyrus after status epilepticus. J Neurosci 21:2048-2057.

Draganski B, Gaser C, Busch V, Schuierer G, Bogdahn U, May A (2004) Neuroplasticity: changes in grey matter induced by training. Nature 427:311.

Dubois NC, Hofmann D, Kaloulis K, Bishop J, Trumpp A (2006) Nestin-Cre transgenic mouse line Nes-Cre1 mediates highly efficient Cre/loxP mediated recombination in the nervous system, kidney, and somite-derived tissues. genesis 44:355-360.

Ekonomou A, Sperk G, Kostopoulos G, Angelatou F (2000) Reduction of A1 adenosine receptors in rat hippocampus after kainic acid-induced limbic seizures. Neuroscience Letters 284:49-52.

Engel J (2013) Seizures and epilepsy: Oxford University Press.

Epsztein J, Represa A, Jorquera I, Ben-Ari Y, Crepel V (2005) Recurrent mossy fibers establish aberrant kainate receptor-operated synapses on granule cells from epileptic rats. J Neurosci 25:8229-8239.

Fedele DE, Gouder N, Güttinger M, Gabernet L, Scheurer L, Rülicke T, Crestani F, Boison D (2005) Astrogliosis in epilepsy leads to overexpression of adenosine kinase, resulting in seizure aggravation. Brain 128:2383-2395.

Feng L, Molnár P, Nadler JV (2003) Short-Term Frequency-Dependent Plasticity at Recurrent Mossy Fiber Synapses of the Epileptic Brain. The Journal of Neuroscience 23:5381-5390.

Frotscher M, Zimmer J (1983) Lesion-induced mossy fibers to the molecular layer of the rat fascia dentata: Identification of postsynaptic granule cells

by the Golgi-EM technique. Journal of Comparative Neurology 215:299-311.

Gao X, Arlotta P, Macklis JD, Chen J (2007) Conditional Knock-Out of -Catenin in Postnatal-Born Dentate Gyrus Granule Neurons Results in Dendritic Malformation. Journal of Neuroscience 27:14317-14325.

Golarai G, Sutula TP (1996) Functional alterations in the dentate gyrus after induction of long-term potentiation, kindling, and mossy fiber sprouting. Journal of Neurophysiology 75:343-353.

Gouder N, Fritschy JM, Boison D (2003) Seizure suppression by adenosine A1 receptor activation in a mouse model of pharmacoresistant epilepsy. Epilepsia 44:877-885.

Gould E, Tanapat P, McEwen BS, Flügge G, Fuchs E (1998) Proliferation of granule cell precursors in the dentate gyrus of adult monkeys is diminished by stress. Proceedings of the National Academy of Sciences 95:3168-3171.

Goussakov IV, Fink K, Elger CE, Beck H (2000) Metaplasticity of Mossy Fiber Synaptic Transmission Involves Altered Release Probability. The Journal of Neuroscience 20:3434-3441.

Gu Y, Arruda-Carvalho M, Wang J, Janoschka SR, Josselyn SA, Frankland PW, Ge S (2012) Optical controlling reveals time-dependent roles for adult-born dentate granule cells. Nat Neurosci 15:1700-1706.

Gutierrez R, Romo-Parra H, Maqueda J, Vivar C, Ramirez M, Morales MA, Lamas M (2003) Plasticity of the GABAergic phenotype of the

"glutamatergic" granule cells of the rat dentate gyrus. J Neurosci 23:5594-5598.

Gutiérrez R (2000) Seizures Induce Simultaneous GABAergic and Glutamatergic Transmission in the Dentate Gyrus-CA3 System. Journal of Neurophysiology 84:3088-3090.

Gutiérrez R, Heinemann U (2001) Kindling induces transient fast inhibition in the dentate gyrus-CA3 projection: Kindling induces fast inhibition in the DG-CA3 projection. European Journal of Neuroscience 13:1371-1379.

Guzman SJ, Schlogl A, Frotscher M, Jonas P (2016) Synaptic mechanisms of pattern completion in the hippocampal CA3 network. Science 353:1117-1123.

Hardison JL, Okazaki MM, Nadler JV (2000) Modest increase in extracellular potassium unmasks effect of recurrent mossy fiber growth. J Neurophysiol 84:2380-2389.

Harris EW, Cotman CW (1986) Long-term potentiation of guinea pig mossy fiber responses is not blocked by N-methyl D-aspartate antagonists. Neuroscience letters 70:132-137.

Hauser WA, Hesdorffer DC (1990) Epilepsy: frequency, causes, and consequences: Epilepsy Foundation of America Landover, MD.

Haussler U, Rinas K, Kilias A, Egert U, Haas CA (2016) Mossy fiber sprouting and pyramidal cell dispersion in the hippocampal CA2 region in a mouse model of temporal lobe epilepsy. Hippocampus 26:577-588.

Hendricks WD, Chen Y, Bensen AL, Westbrook GL, Schnell E (2017) Short-Term Depression of Sprouted Mossy Fiber Synapses from Adult-Born Granule Cells. J Neurosci 37:5722-5735.

Heng K, Haney MM, Buckmaster PS (2013) High-dose rapamycin blocks mossy fiber sprouting but not seizures in a mouse model of temporal lobe epilepsy. Epilepsia 54:1535-1541.

Hensch TK (2005) Critical period plasticity in local cortical circuits. Nature Reviews Neuroscience 6:877.

Henze DA, Urban NN, Barrionuevo G (2000) The multifarious hippocampal mossy fiber pathway: a review. Neuroscience 98:407-427.

Henze DA, Wittner L, Buzsaki G (2002) Single granule cells reliably discharge targets in the hippocampal CA3 network in vivo. Nat Neurosci 5:790-795.

Hosford BE, Liska JP, Danzer SC (2016) Ablation of Newly Generated Hippocampal Granule Cells Has Disease-Modifying Effects in Epilepsy. Journal of Neuroscience 36:11013-11023.

Hosford BE, Rowley S, Liska JP, Danzer SC (2017) Ablation of peri-insult generated granule cells after epilepsy onset halts disease progression. Scientific Reports 7.

Houser CR, Miyashiro JE, Swartz BE, Walsh GO, Rich JR, Delgado-Escueta AV (1990) Altered patterns of dynorphin immunoreactivity suggest mossy fiber reorganization in human hippocampal epilepsy. J Neurosci 10:267-282.

Huang X, Zhang H, Yang J, Wu J, McMahon J, Lin Y, Cao Z, Gruenthal M, Huang Y (2010) Pharmacological inhibition of the mammalian target of rapamycin pathway suppresses acquired epilepsy. Neurobiol Dis 40:193-199.

Hunt DL, Puente N, Grandes P, Castillo PE (2013) Bidirectional NMDA receptor plasticity controls CA3 output and heterosynaptic metaplasticity. Nature Neuroscience 16:1049.

Jackman SL, Turecek J, Belinsky JE, Regehr WG (2016) The calcium sensor synaptotagmin 7 is required for synaptic facilitation. Nature 529:88.

Jessberger S, Romer B, Babu H, Kempermann G (2005) Seizures induce proliferation and dispersion of doublecortin-positive hippocampal progenitor cells. Exp Neurol 196:342-351.

Jessberger S, Zhao C, Toni N, Clemenson GD, Li Y, Gage FH (2007) Seizure-Associated, Aberrant Neurogenesis in Adult Rats Characterized with Retrovirus-Mediated Cell Labeling. Journal of Neuroscience 27:9400-9407.

Jonas P, Major G, Sakmann B (1993) Quantal components of unitary EPSCs at the mossy fibre synapse on CA3 pyramidal cells of rat hippocampus. The Journal of Physiology 472:615-663.

Jung K-H, Chu K, Lee S-T, Kim J, Sinn D-I, Kim J-M, Park D-K, Lee J-J, Kim SU, Kim M (2006) Cyclooxygenase-2 inhibitor, celecoxib, inhibits the altered hippocampal neurogenesis with attenuation of spontaneous recurrent seizures following pilocarpine-induced status epilepticus. Neurobiology of disease 23:237-246.

Jung KH, Chu K, Kim M, Jeong SW, Song YM, Lee ST, Kim JY, Lee SK, Roh JK (2004) Continuous cytosine-b-D-arabinofuranoside infusion reduces ectopic granule cells in adult rat hippocampus with attenuation of spontaneous recurrent seizures following pilocarpine-induced status epilepticus. Eur J Neurosci 19:3219-3226.

Jung M, McNaughton B (1993) Spatial selectivity of unit activity in the hippocampal granular layer. Hippocampus 3:165-182.

Kanamatsu T, Obie J, Grimes L, McGinty JF, Yoshikawa K, Sabol S, Hong JS (1986) Kainic acid alters the metabolism of Met5-enkephalin and the level of dynorphin A in the rat hippocampus. J Neurosci 6:3094-3102.

Kelly T, Beck H (2017) Functional properties of granule cells with hilar basal dendrites in the epileptic dentate gyrus. Epilepsia 58:160-171.

Kempermann G, Kuhn HG, Gage FH (1998) Experience-induced neurogenesis in the senescent dentate gyrus. Journal of Neuroscience 18:3206-3212.

Kerchner GA, Nicoll RA (2008) Silent synapses and the emergence of a postsynaptic mechanism for LTP. Nature Reviews Neuroscience 9:813.

Klug A, Borst JGG, Carlson BA, Kopp-Scheinpflug C, Klyachko VA, Xu-Friedman MA (2012) How do short-term changes at synapses fine-tune information processing? Journal of Neuroscience 32:14058-14063.

Kourdougli N, Pellegrino C, Renko JM, Khirug S, Chazal G, Kukko-Lukjanov TK, Lauri SE, Gaiarsa JL, Zhou L, Peret A (2017) Depolarizing GABA contributes to glutamatergic network rewiring in epilepsy. Annals of Neurology.

Kron MM, Zhang H, Parent JM (2010) The Developmental Stage of Dentate Granule Cells Dictates Their Contribution to Seizure-Induced Plasticity. Journal of Neuroscience 30:2051-2059.

Kuhn HG, Dickinson-Anson H, Gage FH (1996) Neurogenesis in the dentate gyrus of the adult rat: age-related decrease of neuronal progenitor proliferation. J Neurosci 16:2027-2033.

Kwon H-B, Castillo PE (2008) Long-term potentiation selectively expressed by NMDA receptors at hippocampal mossy fiber synapses. Neuron 57:108-120.

Langer D, Hammer K, Koszalka P, Schrader J, Robson S, Zimmermann H (2008) Distribution of ectonucleotidases in the rodent brain revisited. Cell and Tissue Research 334:199-217.

Leutgeb JK, Leutgeb S, Moser M-B, Moser EI (2007) Pattern separation in the dentate gyrus and CA3 of the hippocampus. science 315:961-966.

Levin HS (2003) Neuroplasticity following non-penetrating traumatic brain injury. Brain Inj 17:665-674.

Lewis PF, Emerman M (1994) Passage through mitosis is required for oncoretroviruses but not for the human immunodeficiency virus. J Virol 68:510-516.

Lledo P-M, Alonso M, Grubb MS (2006) Adult neurogenesis and functional plasticity in neuronal circuits. Nature Reviews Neuroscience 7:179-193.

Longo BM, Mello LEAM (1997) Blockade of pilocarpine- or kainate-induced mossy fiber sprouting by cycloheximide does not prevent subsequent epileptogenesis in rats. Neuroscience Letters 226:163-166.

Longo BM, Mello LEAM (1998) Supragranular mossy fiber sprouting is not necessary for spontaneous seizures in the intrahippocampal kainate model of epilepsy in the rat. Epilepsy Research 32:172-182.

Löscher W (2011) Critical review of current animal models of seizures and epilepsy used in the discovery and development of new antiepileptic drugs. Seizure 20:359-368.

Löscher W (2017) Animal Models of Seizures and Epilepsy: Past, Present, and Future Role for the Discovery of Antiseizure Drugs. Neurochemical Research 42:1873-1888.

Lynch M, Sutula T (2000) Recurrent Excitatory Connectivity in the Dentate Gyrus of Kindled and Kainic Acid–Treated Rats. Journal of Neurophysiology 83:693-704.

Lynch M, Sayin U, Golarai G, Sutula T (2000) NMDA receptor-dependent plasticity of granule cell spiking in the dentate gyrus of normal and epileptic rats. J Neurophysiol 84:2868-2879.

Magiorkinis E, Sidiropoulou K, Diamantis A (2010) Hallmarks in the history of epilepsy: epilepsy in antiquity. Epilepsy Behav 17:103-108.

Malenka RC, Bear MF (2004) LTP and LTD: an embarrassment of riches. Neuron 44:5-21.

Manita S, Kawamura Y, Sato K, Inoue M, Kudo Y, Miyakawa H (2004) Adenosine A1-receptor-mediated tonic inhibition of glutamate release at rat hippocampal CA3–CA1 synapses is primarily due to inhibition of N-type Ca2+ channels. European Journal of Pharmacology 499:265-274.

Marchal C, Mulle C (2004) Postnatal maturation of mossy fibre excitatory transmission in mouse CA3 pyramidal cells: a potential role for kainate receptors. The Journal of Physiology 561:27-37.

Martin EA, Muralidhar S, Wang Z, Cervantes DC, Basu R, Taylor MR, Hunter J, Cutforth T, Wilke SA, Ghosh A, Williams ME (2015) The intellectual disability gene Kirrel3 regulates target-specific mossy fiber synapse development in the hippocampus. eLife 4:e09395.

Masukawa LM, Wang H, O'Connor MJ, Uruno K (1996) Prolonged field potentials evoked by 1 Hz stimulation in the dentate gyrus of temporal lobe epileptic human brain slices. Brain Res 721:132-139.

McGinty JF, Henriksen SJ, Goldstein A, Terenius L, Bloom FE (1983) Dynorphin is contained within hippocampal mossy fibers: immunochemical alterations after kainic acid administration and colchicine-induced neurotoxicity. Proceedings of the National Academy of Sciences 80:589-593.

McNamara J (1994) Cellular and molecular basis of epilepsy. The Journal of Neuroscience 14:3413-3425.

Mello LE, Cavalheiro EA, Tan AM, Kupfer WR, Pretorius JK, Babb TL, Finch DM (1993) Circuit mechanisms of seizures in the pilocarpine model of chronic epilepsy: cell loss and mossy fiber sprouting. Epilepsia 34:985-995.

Mellor J, Nicoll RA (2001) Hippocampal mossy fiber LTP is independent of postsynaptic calcium. Nature neuroscience 4:125.

Mistry R, Dennis S, Frerking M, Mellor JR (2011) Dentate gyrus granule cell firing patterns can induce mossy fiber long-term potentiation in vitro. Hippocampus 21:1157-1168.

Molnar P, Nadler JV (1999) Mossy fiber-granule cell synapses in the normal and epileptic rat dentate gyrus studied with minimal laser photostimulation. J Neurophysiol 82:1883-1894.

Molnár P, Nadler JV (1999) Mossy Fiber–Granule Cell Synapses in the Normal and Epileptic Rat Dentate Gyrus Studied With Minimal Laser Photostimulation. Journal of Neurophysiology 82:1883-1894.

Moore KA, Nicoll RA, Schmitz D (2003) Adenosine Gates Synaptic Plasticity at Hippocampal Mossy Fiber Synapses. Proceedings of the National Academy of Sciences of the United States of America 100:14397-14402.

Münte TF, Altenmüller E, Jäncke L (2002) The musician's brain as a model of neuroplasticity. Nature Reviews Neuroscience 3:473.

Nadler JV, Perry BW, Cotman CW (1980) Selective reinnervation of hippocampal area CA1 and the fascia dentata after destruction of CA3-CA4 afferents with kainic acid. Brain Res 182:1-9.

Nicoll RA, Malenka RC (1995) Contrasting properties of two forms of long-term potentiation in the hippocampus. Nature 377:115-118.

Nicoll RA, Schmitz D (2005) Synaptic plasticity at hippocampal mossy fibre synapses. Nat Rev Neurosci 6:863-876.

Okazaki MM, Evenson DA, Nadler JV (1995) Hippocampal mossy fiber sprouting and synapse formation after status epilepticus in rats: visualization after retrograde transport of biocytin. J Comp Neurol 352:515-534.

Okazaki MM, Molnár P, Nadler JV (1999) Recurrent Mossy Fiber Pathway in Rat Dentate Gyrus: Synaptic Currents Evoked in Presence and Absence of Seizure-Induced Growth. Journal of Neurophysiology 81:1645-1660.

Overstreet-Wadiche LS, Bromberg DA, Bensen AL, Westbrook GL (2006) Seizures accelerate functional integration of adult-generated granule cells. J Neurosci 26:4095-4103.

Parent JM (2007) Adult neurogenesis in the intact and epileptic dentate gyrus. Prog Brain Res 163:529-540.

Parent JM, Tada E, Fike JR, Lowenstein DH (1999) Inhibition of Dentate Granule Cell Neurogenesis with Brain Irradiation Does Not Prevent Seizure-Induced Mossy Fiber Synaptic Reorganization in the Rat. The Journal of Neuroscience 19:4508-4519.

Parent JM, Elliott RC, Pleasure SJ, Barbaro NM, Lowenstein DH (2006) Aberrant seizure-induced neurogenesis in experimental temporal lobe epilepsy. Annals of Neurology 59:81-91.

Parent JM, Yu TW, Leibowitz RT, Geschwind DH, Sloviter RS, Lowenstein DH (1997) Dentate Granule Cell Neurogenesis Is Increased by Seizures and Contributes to Aberrant Network Reorganization in the Adult Rat Hippocampus. The Journal of Neuroscience 17:3727-3738.

Patrylo PR, Dudek FE (1998) Physiological unmasking of new glutamatergic pathways in the dentate gyrus of hippocampal slices from kainate-induced epileptic rats. J Neurophysiol 79:418-429.

Patrylo PR, Schweitzer JS, Dudek FE (1999) Abnormal responses to perforant path stimulation in the dentate gyrus of slices from rats with kainate-induced epilepsy and mossy fiber reorganization. Epilepsy Research 36:31-42.

Peret A, Christie LA, Ouedraogo DW, Gorlewicz A, Epsztein J, Mulle C, Crepel V (2014) Contribution of aberrant GluK2-containing kainate receptors to chronic seizures in temporal lobe epilepsy. Cell Rep 8:347-354.

Pierce JP, Melton J, Punsoni M, McCloskey DP, Scharfman HE (2005) Mossy fibers are the primary source of afferent input to ectopic granule cells that are born after pilocarpine-induced seizures. Experimental neurology 196:316-331.

Ramírez M, Gutiérrez R (2001) Activity-dependent expression of GAD67 in the granule cells of the rat hippocampus. Brain Research 917:139-146.

Represa A, Jorquera I, le gal la Salle G, Ben-Ari Y (1993) Epilepsy induced collateral sprouting of hippocampal mossy fibers: does it induce the development of ectopic synapses with granule cell dendrites? Hippocampus 3:257-268.

Represa A, Niquet J, Pollard H, Ben-Ari Y (1995) Cell death, gliosis, and synaptic remodeling in the hippocampus of epileptic rats. J Neurobiol 26:413-425.

Ribak CE, Shapiro LA (2007) Ultrastructure and synaptic connectivity of cell types in the adult rat dentate gyrus. Prog Brain Res 163:155-166.

Ribak CE, Tran PH, Spigelman I, Okazaki MM, Nadler JV (2000) Status epilepticus-induced hilar basal dendrites on rodent granule cells contribute to recurrent excitatory circuitry. The Journal of Comparative Neurology 428:240-253.

Rosenmund C, Clements J, Westbrook G (1993) Nonuniform probability of glutamate release at a hippocampal synapse. Science 262:754-757.

Rothman JS, Cathala L, Steuber V, Silver RA (2009) Synaptic depression enables neuronal gain control. Nature 457:1015-1018.

Sachidhanandam S, Blanchet C, Jeantet Y, Cho YH, Mulle C (2009) Kainate receptors act as conditional amplifiers of spike transmission at hippocampal mossy fiber synapses. J Neurosci 29:5000-5008.

Salin PA, Scanziani M, Malenka RC, Nicoll RA (1996) Distinct short-term plasticity at two excitatory synapses in the hippocampus. Proc Natl Acad Sci U S A 93:13304-13309.

Sandau US, Colino-Oliveira M, Jones A, Saleumvong B, Coffman SQ, Liu L, Miranda-Lourenco C, Palminha C, Batalha VL, Xu Y, Huo Y, Diogenes MJ, Sebastiao AM, Boison D (2016) Adenosine Kinase Deficiency in the Brain Results in Maladaptive Synaptic Plasticity. J Neurosci 36:12117-12128.

Sansing LH, Tüzün E, Ko MW, Baccon J, Lynch DR, Dalmau J (2007) A patient with encephalitis associated with NMDA receptor antibodies. Nature Reviews Neurology 3:291.

Santhakumar V, Aradi I, Soltesz I (2005) Role of mossy fiber sprouting and mossy cell loss in hyperexcitability: a network model of the dentate gyrus incorporating cell types and axonal topography. J Neurophysiol 93:437-453.

Santhakumar V, Bender R, Frotscher M, Ross ST, Hollrigel GS, Toth Z, Soltesz I (2000) Granule cell hyperexcitability in the early post-traumatic rat dentate gyrus: the 'irritable mossy cell'hypothesis. The Journal of physiology 524:117-134.

Scharfman H, Sollas A, Berger R, Goodman J, Pierce J (2003a) Perforant path activation of ectopic granule cells that are born after pilocarpine-induced seizures. Neuroscience 121:1017-1029.

Scharfman HE (1995) Electrophysiological evidence that dentate hilar mossy cells are excitatory and innervate both granule cells and interneurons. Journal of neurophysiology 74:179-194.

Scharfman HE, Sollas AL, Berger RE, Goodman JH (2003b) Electrophysiological evidence of monosynaptic excitatory transmission between granule cells after seizure-induced mossy fiber sprouting. J Neurophysiol 90:2536-2547.

Schoen S, Ebert U, Löscher W (1999) 5′-Nucleotidase activity of mossy fibers in the dentate gyrus of normal and epileptic rats. Neuroscience 93:519-526.

Semah F, Picot M-C, Adam C, Broglin D, Arzimanoglou A, Bazin B, Cavalcanti D, Baulac M (1998) Is the underlying cause of epilepsy a major prognostic factor for recurrence? Neurology 51:1256-1262.

Severa W, Parekh O, James CD, Aimone JB (2017) A combinatorial model for dentate gyrus sparse coding. Neural computation 29:94-117.

Shibley H, Smith BN (2002) Pilocarpine-induced status epilepticus results in mossy fiber sprouting and spontaneous seizures in C57BL/6 and CD-1 mice. Epilepsy Res 49:109-120.

Simmons ML, Terman GW, Chavkin C (1997) Spontaneous excitatory currents and kappa-opioid receptor inhibition in dentate gyrus are increased in the rat pilocarpine model of temporal lobe epilepsy. J Neurophysiol 78:1860-1868.

Sloviter RS (1987) Decreased hippocampal inhibition and a selective loss of interneurons in experimental epilepsy. Science 235:73-76.

Sloviter RS (1991) Permanently altered hippocampal structure, excitability, and inhibition after experimental status epilepticus in the rat: the “dormant basket cell” hypothesis and its possible relevance to temporal lobe epilepsy. Hippocampus 1:41-66.

Sloviter RS (1992) Possible functional consequences of synaptic reorganization in the dentate gyrus of kainate-treated rats. Neurosci Lett 137:91-96.

Sloviter RS, Zappone CA, Harvey BD, Frotscher M (2006a) Kainic acid-induced recurrent mossy fiber innervation of dentate gyrus inhibitory interneurons:

possible anatomical substrate of granule cell hyper-inhibition in chronically epileptic rats. J Comp Neurol 494:944-960.

Sloviter RS, Zappone CA, Harvey BD, Frotscher M (2006b) Kainic acid-induced recurrent mossy fiber innervation of dentate gyrus inhibitory interneurons: Possible anatomical substrate of granule cell hyperinhibition in chronically epileptic rats. The Journal of Comparative Neurology 494:944-960.

Smith BN (2017) Sprouted Mossy Fiber Connections of Adult-Born Granule Cells: Detonate or Fizzle? Epilepsy Curr 17:379-380.

Spigelman I, Yan XX, Obenaus A, Lee EY, Wasterlain CG, Ribak CE (1998) Dentate granule cells form novel basal dendrites in a rat model of temporal lobe epilepsy. Neuroscience 86:109-120.

Sutula T, He XX, Cavazos J, Scott G (1988) Synaptic reorganization in the hippocampus induced by abnormal functional activity. Science 239:1147-1150.

Sutula T, Cascino G, Cavazos J, Parada I, Ramirez L (1989) Mossy fiber synaptic reorganization in the epileptic human temporal lobe. Ann Neurol 26:321-330.

Sutula T, Koch J, Golarai G, Watanabe Y, McNamara JO (1996) NMDA receptor dependence of kindling and mossy fiber sprouting: evidence that the NMDA receptor regulates patterning of hippocampal circuits in the adult brain. J Neurosci 16:7398-7406.

Sutula T, Zhang P, Lynch M, Sayin U, Golarai G, Rod R (1998) Synaptic and axonal remodeling of mossy fibers in the hilus and supragranular region of the dentate gyrus in kainate-treated rats. J Comp Neurol 390:578-594.

Sutula TP, Dudek FE (2007) Unmasking recurrent excitation generated by mossy fiber sprouting in the epileptic dentate gyrus: an emergent property of a complex system. In: Progress in Brain Research, pp 541-563: Elsevier.

Tashiro A, Zhao C, Gage FH (2006) Retrovirus-mediated single-cell gene knockout technique in adult newborn neurons in vivo. Nature protocols 1:3049.

Tauck DL, Nadler JV (1985) Evidence of functional mossy fiber sprouting in hippocampal formation of kainic acid-treated rats. J Neurosci 5:1016-1022.

Ting JT, Daigle TL, Chen Q, Feng G (2014) Acute brain slice methods for adult and aging animals: application of targeted patch clamp analysis and optogenetics. Methods Mol Biol 1183:221-242.

Toni N, Laplagne DA, Zhao C, Lombardi G, Ribak CE, Gage FH, Schinder AF (2008) Neurons born in the adult dentate gyrus form functional synapses with target cells. Nat Neurosci 11:901-907.

Toth K, Suares G, Lawrence JJ, Philips-Tansey E, McBain CJ (2000) Differential Mechanisms of Transmission at Three Types of Mossy Fiber Synapse. The Journal of Neuroscience 20:8279-8289.

Turski WA, Cavalheiro EA, Schwarz M, Czuczwar SJ, Kleinrok Z, Turski L (1983) Limbic seizures produced by pilocarpine in rats: behavioural,

electroencephalographic and neuropathological study. Behav Brain Res 9:315-335.

Van Praag H, Kempermann G, Gage FH (1999) Running increases cell proliferation and neurogenesis in the adult mouse dentate gyrus. Nature neuroscience 2:266.

Van Praag H, Shubert T, Zhao C, Gage FH (2005) Exercise enhances learning and hippocampal neurogenesis in aged mice. Journal of Neuroscience 25:8680-8685.

van Praag H, Schinder AF, Christie BR, Toni N, Palmer TD, Gage FH (2002) Functional neurogenesis in the adult hippocampus. Nature 415:1030-1034.

Villasana LE, Kim KN, Westbrook GL, Schnell E (2015) Functional Integration of Adult-Born Hippocampal Neurons after Traumatic Brain Injury(1,2,3). eNeuro 2.

von Kitzing E, Jonas P, Sakmann B (1994) Quantal analysis of excitatory postsynaptic currents at the hippocampal mossy fiber-CA3 pyramidal cell synapse. Advances in second messenger and phosphoprotein research 29:235-260.

Vyleta NP, Borges-Merjane C, Jonas P (2016) Plasticity-dependent, full detonation at hippocampal mossy fiber-CA3 pyramidal neuron synapses. Elife 5.

Wagner JJ, Terman GW, Chavkin C (1993) Endogenous dynorphins inhibit excitatory neurotransmission and block LTP induction in the hippocampus. Nature 363:451-454.

Walter C, Murphy BL, Pun RY, Spieles-Engemann AL, Danzer SC (2007) Pilocarpine-induced seizures cause selective time-dependent changes to adult-generated hippocampal dentate granule cells. J Neurosci 27:7541-7552.

Weisskopf MG, Nicoll RA (1995) Presynaptic changes during mossy fibre LTP revealed by NMDA receptor-mediated synaptic responses. Nature 376:256-259.

Weisskopf MG, Zalutsky RA, Nicoll RA (1993) The opioid peptide dynorphin mediates heterosynaptic depression of hippocampal mossy fibre synapses and modulates long-term potentiation. Nature 362:423-427.

Weisskopf MG, Castillo PE, Zalutsky RA, Nicoll RA (1994) Mediation of hippocampal mossy fiber long-term potentiation by cyclic AMP. Science 265:1878-1882.

Wiebe S, Blume WT, Girvin JP, Eliasziw M (2001) A randomized, controlled trial of surgery for temporal-lobe epilepsy. N Engl J Med 345:311-318.

Williams Megan E, Wilke Scott A, Daggett A, Davis E, Otto S, Ravi D, Ripley B, Bushong Eric A, Ellisman Mark H, Klein G, Ghosh A (2011) Cadherin-9 Regulates Synapse-Specific Differentiation in the Developing Hippocampus. Neuron 71:640-655.

Williams PA, Wuarin J-P, Dou P, Ferraro DJ, Dudek FE (2002) Reassessment of the Effects of Cycloheximide on Mossy Fiber Sprouting and Epileptogenesis in the Pilocarpine Model of Temporal Lobe Epilepsy. Journal of Neurophysiology 88:2075-2087.

Williams-Karnesky RL, Sandau US, Lusardi TA, Lytle NK, Farrell JM, Pritchard EM, Kaplan DL, Boison D (2013) Epigenetic changes induced by adenosine augmentation therapy prevent epileptogenesis. J Clin Invest 123:3552-3563.

Williamson PD, French JA, Thadani VM, Kim JH, Novelly RA, Spencer SS, Spencer DD, Mattson RH (1993) Characteristics of medial temporal lobe epilepsy: II. Interictal and ictal scalp electroencephalography, neuropsychological testing, neuroimaging, surgical results, and pathology. Ann Neurol 34:781-787.

Wong M (2013) Mammalian target of rapamycin (mTOR) pathways in neurological diseases. Biomedical journal 36:40-50.

Wu K, Leung LS (2001) Enhanced but fragile inhibition in the dentate gyrus in vivo in the kainic acid model of temporal lobe epilepsy: a study using current source density analysis. Neuroscience 104:379-396.

Wu L-G, Saggau P (1994) Adenosine inhibits evoked synaptic transmission primarily by reducing presynaptic calcium influx in area CA1 of hippocampus. Neuron 12:1139-1148.

Wuarin J-P, Dudek FE (1996) Electrographic Seizures and New Recurrent Excitatory Circuits in the Dentate Gyrus of Hippocampal Slices from

Kainate-Treated Epileptic Rats. The Journal of Neuroscience 16:4438-4448.

Wuarin JP, Dudek FE (2001) Excitatory synaptic input to granule cells increases with time after kainate treatment. J Neurophysiol 85:1067-1077.

Yang SM, Alvarez DD, Schinder AF (2015) Reliable Genetic Labeling of Adult-Born Dentate Granule Cells Using Ascl1CreERT2 and GlastCreERT2 Murine Lines. Journal of Neuroscience 35:15379-15390.

Zeng LH, Rensing NR, Wong M (2009) The mammalian target of rapamycin signaling pathway mediates epileptogenesis in a model of temporal lobe epilepsy. J Neurosci 29:6964-6972.

Zhan R-Z, Timofeeva O, Nadler JV (2010) High ratio of synaptic excitation to synaptic inhibition in hilar ectopic granule cells of pilocarpine-treated rats. American Journal of Physiology-Heart and Circulatory Physiology.

Zhou QG, Nemes AD, Lee D, Ro EJ, Zhang J, Nowacki AS, Dymecki SM, Najm IM, Suh H (2019) Chemogenetic silencing of hippocampal neurons suppresses epileptic neural circuits. J Clin Invest 129:310-323.

Zimmermann H, Vogel M, Laube U (1993) Hippocampal localization of 5′-nucleotidase as revealed by immunocytochemistry. Neuroscience 55:105-112.

Zucca S, Griguoli M, Malézieux M, Grosjean N, Carta M, Mulle C (2017) Control of Spike Transfer at Hippocampal Mossy Fiber Synapses *In Vivo* by $GABA_A$ and $GABA_B$ Receptor-Mediated Inhibition. The Journal of Neuroscience 37:587-598.

Zucker RS, Regehr WG (2002) Short-Term Synaptic Plasticity. Annual Review of Physiology 64:355-405.